

---

Theses and Dissertations

---

Spring 2015

## Predicting episodic ammonium excretion by freshwater mussels via gape response and heart rate

Lee W Hauser  
*University of Iowa*

Follow this and additional works at: <https://ir.uiowa.edu/etd>

 Part of the [Civil and Environmental Engineering Commons](#)

Copyright 2015 Lee Hauser

This thesis is available at Iowa Research Online: <https://ir.uiowa.edu/etd/1621>

---

### Recommended Citation

Hauser, Lee W. "Predicting episodic ammonium excretion by freshwater mussels via gape response and heart rate." MS (Master of Science) thesis, University of Iowa, 2015.  
<https://doi.org/10.17077/etd.ds4ka6u7>

---

Follow this and additional works at: <https://ir.uiowa.edu/etd>

 Part of the [Civil and Environmental Engineering Commons](#)

PREDICTING EPISODIC AMMONIUM EXCRETION BY FRESHWATER  
MUSSELS VIA GAPE RESPONSE AND HEART RATE

by  
Lee W Hauser

A thesis submitted in partial fulfillment  
of the requirements for the Master of  
Science degree in Civil and  
Environmental Engineering in the  
Graduate College of  
The University of Iowa

May 2015

Thesis Supervisor: Assistant Professor Craig L. Just

Copyright by  
LEE W HAUSER  
2015  
All Rights Reserved

Graduate College  
The University of Iowa  
Iowa City, Iowa

CERTIFICATE OF APPROVAL

---

MASTER'S THESIS

---

This is to certify that the Master's thesis of

Lee W Hauser

has been approved by the Examining Committee for the  
thesis requirement for the Master of Science degree in  
Civil and Environmental Engineering at the May 2015  
graduation.

Thesis Committee:

\_\_\_\_\_  
Craig L. Just, Thesis Supervisor

\_\_\_\_\_  
Richard L. Valentine

\_\_\_\_\_  
David M. Cwiertyny

To all the people that have helped me on my journey and to the people lost  
along the way

Fear is a reaction, courage is a decision; perseverance is making that decision  
day after day after day.

Joe Tye

## ACKNOWLEDGMENTS

First, I would like to thank all of my family and friends for their encouragement throughout my time in academics. Specifically, I would like to thank my mom and dad for their love and support. Secondly, I would like to thank my advisor Craig Just. Not only were you encouraging throughout my research, but you also provided me with opportunities that will make me a better engineer.

Next I would like to thank all of the people that assisted me in finishing my thesis. Firstly, I would like to specifically thank Daniel Vial and Jim Niemeier for building the heart rate and gape sensors. Secondly, I would like to thank Katie Langenfeld for helping me collect samples and for her work on the STELLA model. Lastly, I would like to thank Jon Durst, Brandon Barquist, and Eric Jetter for their in fixing problems with the mussel habitats and ensuring I had all of the necessary equipment to conduct my research.

## ABSTRACT

Freshwater mussels are a viable option to detect real-time changes in water quality within aquatic ecosystems. Known as ecosystem engineers, freshwater mussels are constantly filtering particles and recycling nutrients in the benthic community. Therefore, identifying their physiological responses to alterations in water quality will enable mussels to not only serve as biomonitors but help model their impact on nitrogen cycle. This research focuses on identifying how mussel gape and heart rate respond to the addition of phytoplankton following a period of limited food availability. Immediately following phytoplankton addition, mussels show a decreased gape position linked with changes heart rate. As the gape returns to an open position, overlying ammonia concentrations increase showing an end of the metabolism process. As a result, pairing physiological changes with increased concentrations of phytoplankton, freshwater mussels' impact on ammonium concentrations can be accurately predicted. By inputting experimental excretion rates combined with variations in gape position, dynamic models will be simulate ammonium concentrations in the overlying water.



## PUBLIC ABSTRACT

Freshwater mussels are a viable option to detect real-time changes in water quality within aquatic ecosystems. Known as ecosystem engineers, freshwater mussels are constantly filtering particles and recycling nutrients in the benthic community. Therefore, identifying their physiological responses to alterations in water quality will enable mussels to not only serve as biomonitors but help model their impact on nitrogen cycle. This research focuses on identifying how mussel gape and heart rate respond to the addition of phytoplankton following a period of limited food availability. Immediately following phytoplankton addition, mussels show a decreased gape position linked with changes heart rate. As the gape returns to an open position, overlying ammonia concentrations increase showing an end of the metabolism process. As a result, pairing physiological changes with increased concentrations of phytoplankton, freshwater mussels' impact on ammonium concentrations can be accurately predicted. By inputting experimental excretion rates combined with variations in gape position, dynamic models will be simulate ammonium concentrations in the overlying water.

## TABLE CONTENTS

LIST OF TABLES .....	ix
LIST OF FIGURES .....	x
CHAPTER 1 INTRODUCTION AND OBJECTIVE .....	1
CHAPTER 2 LITERATURE REVIEW .....	7
2.1 Freshwater Mussel impacts on Aquatic Nitrogen .....	7
2.2 Monitoring Physiological Changes in Mussels .....	12
2.3 Using Mussels Gape Responses to Model Dynamic Ecosystems .....	15
CHAPTER 3 MATERIALS AND METHODS .....	19
3.1 Mussel Collection and Transitory Habitat .....	19
3.2 Mussel Mesocosm .....	19
3.3 Water Chemistry Sensing .....	20
3.4 Heart Rate and Gape Sensors .....	21
3.5 Experiment 1: Ammonium Excretion, Heart Rate, and Gape response by Two Mussels in a 93 Liter Mesocosm .....	22
3.6 Experiment 2: Ammonium Excretion, Heart Rate, and Gape Response by One Mussel in a 61 Liter Mesocosm .....	23
3.7 Experiment 3: Ammonium Excretion, Heart Rate, and Gape Response by One Mussel in a 10 L Microcosm .....	23
3.8 Data Analysis .....	24
CHAPTER 4 AMMONIUM EXCRETION, HEART RATE, AND GAPE RESPONSE BY MUSSELS IN A MESOCOSM .....	34
4.1 Results: Experiment 1 .....	34
4.2 Results: Experiment 2 .....	36
4.2.1 Experiment 2A .....	36
4.2.2 Experiment 2B .....	39
4.2.3 Ammonium Mass Flux Comparison between Experiment 2A and 2B .....	41
CHAPTER 5 AMMONIUM EXCRETION, HEART RATE, AND GAPE RESPONSE BY ONE MUSSEL IN A 10 L MICROCOSM .....	47
5.1 Results of Experiment 3 .....	47
5.1.1 Experiment 3A .....	47
5.1.2 Experiment 3B .....	50
5.1.3 Ammonium Mass Flux Comparison between Experiments 3A and 3B .....	52
5.2 Experimental Discussion .....	53
CHAPTER 6 MODELING THE IMPACT FRESHWATER MUSSELS HAVE ON AQUATIC AMMONIUM CONCENTRATIONS VIA GAPE RESPONSE .....	62

6.1 Model Parameters .....	62
6.2 Stella Model.....	65
REFERENCES .....	83

## LIST OF TABLES

Table 6.1 Variables used in the development of the STELLA model. ....	73
Table 6.2 Range of variables and rates used for the dynamic STELLA model.....	76

## LIST OF FIGURES

Figure 1.1 Dissolved oxygen concentration at the Mississippi River Delta in the Gulf of Mexico in 2014. ....	5
Figure 1.2 Total nitrogen yield delivered to the Gulf of Mexico from the incremental drainage reaches within the basin of the Mississippi and Atchafalaya Rivers. ....	6
Figure 2.1 Freshwater mussels' typical anatomy .....	16
Figure 2.2 Reproductive life cycle of mussels.....	17
Figure 2.3 Accumulation of excess nutrients in aquatic ecosystems during different flow conditions. ....	18
Figure 3.1 Location of mussel bed used for this research in Iowa River (Image from Google Earth).....	25
Figure 3.2 Six experimental mesocosms used for this research. ....	26
Figure 3.3 Digital representation of the experimental setup for experiments 1, 2A, and 2B.....	27
Figure 3.4 Digital representation of 10 liter microcosm for experiment 3 (3A and 3B). ....	28
Figure 3.5 Sampled heart rate data to determine sensor placement on the mussel. The y-axis is a unitless value outputted by Tera Term. ....	29
Figure 3.6 Raw heart rate from Tera Tram after being automated by MATLAB script. The y-axis is a unitless value. ....	30
Figure 3.7 A digital image of electronic sensor placement on freshwater mussels.....	31
Figure 3.8 Experimental placement of hall sensor and rare earth magnet on freshwater mussel. ....	32
Figure 3.9 Experimental placement of battery clip and heart rate sensor near the hinge of the mussel. ....	33
Figure 4.1 Experiment 1 results: (a) phytoplankton concentrations in overlying water, (b) changes in $\text{NH}_4^+$ concentrations for mussel and control mesocosms ( $\text{mg-N L}^{-1}$ ), and (c) changes in the mussels heart rate (bpm) and gape response (open or closed). The blue dashed lines mark changes in gape position.....	42
Figure 4.2 $\text{NH}_4^+$ mass flux immediately after Phyto-Feast addition for both control and mussel microcosms in Experiment 1. ....	43

Figure 4.3 Experiment 2A results: (a) phytoplankton concentrations in overlying water, (b) changes in $\text{NH}_4^+$ concentrations for mussel and control mesocosms( $\text{mg-N L}^{-1}$ ), and (c) changes in the mussels heart rate (bpm) and gape response (open or closed). The blue dashed lines mark changes in gape position.....	44
Figure 4.4 Experiment 2B results: (a) phytoplankton concentrations in overlying water, (b) changes in $\text{NH}_4^+$ concentrations for mussel and control mesocosms ( $\text{mg-N L}^{-1}$ ), and (c) changes in the mussels heart rate (bpm) and gape response (open or closed). The blue dashed lines mark changes in gape position.....	45
Figure 4.5 $\text{NH}_4^+$ mass flux immediately after Phyto-Feast addition for both control and mussel microcosms in experiments 2A and 2B. ....	46
Figure 5.1 Experiment 3A results: (a) phytoplankton concentrations in overlying water, (b) changes in $\text{NH}_4^+$ concentrations for mussel and control microcosms ( $\text{mg-N L}^{-1}$ ), and (c) changes in the mussels heart rate (bpm) and gape response (open or closed). The blue dashed lines mark changes in gape position.....	58
Figure 5.2 Experiment 3B results: (a) phytoplankton concentrations in overlying water, (b) changes in $\text{NH}_4^+$ concentrations for mussel and control microcosms ( $\text{mg-N L}^{-1}$ ), and (c) mussels gape response (open or closed). The blue dashed lines mark changes in gape position. ....	59
Figure 5.3 $\text{NH}_4^+$ mass flux immediately after Phyto-Feast addition for both control and mussel microcosms in experiments 3A and 3B. ....	60
Figure 5.4 $\text{NH}_4^+$ mass flux after mussel gape re-opened following the addition of Phyto-Feast for both the control and mussel microcosm for experiment 3A and 3B. ....	61
Figure 6.1 Stocks, flows, and converters for phytoplankton in the STELLA model adapted from Bril Dissertation.....	69
Figure 6.2 Stocks, flows, and converters for ammonium in the STELLA model adapted from Bril Dissertation.....	70
Figure 6.3 Stocks, flows, and converters for both organic nitrogen and nitrate in the STELLA model adapted from Bril Dissertation.....	71
Figure 6.4 Stocks, flows, and converters for nitrite in the STELLA model adapted from Bril Dissertation. ....	72
Figure 6.5 Simulated overlying water $\text{NH}_4^+$ concentrations for one mussel and phytoplankton biomass one $\text{mg L}^{-1}$ during various gape position changes. ....	77
Figure 6.6 Simulated overlying water $\text{NH}_4^+$ concentrations for one mussel and phytoplankton biomass five $\text{mg L}^{-1}$ during various gape position changes.....	78
Figure 6.7 Simulated overlying water $\text{NH}_4^+$ concentrations for one mussel and phytoplankton biomass of ten $\text{mg L}^{-1}$ during various gape position changes.....	79

Figure 6.8 Simulated overlying NH <sub>4</sub> <sup>+</sup> concentrations for 200 mussels and phytoplankton biomass of one mg L <sup>-1</sup> during various gape position changes.....	80
Figure 6.9 Simulated overlying NH <sub>4</sub> <sup>+</sup> concentrations for 200 mussel and phytoplankton biomass of five mg L <sup>-1</sup> during various gape position changes. ....	81
Figure 6.10 Simulated overlying NH <sub>4</sub> <sup>+</sup> concentrations for 200 mussel and phytoplankton biomass of ten mg L <sup>-1</sup> during various gape position changes.....	82

## CHAPTER 1

### INTRODUCTION AND OBJECTIVE

The unbridled growth of the human population continues to place new economic and environmental stressor on the planet. Since the turn of the 20<sup>th</sup> century, the human population has more than tripled to a level exceeding 7 billion people.<sup>1</sup> During this time frame, farming practices have changed to meet the ever increasing food demand. In the United States, the land area devoted to agricultural has increased and the fertilizer application rates have risen maximize crop yield. Inorganic nitrogen, anthropogenically derived from the atmosphere, has become the dominant form of fertilizer.<sup>2</sup> As humans account for more than half of the annual fixation of atmospheric nitrogen. Unfortunately, between 1990 and 2000, approximately 30% of the nitrogen fertilizer that was applied to agricultural fields was lost to receiving waters due to runoff.<sup>3, 4</sup> Consequently, the Des Moines Water Works has threatened a lawsuit against three upstream counties in the Des Moines River watershed that have had high concentrations of nitrate which is costly to remove during drinking water treatment.<sup>5</sup>

The environmental consequence of nitrogen runoff to rivers, streams and coastal water are great. Water reaches characterized by low dissolved oxygen concentrations (i.e., hypoxic zones), are forming with increased size and frequency. The well documented 'Dead Zone' and is located in the Gulf of Mexico and extends from the mouth of the Mississippi River-(Figure 1.1). In 2014, the United States Environmental Protection Agency (EPA) estimated the hypoxic zone to be 13,080 square kilometers in size, which was slightly below the five year average (14,353 square kilometers). Since 1985, has been between 7,000 and 22,000 square kilometers. <sup>6</sup> As the Mississippi River watershed covers the entire Corn Belt, most of the excess nitrogen dumped into the Gulf of Mexico (Figure 1.2) is attributed to agricultural practices in the Midwest. And, the increasing variability of precipitation and more frequent extremes of drought and flood



has made the nitrogen loading increasingly dynamic. Researchers are continually seeking new and improved ways to quantify this variable nitrogen loading and to study the impacts of this loading on receiving waters. Recognizing that some aquatic organisms influence the nitrogen cycle more than others, researchers have turned to biomonitoring of certain species to improve scientific understanding and potential engineered solutions and/or mitigations.

Biomonitoring is defined as “the systematic use of living organisms or their responses as bioindicators to determine the condition or changes of the environment.”<sup>7</sup> Bioindicators can be used to study sudden environmental changes and to develop a baseline off longer-term environmental conditions.<sup>7</sup> In aquatic ecosystems, benthic invertebrates are well equipped as bioindicators. Since they are relatively immobile, and representative of the area where they are collected. Secondly, compared to fish, invertebrates have longer life cycles. Therefore changes in their population and community structure are more indicative of environmental changes. Lastly, invertebrates live and feed in, on, and around the benthic region where toxins typically accumulate. As invertebrates assimilate toxic pollutants, researchers are able to track the presence of toxic chemicals in the skeletal structure.<sup>8</sup> One benthic invertebrate that meets the previously stated criteria is freshwater mussels. Freshwater mussels are essential members of benthic community and can be a reliable indicator of changes in aquatic ecosystems.

For decades, freshwater mussels have been used to monitor pollutants as a result of living in nearshore habitats, being relatively sedentary, and long life expectancies. Additionally, mussel shells show physical and chemical changes in aquatic ecosystems, and their taxonomy, physiological behavior, and genetic makeup have been well documented.<sup>8</sup> Inefficiently, mussels are primarily used to determine the presence or absence of a specific chemicals or sudden life-style changes. As mussels filter the overlying water, toxic chemicals are typically stored in the shell or the soft tissue inside

the shell. As mussel population unexpectedly decrease, scientists can examine the chemical composition of the anatomy to determine if the decreases in populations was due to water quality issues.<sup>9</sup> To maximize the biomonitoring capabilities of mussels, researchers need to understand how real-time changes in overlying water conditions, specifically phytoplankton concentrations, impact physiological behavior of mussels.

Under flourishing environmental conditions, phytoplankton is the primary food source for freshwater mussels. Phytoplankton are photosynthesizing organism that require sunlight and dissolved inorganic nitrogen and phosphorus in the overlying water. During growth, phytoplankton remove nitrate or ammonium along with phosphorus from the overlying water until nutrient concentrations become unusable.<sup>10</sup> Being filter feeders, freshwater mussels remove phytoplankton from the overlying water while metabolizing valuable nutrients and discharging the unusable material through feces, pseudofeces, or excretion.<sup>11</sup> Depending on make-up of the benthic community, the discharged nutrients can either be taken up by plants, used by other macroinvertebrates, or go through chemical alteration (i.e., nitrification and denitrification). Aquatic ecosystems not located in agricultural regions need the discharged nutrients for sustainable life.<sup>12, 13</sup> Therefore, further understanding the impact of freshwater mussels on ammonia concentrations in rivers and streams will help accurately model their impact on the nitrogen cycle.

Our study interpreted real-time changes in ammonium concentrations attributed to mussel excretion and physiological behavior during periods of elevated phytoplankton concentrations. Specifically, detect real-time abduction and adduction of the bivalve shell along with changes in heart rate while investigating if there is a direct correlation between heart rate and changes in gape position. In an effort to fully understand the impact freshwater mussels have on the nitrogen cycle, another goal of this study was to understand how ammonium concentrations change during times of increased phytoplankton concentrations. More specifically, monitor and model the amount of

ammonia excreted by an individual freshwater mussel after the addition of phytoplankton.

Thus the specific objectives of our study were:

- Measure changes in overlying water ammonium concentration resulting from phytoplankton decay by bacteria and excretion by mussels
- Measure mussel heart rate and gape responses to changes in phytoplankton concentration and subsequent ammonium excretion
- Correlate changes in mussel heart rate and gape response to changes in overlying water ammonium concentration
- Evaluate the engineering significance of ammonium excretion by mussels in a river with excess nutrients using mussel biomonitoring data with nutrient prediction model

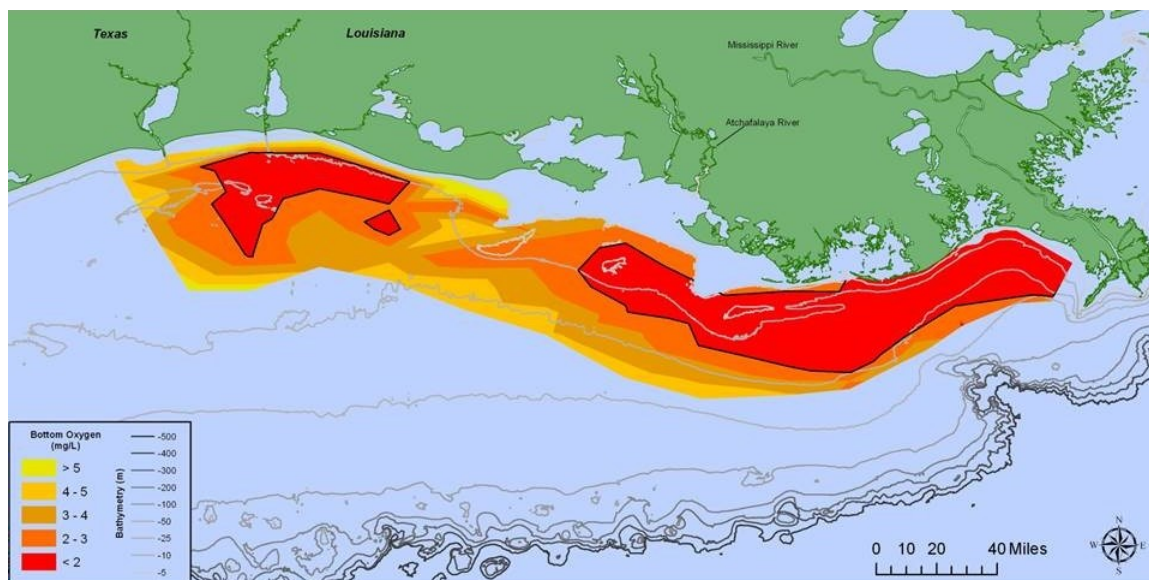


Figure 1.1 Dissolved oxygen concentration at the Mississippi River Delta in the Gulf of Mexico in 2014.<sup>14</sup>

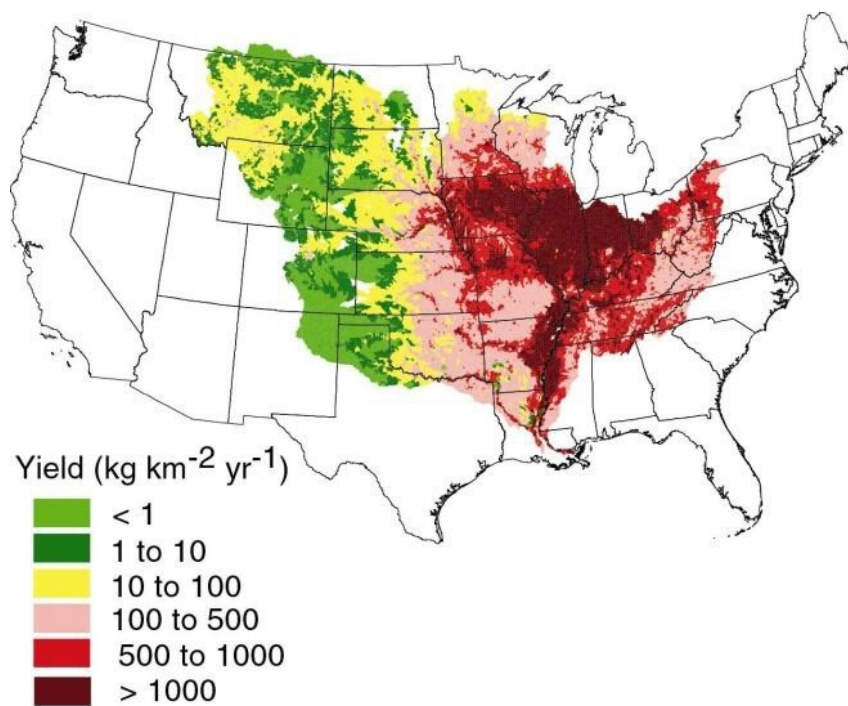


Figure 1.2 Total nitrogen yield delivered to the Gulf of Mexico from the incremental drainage reaches within the basin of the Mississippi and Atchafalaya Rivers.<sup>15</sup>

## CHAPTER 2

### LITERATURE REVIEW

This chapter is structured to first highlight the impact of freshwater mussels on the aquatic nitrogen cycle. This is followed by research overview of various studies that measured mussel physiology (e.g. gape response and heart rate) and some studies that correlated these physiological responses to changes in water chemistry. Lastly, the chapter highlights various ways that mussel impacts have been numerically modelled and specifically outlines the utility of the STELLA modeling program for this purpose.

#### 2.1 Freshwater Mussel impacts on Aquatic Nitrogen

Freshwater mussels have the ability to control water conditions in multiple trophic levels, resulting in the label of “ecosystem engineers.” As mussels filter particulates from the overlying water, they not only metabolize some of the filtered particles for growth, but release nutrients back into the water for other aquatic organism to use.<sup>16</sup> In ecosystems with limited nutrients, high filtering capabilities of mussels ensure enough nutrients are available for other organisms to grow.<sup>17</sup> Not only do mussels provide nutrients for other organisms, but their dependence on a fish host for reproduction make mussels a valuable tool to asses ecosystem health. As mussel populations increase, aquatic ecosystems are thought to be flourishing as there will be an abundance of nutrients for organisms to use during growth and a diverse amount of indigenous fish species. However, as mussel population decline, ecosystems typically have water quality issues leading to decreased populations of aquatic organisms.<sup>18</sup> Identifying the relationship between the benthic region and freshwater mussels will help preserve ecosystems for aquatic organisms.

Freshwater mussels are classified as a mollusk that inhabit the benthic region of lakes and rivers. There are over 900 freshwater mussel species throughout Earth’s freshwater ecosystems.<sup>19</sup> Of that, approximately 300 species occupy United States

freshwater system.<sup>20</sup> In the majority of freshwater ecosystems, mussels live in interspecies beds ranging from 1-100 mussels m<sup>-2</sup> and depending on the species, mussels can live anywhere from 5-100 years.<sup>21,22</sup> Mussels are able to live for long periods of time since the fundamental nutrients required for growth are easily accessible.

The internal biomass of freshwater mussels is protected by two rigid shells made up of calcium carbonate, hinged together. The soft tissue of the internal body is made up predominately carbon, nitrogen, and phosphorus. The internal body consists of gills, a digestive tract, muscular foot for movement, and mantle tissue that continually builds the shell-(Figure 2.1). Mussels obtain all of the required nutrients by filtering suspended particles from the overlying water.<sup>23,24</sup> With limited space inside the shell, mussel have a unique reproduction cycle that requires a fish to complete the process-(Figure 2.2). Sperm is released into the overlying water by male mussels, which is then filtered by the female mussel to fertilize the eggs. Once the eggs become fertilized, the female mussel attracts a fish host and attaches the fertilized eggs, glochidia, onto fish's gills. Each mussel species requires certain fish that will nurture and protect the glochidia until they are ready to detach.<sup>23</sup> As a result of the unique reproduction cycle, water quality issues can limit the reproduction of mussels.

Of the 300 mussel species existing in the United States, there are, depending on how many have gone extinct since the last survey, 78 species that inhabit the Midwest. Over half of those are classified as federally endangered, threatened or state species of concern. Destruction of habitats, water pollution, and invasive species have been the main cause in declining mussel populations.<sup>20</sup> As water bodies continue to be polluted, mussels' habitats continue to deteriorate. Not only does eroded sediment alter the preferred substrate for mussels to move around in, but sediment can suffocate them. Mussels prefer a mixture of cobble and coarse material as it allows them to still move, but the larger rocks help protect mussels from high flow velocities.<sup>25</sup> Depending on the species, mussels will either burrow or partially submerge themselves in substrate.<sup>26</sup> As

soil is washed into rivers and lakes, it settles to the bottom, forming a blanket over the portion of the mussel that is not burrowed and results in suffocation.<sup>27</sup> Even though mussels are known as ecosystem engineers, issues with water quality can limit improvements in aquatic ecosystems made by mussels.

Mussels get their label as ecosystem engineers due to their extensive filtering ability. Mussel beds have the ability to filter anywhere from 10 to 100% of the water column.<sup>28</sup> Individual filtering rates are dependent on both size and species, with larger mussels demonstrating filtration rates as high as 0.5-1 liter hour<sup>-1</sup>. The higher the filtration rate, the higher the clearance rate can be (removal of suspended particles).<sup>29</sup> Even though mussels can remove and store toxic metals, they are most beneficial to ecosystems when they are recycling nutrients.<sup>30</sup> Mussels fundamental assistance to ecosystems is when they remove algae and recycle nitrogen and phosphorus for other organisms to use.

With nitrogen and phosphorus being two of the fundamental building blocks for life, an abundance of nutrients can create ecosystems overgrown with plants. Abnormally high concentrations of nitrogen and phosphorus in rivers and streams is primarily a result of agricultural runoff. The fertilizer not used by plants either goes through chemical alteration in the form of nitrification or denitrification, sorb onto soil particles, or leaches into neighboring water bodies. In most fields, ammonium is quickly oxidized to either nitrite or nitrate depending on which nitrifying bacteria are present and the amount of oxygen available for oxidation.<sup>31</sup> Ammonium has a positive charge. Therefore, any leftover becomes attached to the negatively charged soil particles, making it relatively immobile. However, since nitrate and nitrite have a negative charge, it will not attach to soil particles but instead leach into water bodies.<sup>32</sup> Heavy rain events immediately following fertilizer application increase concentrations of ammonium, phosphorus, and nitrate are found in neighboring water. However, when there is enough time for the ammonium to be oxidized and for plants to uptake the phosphorus, only elevated



concentrations of nitrate existed with trace amounts of ammonium and phosphorus.<sup>33, 34</sup> Therefore, the main problem with fertilizer arises once it is nitrified and washed into neighboring rivers and lakes.

In aquatic ecosystems, excess nutrients create hot spots for plants and algal blooms (phytoplankton) creating eutrophic conditions. Eutrophication is not an overnight process but rather a slow evolving process that is directly influenced by the amount of phosphorus and nitrogen compounds present. Eutrophication will cause the following to occur, increases in phytoplankton biomass, diminished visibility, lower dissolved oxygen concentrations, and loss of indigenous fish species.<sup>35</sup> During phytoplankton growth, both nitrogen and phosphorus are removed from the overlying water. In most freshwater systems, phosphorus is the limiting nutrient while nitrogen compounds are limiting in marine systems.<sup>35</sup> Depending on the phytoplankton species, nitrogen to phosphorus ratios can be as large as 107:1 or as small as 4:1.<sup>36</sup> Phytoplankton blooms become widespread three to five days after the increase in nutrient concentrations.<sup>37</sup> With phytoplankton quickly responding to increases in nutrient concentrations, aquatic organisms have to limit the impact algal blooms have.

Depending on the time of the year, ecosystems within the Upper Mississippi Watershed have increased amounts of algae growth, just to what extent. From low productivity to high productivity, rivers and lakes are classified as oligotrophic, mesotrophic, or eutrophic. In terms of algae removal, freshwater mussels will remove algae throughout all trophic levels.<sup>11</sup> However, there are thresholds at both oligotrophic and eutrophic where algae removal stops. During times of lower algae concentrations, mussels quit feeding as an effort to conserve energy.<sup>38</sup> Conversely, during extended periods of high algae concentrations mussels will remove phytoplankton before becoming fully saturated and stopping.<sup>39</sup> Once the mussel has removed phytoplankton from the overlying water, phytoplankton is metabolized and nutrients are recycled for other aquatic organisms to use.

Similar to any other living organism, mussels metabolize the filtered phytoplankton and then discharge it back out as a useable nutrient (ammonium, nitrate, or phosphorus). The metabolized algal is either be allocated for tissue growth, biodeposited (feces or pseudofeces), or excreted. As algae concentrations increase, there is an increase amount of nutrients in the biodeposited and excreted materials.<sup>40</sup> With biodeposited material being a mixture of organic nitrogen, phosphorus, and silt and excreted material being mainly ammonium, other aquatic organisms are able to use the waste for growth. The excreted ammonium and biodeposited material mix in with the substrate before diffusing into the overlying water.<sup>41, 42</sup> As the nutrients are recycled back into the water, microorganisms are able to process them in several ways.

Depending on the microorganisms present in aquatic ecosystems, nitrogen compounds are either be chemically processed or used for growth. Like fertilizer, in aquatic ecosystems bacteria process ammonium and nitrate through nitrification or denitrification. With an abundance of oxygen, nitrifying bacteria oxidize ammonium to first nitrite then nitrate. Following nitrification, denitrifying bacteria reduce nitrate to dinitrogen gas with intermediates of nitrite, nitric oxide, and nitrous oxide. In some aquatic ecosystems, there are not the bacteria required completely convert nitrate to dinitrogen gas.<sup>43, 44</sup> During cell synthesis, microorganisms prefer ammonium as their inorganic nitrogen source as it is already in a useable oxidation state of -III. Compared to other forms of inorganic nitrogen,  $\text{NO}_3^-$  or  $\text{NO}_2^-$ , the nitrogen must be reduced before some microorganisms can use it, which requires additional energy.<sup>45</sup> For various flow conditions, figure 4.3 illustrates the impact different concentrations of ammonium and nitrate have on aquatic ecosystems. Figure 4.3 indicates that of all the nutrients, ammonium is the most influential on plant growth in aquatic ecosystems.

## 2.2 Monitoring Physiological Changes in Mussels

Freshwater mussels have been used as biomonitors to track changes in water chemistry for decades, but none of the information can be processed for real-time analysis. Conservationists use mussel shell composition and size to investigate previous issues with water quality.<sup>9</sup> Mussels are said to be good bioindicators due to being ubiquitous in aquatic ecosystems, long-lived and sedentary, have the ability to incorporate and show annual patterns of the physical and chemical environments after death, along with mussel being easily simulated in a laboratory settings. At environmental extremes, primary responses of mussels can be broken into physiological regulations or survival.<sup>8</sup> By identifying differences in survival strategies and how physiology changes correlate to variations in aquatic environments, mussel behavior can be used for models and as real-time bioindicators.

Physiological behavior for freshwater mussels is broken into three categories, gape response (opening and closing of the bivalve), variations in heart rate, or changes in filtration. Changes in gape are influenced by burrowing events, predation risk, variations in algae concentrations, and the removal from water.<sup>46-49</sup> Variations in heart rate are attributed to both burrowing events and changes in oxygen intake.<sup>50, 51</sup> Changes in filtration are expected during variations in algae concentrations and increases in suspended solid.<sup>48, 52, 53</sup> With this research focusing on gapping events and fluctuations in heart rate, the literature review will focus on those two aspects while highlighting important details about changes in filtration.

The bivalve not only serves as a housing structure for the internal organs but it is a protective casing against threats. Gape closure is an indication of survival strategy. As predation risk increases, the presence of mussel homogenate, the gape position will close until the detection of homogenate has stopped. Even with increased presence of algae, valve gape remains closed until the predation risk disappears.<sup>47</sup> Similar to predation risk, prolonged removal from water evokes survival instinct and leads to the gape closure as a

way to decrease oxygen consumption. When being removed for water, mussels are able to survive while remaining closed by switching the metabolism process from aerobic to anaerobic, requiring less oxygen.<sup>49, 51</sup> Different from survival strategies, physiological regulations govern episodic gaping events.

Episodic gaping events are representative of either burrowing activities or changes in food availability. Burrowing activities can be broken into three phases: 1) penetration of the foot into substrate, 2) lifting of the shell, and 3) deepening of the shell. Throughout the burrowing process, the gape goes through abduction and adduction events enabling freedom of foot movement.<sup>50</sup> Comparable to burrowing, mussels show an increased degree of gape for both low and high algae concentrations. During low algae concentrations, mussels dig for organic matter in the substrate to find and consume nutrients for growth, known as pedal feeding.<sup>54</sup> As there is a transition from limited food availability to an abundance of food, mussels increase the gape angle until the algae concentration drops below a certain threshold before closing.<sup>17</sup> While changes in gape position are easy to monitor, it is more challenging to detect changes in heart rate.

Due to the rigid bivalve, a little research has been done on mussel heart rate but instead focusing on oxygen consumption. Like any living organism, the heart rate of freshwater mussels is influenced by energy expenditure and oxygen consumption. During all three phases of the described burrowing event, mussels show an elevated heart rate compared to a burrowed or immobile mussel. In order to meet the energy demands for burrowing, mussels increase their oxygen consumption rate.<sup>50</sup> Alternatively, during times of stressful environmental conditions their metabolism switches from aerobic to anaerobic, moving away from oxygen consumption subsequently decreasing the heart rate.<sup>55</sup>

With mussels obtaining the required nutrients through filtering suspend solids, it would be expected to be an automated process but fluctuations in aquatic conditions alter the filtration rate of mussels. Most notably, there is an upper and a lower threshold where

mussels will quit filtering. As increased algae conditions persist, mussels quit filtering due to becoming saturated with food. Conversely, at periods of low algae conditions, mussels quit filtering as a result of being unable to obtain enough nutrients and therefore becoming inefficient. With it being inefficient, the decreased filtering serves as a way to conserve energy.<sup>39</sup> With energy conservation being a driving factor for filtration rates, mussels surprisingly do not show slower filtration rates during increased amounts of silt. The increased amounts of silt require more energy to sort valuable nutrients from wastes. However, when increased silt particulates are coupled with high algae concentrations, mussel do not decrease their filtration rates.<sup>53</sup>

It has been shown that many factors influence the physiological behavior of mussels. Therefore, it is important to monitor mussels in various environmental conditions and correlate changes in physiological behavior with chemical conditions in aquatic ecosystems. Early research to detect changes in gape position was done using automated imaging or visual observations.<sup>52, 56</sup> Unfortunately, it is limited to only detecting gape movements of the portion of the mussel not burrowed. Hall-effect sensors are able to detect gape movements below the surface through the use of a hall sensor and a magnet positioned on opposite sides of the shell. Together they create a magnetic field that is not disrupted by sand. The sensor outputs a real-time voltage signal that is directly proportional to the magnetic field as it changes due to gape movements.<sup>47, 57, 58</sup> Inferring changes in gape can easily be done both by observation and sensors but unfortunately the mussel's rigid shell makes it challenging to detect heart beats.

A lot of research that has been done to detect heart rates is done using invasive methods, but new technology has shown its ability to identify changes in mussel heart rate in a noninvasive technique. Initially, the heart rate was determined by carefully inserting metal screws into the cardiorenal region that would output electrocardiogram recordings, showing the heart rate. The metal screws had to be precisely positioned into the cardiorenal region, otherwise they would penetrate life-threatening body tissue.<sup>50</sup> As a

result, researchers tried to identify noninvasive techniques to detect their heart rate. One solution was using optical sensors and IR illumination to monitor changes in cardiac muscle volume. Optical sensors are able to detect changes in volume (heart contractions) through variations in the amount of detectable light.<sup>59</sup> Similarly, research has shown that a light emitting diode (LED) coupled with a phototransistor can detect the heartbeat of the mussel.<sup>60</sup>

### 2.3 Using Mussels Gape Responses to Model Dynamic Ecosystems

With ecosystems being a mix of balancing and reinforcing loops, simulation models are helpful tools to analyze and understand ecological systems and fluctuations in biogeochemical cycles.<sup>61</sup> In terms of mussels, a lot of models around their ecosystem processes are focused on budgeting, if mussels filter a known amount of volume they will produce x amounts of feces, pseudofeces, and excrete a certain amount of ammonia.<sup>41</sup> However, none of the models or predictions look at the dynamic impact it has on the ecosystem. Fortunately, systems-based software is now becoming available that enables researchers to develop dynamic ecological systems models.<sup>62</sup> With an easy-to-use, graphical icon-based interface, STELLA is becoming a commonly used modeling program.<sup>63</sup>

STELLA (isee systems, inc., Lebanon, New Hampshire) is an object-oriented software package that uses stocks and flows to model dynamic systems. Stocks represent a reservoir of material that increases or decreases throughout the simulation. Flows go in and out of stocks that lead to clouds that represent sources or sinks. The rate at which the reservoir fluctuates is influenced by converters, which represents the relationships between the modeled elements. These values can be constants, mathematical or graphical functions, and data sets.<sup>64</sup> This research will use known adaptations in physiological behavior and excretion rates to model changes in overlying ammonium concentrations.

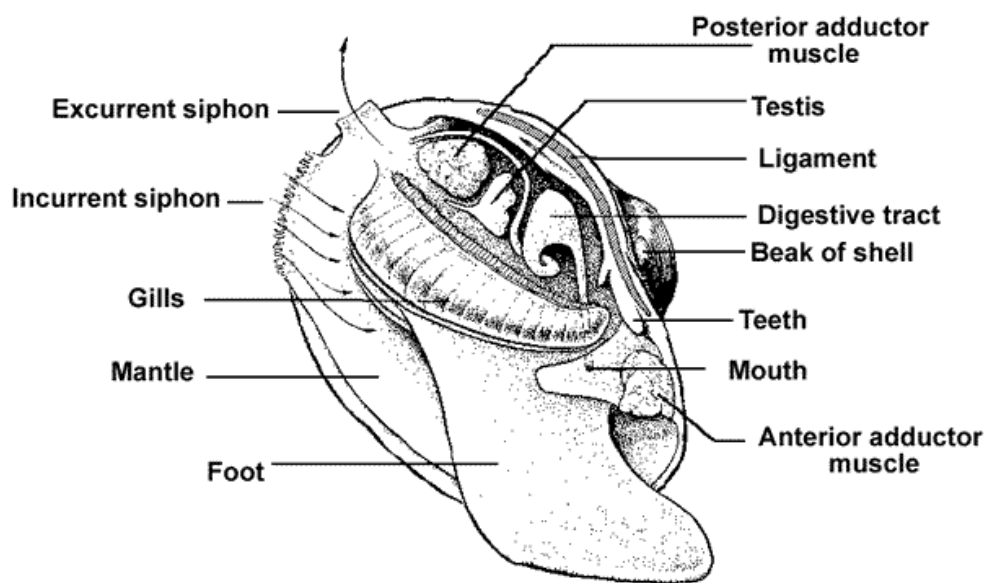


Figure 2.1 Freshwater mussels' typical anatomy<sup>65</sup>

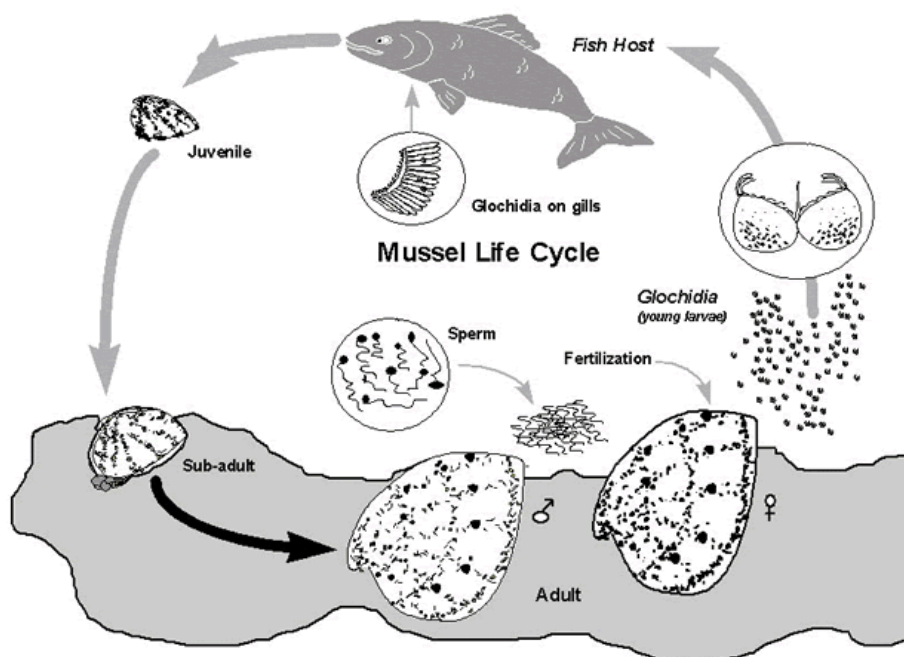


Figure 2.2 Reproductive life cycle of mussels<sup>66</sup>



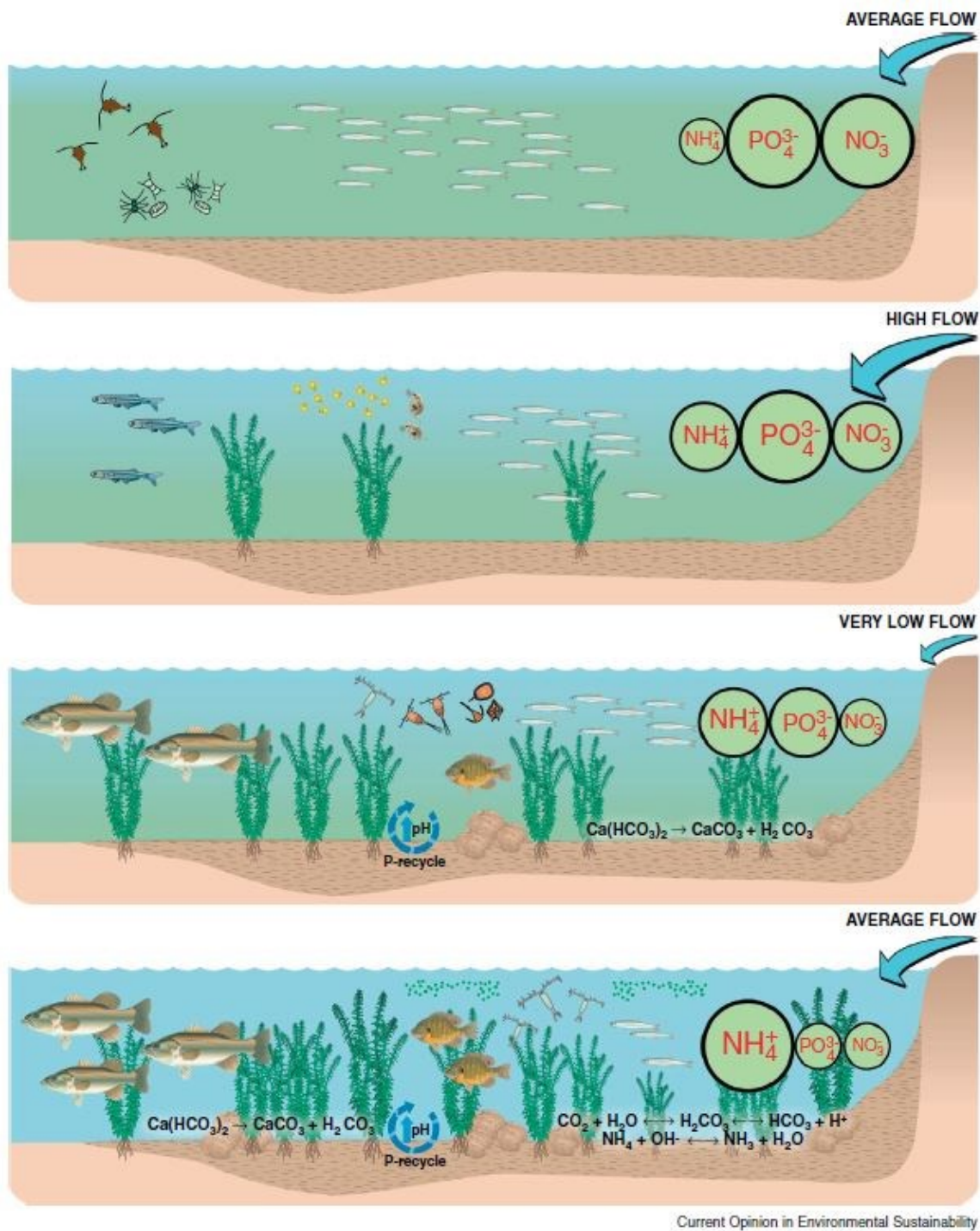


Figure 2.3 Accumulation of excess nutrients in aquatic ecosystems during different flow conditions.

## CHAPTER 3

### MATERIALS AND METHODS

This chapter provides details about the materials and methods used during this study. It describes the experimental mussel habitats, the electronic sensors used to detect changes in physiological behavior, and the equipment and tests used to analyze changes in water quality. All laboratory experiments were conducted at the University of Iowa Water Treatment Plant.

#### 3.1 Mussel Collection and Transitory Habitat

In our study, *Lampsilis cardium*, commonly known as the plain pocketbook mussel, were evaluated to see how excretion rate, heart rate, and gape response were influenced by changes in phytoplankton concentrations. All of the freshwater mussels used for this study were collected from a mussel bed in the Iowa River. The Iowa River runs along 1<sup>st</sup> Avenue in Coralville, IA and the mussel bed is located south of the roller dam on the east bank-(Figure 3.1). The river bottom where the mussel bed is located, is made up of coarse material with patches of cobble. The mussels were removed from the substrate manually and with the assistance of kick nets. After collection, the mussels were transported and kept in a transitory mesocosm(Figure 3.2). The transitory mesocosm functioned not only as a holding tank, but as an ideal habitat for the mussels that provided them with valuable nutrients when experiments were not being conducted. Water was changed on a regular basis and there was an ample food source.

#### 3.2 Mussel Mesocosm

Between October 2014 and January 2015, three experiments were conducted in no-flow mesocosms. Two experiments (experiments 1, 2A, and 2B) were conducted in rectangular mesocosms (61 x 61 x 61), (Figure 3.3). To decrease the volume of the system, one experiment with two trials, 3A and 3B, was conducted in approximately a 10

L microcosm (Figure 3.4). When experiments were not going on, mussels were returned to a transitory mesocosm. No experiments were ever conducted in the transitory mesocosm.

To simulate normal conditions, the controlled variables were: substrate, light, temperature, and mixing. The bottom three inches of both the micro and mesocosms were lined with sand obtained from River Products Co. in Iowa City. To ensure that there was no bacterial growth in the experimental tanks, the sand was washed with water from ion exchange tanks (Hausers Water Systems). All mesocosm were illuminated with one overhanging 1000-watt solar simulator (Sunlight Supply, Inc, Vancouver, WA). Bucket heaters (Allied Precision 742G Bucket Heater) rested on the substrate of each mesocosm. The water temperature in each mesocosm was maintained at 70° Fahrenheit by a JBJ True Temp Digital Heater Controller (TT-1000). Depending on the experiment, the mixing of the overlying water was done using two methods. In the rectangular mesocosms, mixing was generated from a 75 gal h<sup>-1</sup> submersible pump (EcoPlus 66, Sunlight Supply). In the 10 liter microcosm, an aquarium air pump attached to a round diffuser stone was used for mixing (110V Aquaculture Aquarium Air Pump).

### 3.3 Water Chemistry Sensing

During the experiments, water quality was monitored using three different techniques, : real-time sensors, colorimetric tests, and fluorescence. Hydrolab multi-probe sondes (n=5, model DS5, Hach Chemical Company, Loveland, Colorado) were used to measure real time (1.5 minute intervals) water chemistry changes in the overlying water. Specifically, the multi-probe sondes measured the NH<sub>4</sub><sup>+</sup> (ion selective electrode), temperature (variable resistance thermistor), pH (KCl impregnated glass bulb), and conductivity (fixed potential electrodes). Prior to each experiment, NH<sub>4</sub><sup>+</sup>, pH, and conductivity probes were calibrated using Hach standards. During experiments, periodic grab samples were taken to monitor both ammonium and phytoplankton concentrations in

the overlying water. Hach ammonia ultra-low Test N Tube kits (TNT 830 ULR, Loveland, Colorado) were used as a second source of measuring  $\text{NH}_4^+$  concentrations. Phytoplankton concentrations were determined by using a fluorimeter (Trilogy Laboratory Fluorometer Model 7200-000, Turner Design). Higher fluorescence (NTU) values were associated with increased phytoplankton concentrations.

### 3.4 Heart Rate and Gape Sensors

All of the electronic sensors used to monitor changes in the physiological behavior of mussels were modeled after previously conducted research. The Hall sensor, used to monitor changes in gape angle, was modeled after findings described in literature.<sup>58</sup> Using electrical wires, the Hall sensor was directly connected to an eight channel data acquisition starter kit (DATAQ Instruments, Model DI-149). Using a USB connection, the DATAQ Instrument sent real-time gape changes to a laptop. WinDaq software recorded the data and enabled the conversion to Microsoft Excel. Similar to the Hall sensors, the heart rate sensor was modeled after previous research.

The heart rate sensor was modeled after research that used a noninvasive technique.<sup>56</sup> The heart rate sensor was made up of an infrared (IR) LED sensor that was firmly held against the shell of the mussel. It is vital that the LED sensor remained in contact with the shell as it enabled the light to pass through the shell and reflect off internal organs without any noise. The reflected light was then detected by a phototransistor, sampled by an analog-to digital converter, and analyzed by a microcontroller. The heart rate sensor was connected to a breadboard that transferred the signal to a computer. Tera Term (Tera Term Project, T. Teranishi) software recorded the raw real-time results from the sensor-(figure 3.5) before being automated with MATLAB to show a visual representation of the heart rate-(Figure 3.6).

The Hall sensor and the heart rate sensor were attached in specific spots using Gorilla Epoxy (The Gorilla Glue Company)-(Figure 3.7). This two-part epoxy had to be

mixed before applying to the surfaces. All of the sensors were held in place with applied pressure for 30 minutes and an extra five minutes without pressure before the mussel was submerged back into water. The hall sensor was positioned on the opposite sides of the mussel's bivalve from a rare earth magnet-(Figure 3.8). Instead of gluing the heart rate sensor to the shell, a battery clip (Digi-Key, PN BK-5044-ND) held the LED in contact with the shell but also enabled the sensor to be moved or replaced if there were software issues. Depending on the ability to obtain a good heart rate signal-(Figure 3.5) the battery clip was glued near the hinge of the mussel (figure 3.9)

### 3.5 Experiment 1: Ammonium Excretion, Heart Rate, and Gape response by Two Mussels in a 93 Liter Mesocosm

Experiment 1 was conducted in two rectangular mesocosms, a control tank and a mussel tank. Both mesocosms were filled up with 93 liters of water from ion exchange tanks. One day before the experiment began, a bucket heater was placed in each experimental mesocosm to ensure the temperature was at 70° Fahrenheit. Two mussels were then transferred into the mussel mesocosm but only one of mussels had electronic sensors attached. For four days, mussels had limited food availability with periodic grab samples ensuring these conditions. On the 5<sup>th</sup> day, 60 mL of Phyto-Feast (Reef Nutrition, Campbell, CA) was added to both tanks. To guarantee that the system became well mixed, a stirring stick was used to mix the overlying water immediately after the addition of Phyto-Feast. Grab samples were taken approximately every 30 minutes, testing for both  $\text{NH}_4^+$  and phytoplankton concentrations. Other than grab samples, the mesocosm were left untouched for 28 hours. Upon the completion of the experiment, both mussels were returned to the transitory tank and the experimental tanks were cleaned prior to the next experiment.

### 3.6 Experiment 2: Ammonium Excretion, Heart Rate, and Gape Response by One Mussel in a 61 Liter Mesocosm

After Experiment 1, it was concluded that the next experiment would be conducted with only one mussel and a smaller volume of water. Therefore, two mesocosm were filled up with 61 liters of water from ion exchange tanks. As in Experiment 1, the bucket heater was added to each tank one day prior to the beginning of the experiment. The first four days consisted of limited food availability, but on the fifth day, 50 mL of Phyto-Feast was added to both mesocosms. To ensure a well-mixed mesocosm, a stirring stick was used immediately to stir the overlying water. Grab samples monitored changes in  $\text{NH}_4^+$  and phytoplankton concentration approximately every hour and a half after the food spike. Experiment 2 consisted of two trials, 2A and 2B. Experiment 2A lasted 66 hours (2.7 days) while Experiment 2B lasted for 40 hours (1.7 days). After both trials, the mussel was returned to the transitory mesocosm and both experimental mesocosm were cleaned.

### 3.7 Experiment 3: Ammonium Excretion, Heart Rate, and Gape Response by One Mussel in a 10 L Microcosm

Trying to ensure that the mussel was in close proximity to the sensor, Experiment 3 (3A and 3B) was conducted in cylindrical microcosms with diameters of approximately 29 cm. Both microcosm were filled up with 10 liters of water from ion exchange tanks. Due to limited space, a bucket heater was not added to the microcosms. Instead, both microcosms were partially submerged in water bath where the temperature was controlled with bucket heater (Figure 3.4). One mussel was placed in a microcosm for four days with limited food availability. On the fifth day, 10 mL of Phyto-Feast was added to each microcosm. To ensure each microcosm became well-mixed, a stirring stick was used to mix the overlying water. Immediately after the spike, grab samples were taken every hour and a half to monitor changes  $\text{NH}_4^+$  and phytoplankton concentrations.

Experiment 3A lasted for 42 hours while Experiment 3B lasted for 40 hours. After each trial, the mussel was returned to the transitory tank and the microcosm cleaned.

### 3.8 Data Analysis

Prior to data analysis,  $\text{NH}_4^+$  concentrations from the multi-probe sondes were normalized with grab samples from the overlying water. Using the same grab sample for both tanks,  $\text{NH}_4^+$  concentrations were normalized at the beginning of the experiment and immediately after the addition of Phyto-Feast. By normalizing the data for both tanks, it could be determined if the difference in  $\text{NH}_4^+$  concentrations were statistically significant. Using SigmaPlot 13 (Systat Software Inc) built in analysis functions, statistical significance was tested using Mann-Whitney Ranks Sum Test. Instead of testing  $\text{NH}_4^+$  concentrations for the entire experiment, statistical significance was only looked at following the addition of Phyto-Feast.





Figure 3.1 Location of mussel bed used for this research in Iowa River (Image from Google Earth).



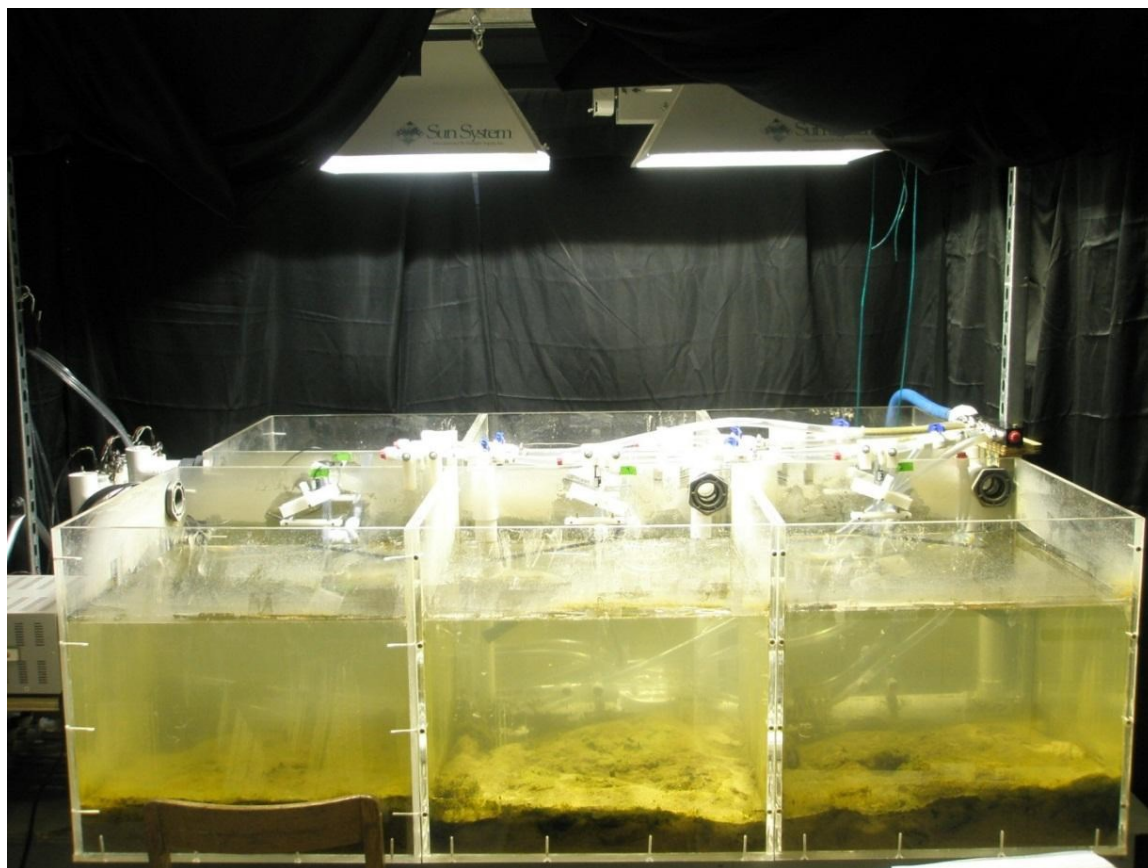


Figure 3.2 Six experimental mesocosms used for this research.

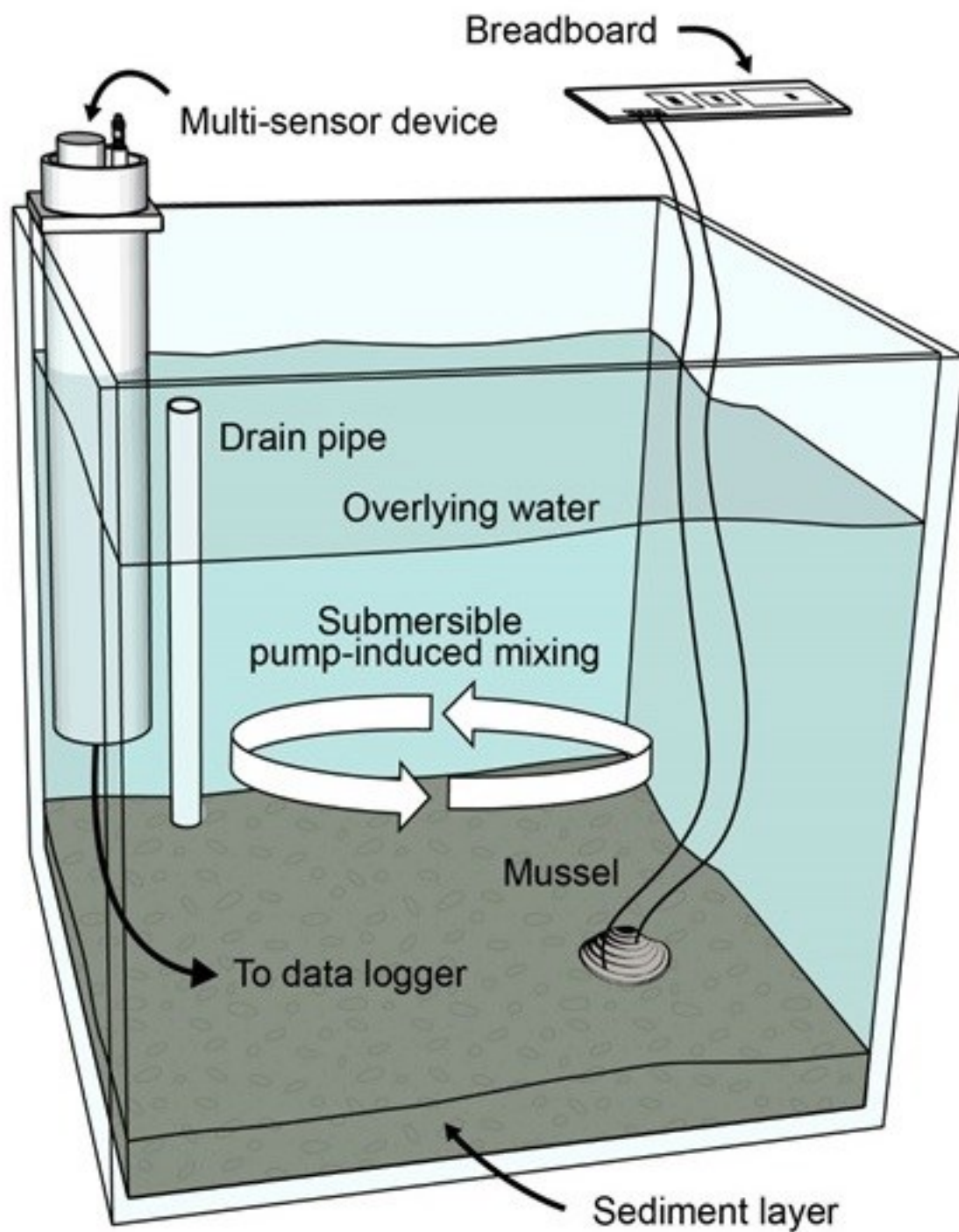


Figure 3.3 Digital representation of the experimental setup for experiments 1, 2A, and 2B.

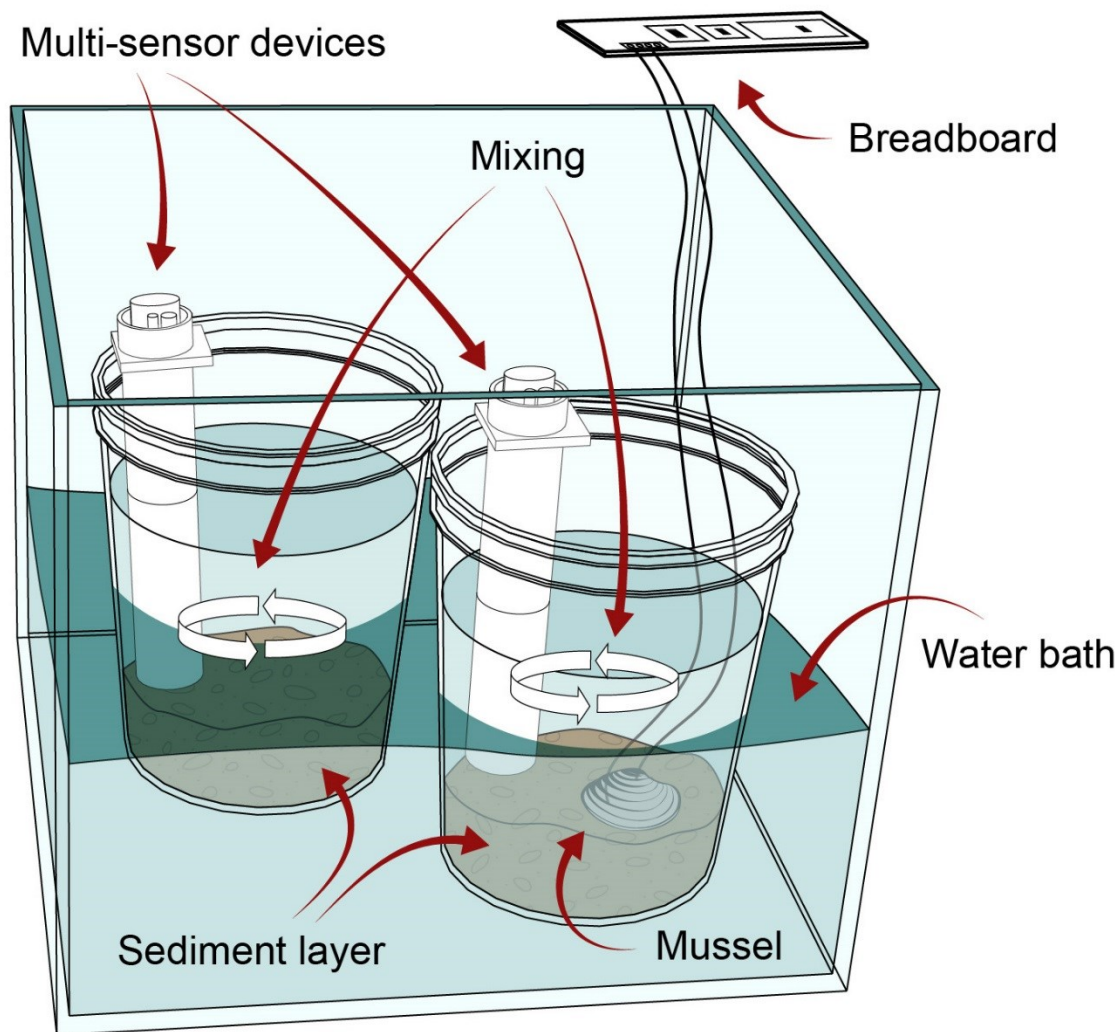


Figure 3.4 Digital representation of 10 liter microcosm for experiment 3 (3A and 3B).

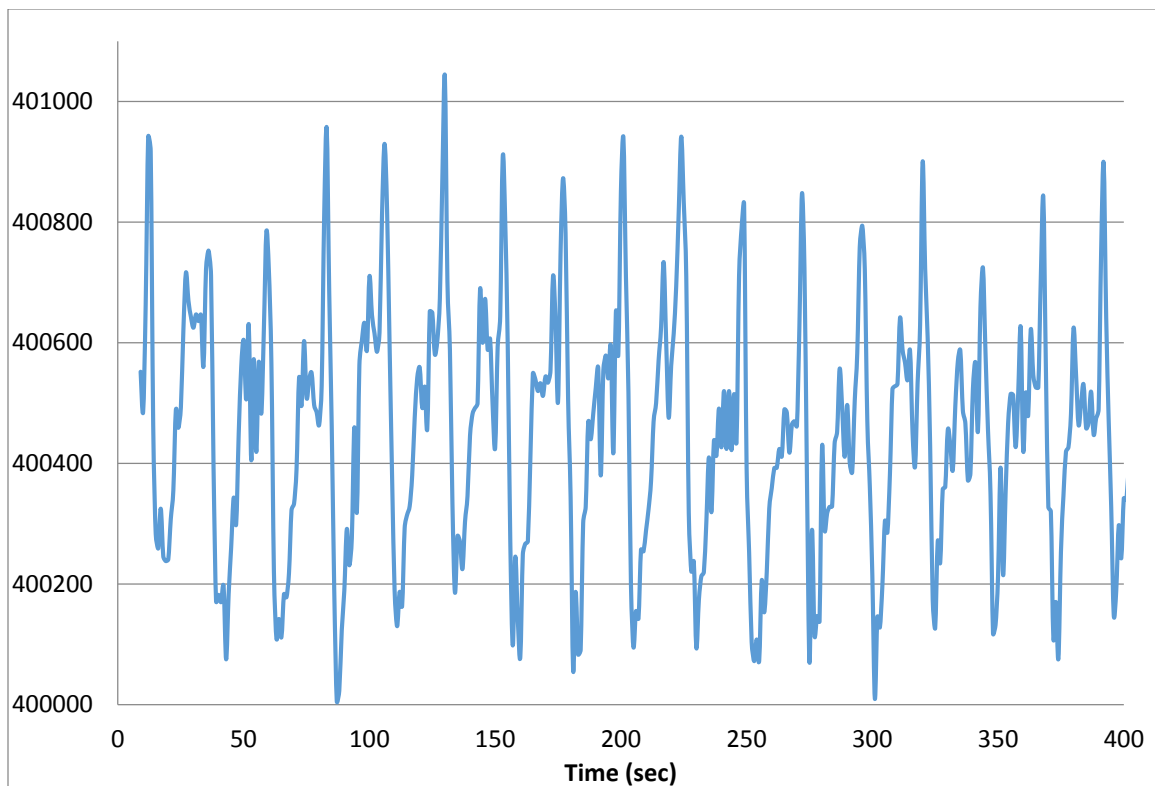


Figure 3.5 Sampled heart rate data to determine sensor placement on the mussel. The y-axis is a unitless value outputted by Tera Term.

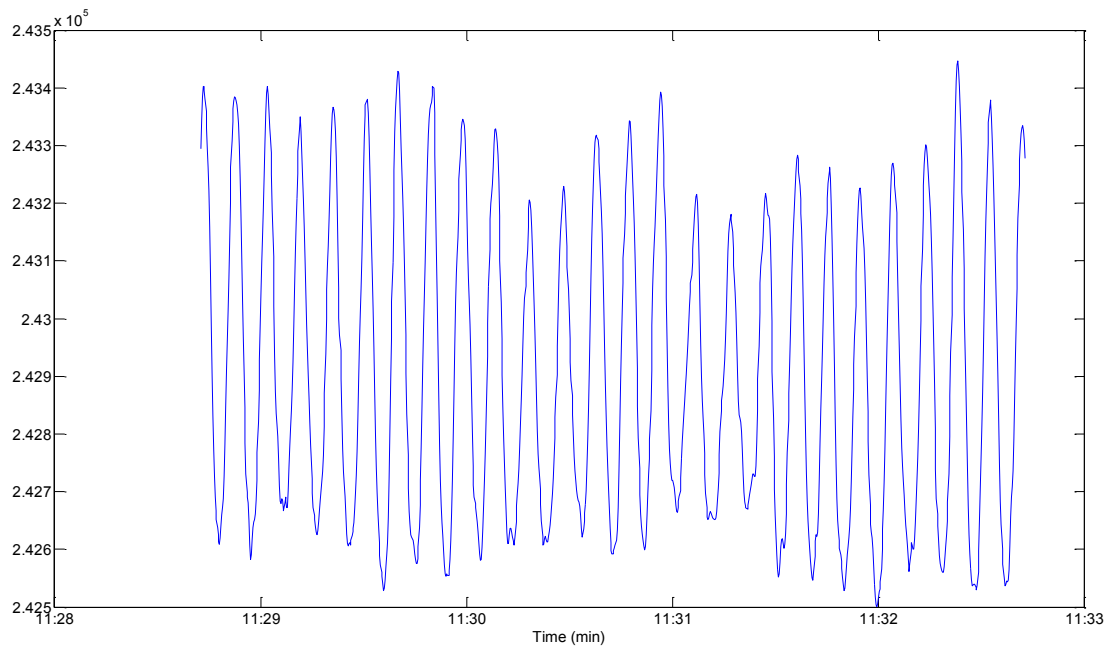


Figure 3.6 Raw heart rate from Tera Tram after being automated by MATLAB script.  
The y-axis is a unitless value.

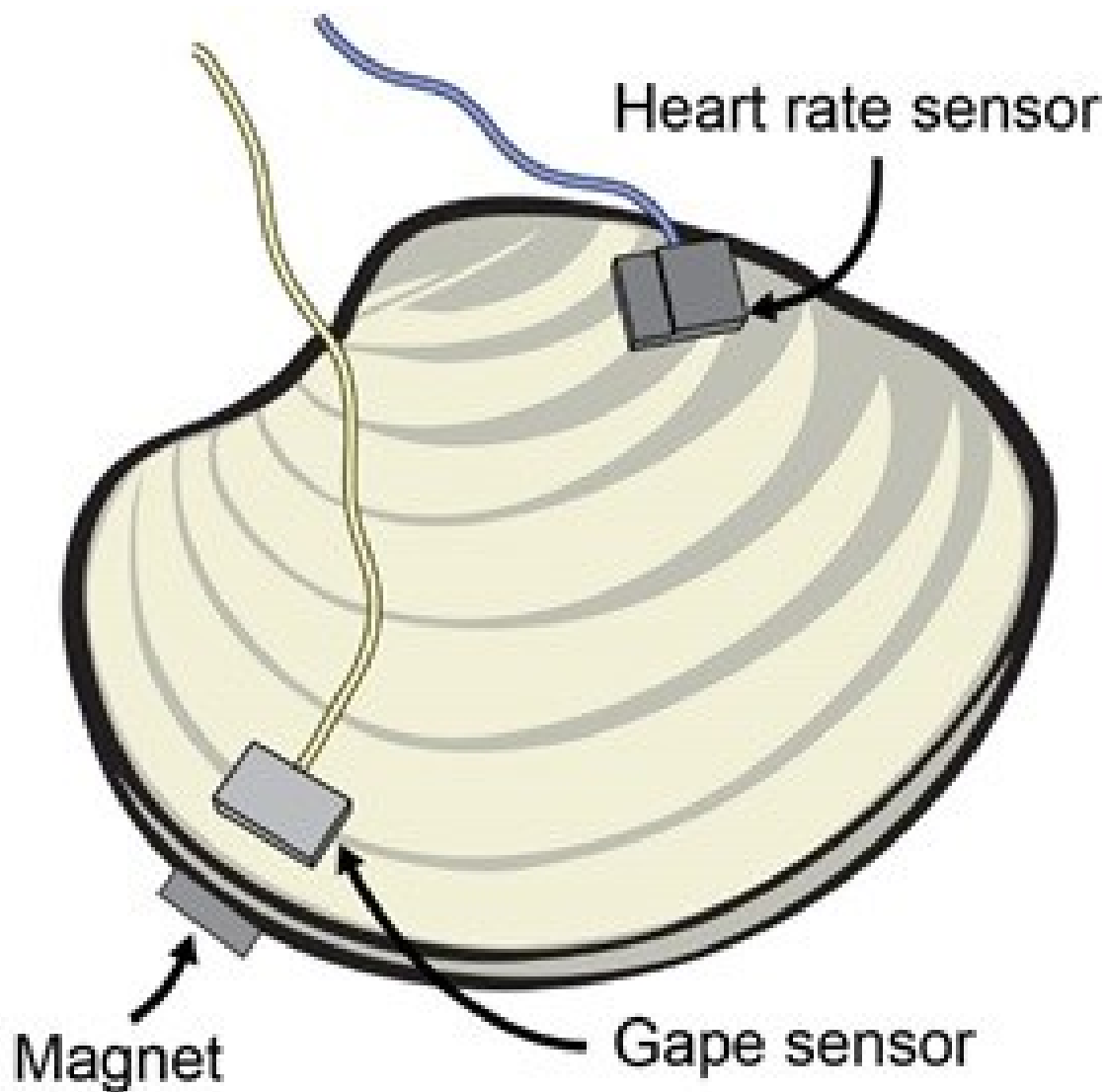


Figure 3.7 A digital image of electronic sensor placement on freshwater mussels.





Figure 3.8 Experimental placement of hall sensor and rare earth magnet on freshwater mussel.

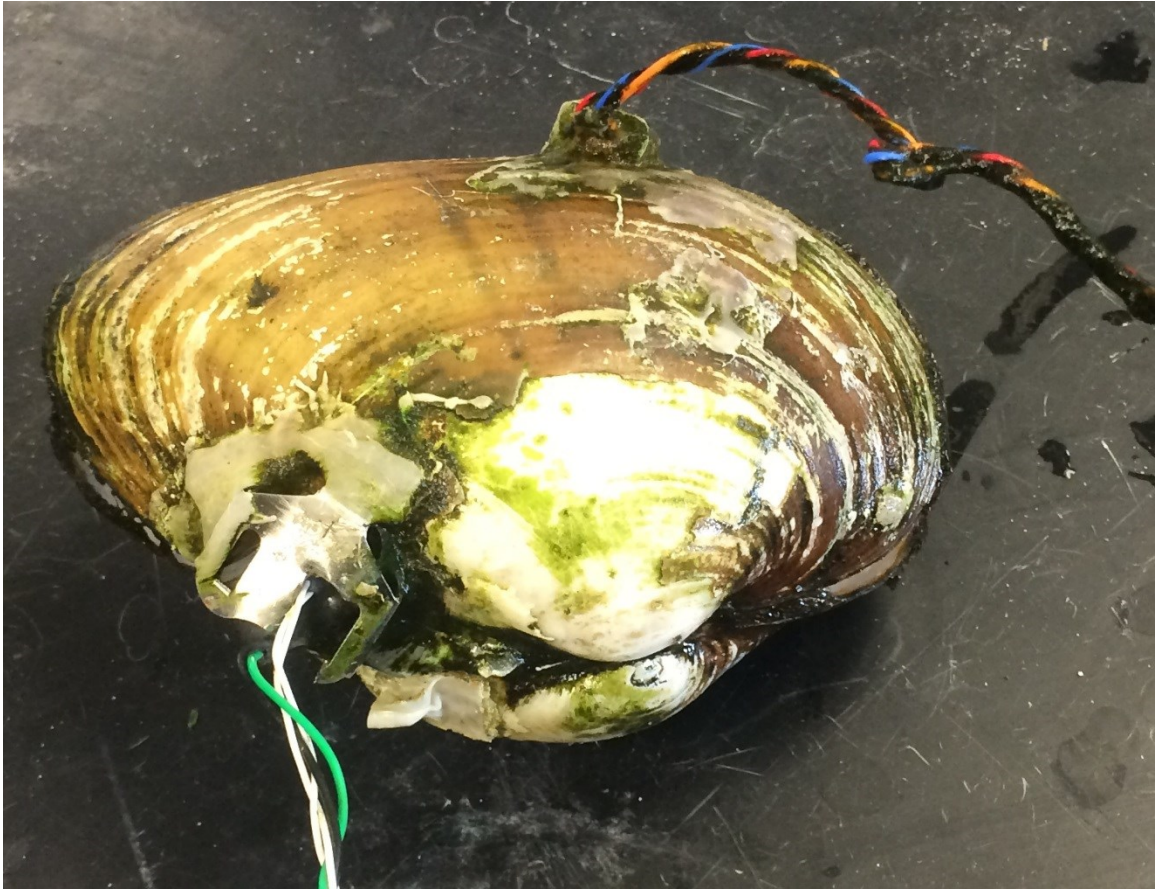


Figure 3.9 Experimental placement of battery clip and heart rate sensor near the hinge of the mussel.



CHAPTER 4  
AMMONIUM EXCRETION, HEART RATE, AND GAPE RESPONSE  
BY MUSSELS IN A MESOCOSM

This chapter will present the results from experiments 1, 2A, and 2B, showing increases in phytoplankton impact mussel  $\text{NH}_4^+$  excretion, heart rate and gape position following a period of limited food availability. This is followed by a comparison of  $\text{NH}_4^+$  mass fluxes for the mussel and control microcosm.

4.1 Results: Experiment 1

Prior to the phytoplankton addition,  $\text{NH}_4^+$  concentrations, gape position, and heart rate were relatively stable. After the addition of Phyto-Feast,  $\text{NH}_4^+$  concentrations increased and heart rate went through sudden increases and decreases while the mussel gape went through one closing event (Figure 4.1). Figure 4.1A shows the change in phytoplankton concentrations (RFU) for both the mussel and the control tank. Figure 4.1B shows the changes in  $\text{NH}_4^+$  concentration ( $\text{mg-N L}^{-1}$ ) for both the mussel and the control mesocosm. The changes in the mussel mesocosm are represented by the shaded region while the control mesocosm is represented by the red line. In Figure 4.1C, the left y-axis shows the mussel gape position (open or closed) and the right y-axis shows the mussel heart rate (bpm). The changes in gape position are shown by the shaded region while the heart rate is represented by the red line. All of the graphs are over the range of 26 hours on the x-axis, with the first ten hours being the end of low food availability.

During the five-day, low food availability period it was expected that the phytoplankton concentrations in the overlying water would be lower when compared to the concentrations after the addition of Phyto-Feast. Throughout the low food availability period, the phytoplankton concentrations in the control and mussel mesocosms averaged 168 and 170 RFU. With the addition of Phyto-Feast at hour 10, the phytoplankton concentration suddenly increased to 5,170 RFU in the control mesocosm and 5,380 RFU

in the mussel mesocosm (Figure 5.1A). Even with submersible pumps, the relative phytoplankton concentrations decreased exponentially to 584 RFU in the control mesocosm and 820 RFU in the mussel mesocosm during a time span of approximately 14.3 hours. Translating to a phytoplankton first-order settling rate of  $0.16 \text{ hr}^{-1}$  for the control mesocosm and  $0.13 \text{ hr}^{-1}$  in the mussel mesocosm. As a result of increases in phytoplankton concentrations at the end of the low food availability period,  $\text{NH}_4^+$  concentration increased in both mesocosms.

To determine changes in  $\text{NH}_4^+$  concentration attributed to mussel excretion, a comparison was made between the control mesocosm and the mussel mesocosm. The Phyto-Feast addition caused an immediate increase in  $\text{NH}_4^+$  concentration from approximately 0.5 to 0.57 mg-N/L in the control and mussel mesocosm (Figure 4.1B). The  $\text{NH}_4^+$  concentration remained relatively stable in both mesocosms until a rise and fall in  $\text{NH}_4^+$  concentrations, spanning 1.8 hr, occurred in the mussel mesocosm only. Initially, the  $\text{NH}_4^+$  peak in the mussel mesocosm, 12.5 hr after the Phyto-Feast addition, was presumed to be a result of phytoplankton digestion followed by an excretion event. But, this assertion could not explain the subsequent  $\text{NH}_4^+$  concentration decrease since volatilization and/or biological oxidation of  $\text{NH}_4^+$  would be relatively slow. However, the calculated mass flux for the control mesocosm was  $0.02 \text{ mg-N hr}^{-1}$  and  $0.15 \text{ mg-N hr}^{-1}$  for the mussel mesocosm during the  $\text{NH}_4^+$  rise indicating higher excretion rates attributed to mussels (Figure 4.2). The  $\text{NH}_4^+$  concentrations were not statistically different between the control and mussel mesocosm.

The objectives of this research were to measure and correlate changes in mussel heart rate and gape in response to changes in phytoplankton and  $\text{NH}_4^+$  concentrations in the overlying water (Figure 4.1C). At the end of the low food availability, the gape position was open. The gape closed approximately 1.3 hours after the addition of Phyto-Feast and remained closed for 8.5 hours before re-opening. While the gape went through only one position change, the heart rate responded differently following the Phyto-Feast

addition. The mussel heart rate was approximately 7.4 beats per minute (bpm) at the beginning of the experiment (Figure 1C) before dropping to 6.9 bpm right before the gaping event. Following the gaping event, the heart rate oscillated between 6.5 and 7.8 bpm before rapidly decreasing to 5.3 bpm 20 hours into the experiment. This was followed by a rapid heart rate increase to over 8 bpm after the gape reopened. Overall, the mussel had an average heart rate of  $7 \pm 0.7$  bpm.

## 4.2 Results: Experiment 2

After Experiment 1, two changes were made to the experimental procedure. First, experiments would only be conducted with one mussel. With both mussels not connected to sensors, it was impossible to identify how  $\text{NH}_4^+$  concentrations were influenced by changes in gape position and heart rate. Similarly, using two mussels made it impossible to accurately determine individual mussel excretion rates. Secondly, the volume of the overlying water was decreased to strengthen the ability to detect changes in  $\text{NH}_4^+$  concentrations.

### 4.2.1 Experiment 2A

A visual representation of how phytoplankton concentrations,  $\text{NH}_4^+$  concentrations, heart rate, and gape position changed over the course of 66 hours in Experiment 2A can be seen in Figure 4.3. This experiment was conducted over a longer period of time than the other experiments due to a gaping event not happening immediately after the addition of Phyto-Feast. Figure 4.3A shows changes in phytoplankton concentrations (RFU) in both the mussel and control mesocosm. Figure 4.3B shows the changes in  $\text{NH}_4^+$  concentrations ( $\text{mg-N L}^{-1}$ ) for both the control and mussel mesocosm. Both of these figures show changes in the mussel mesocosm with a brown filled region while the control mesocosm is represented by a red line. Figure 4.3C shows both changes in mussel gape and the mussel heart rate. The mussel gape position is represented by the brown filled region with which position shown on the left y-axis (open

or closed). The mussel heart rate is indicated by the red line with right y-axis showing the beats per min (bpm). All of the graphs in figure 4.3 are represented by time in hours on the x-axis with tick marks every four hours. Figure 4.3 shows that all four of the variables responded differently throughout the experiment.

The low food availability period ensured there were minimal phytoplankton concentrations in the overlying water. As a result, the phytoplankton concentrations in the overlying water average 165.4 RFU in the control mesocosm and 113 RFU in the mussel mesocosm. Immediately after the addition of Phyto-Feast at 14.2 hours, the phytoplankton concentrations jumped to 4,447 and 4,434 RFU in the control and mussel mesocosm respectively (Figure 4.3A). Over the next 33 hours, the phytoplankton concentrations decreased exponentially to 525 RFU in the control mesocosm and 293 RFU in the mussel mesocosm which translates to a first-order settling rate of  $0.06 \text{ hr}^{-1}$  for the control mesocosm and  $0.08 \text{ hr}^{-1}$  for the mussel mesocosm. Similar to phytoplankton concentrations,  $\text{NH}_4^+$  concentrations jumped after the addition of Phyto-Feast.

One of the objectives of this study was to measure changes in overlying water  $\text{NH}_4^+$  concentration resulting from phytoplankton decay by bacteria and excretion by mussels. During the low food availability period, the first 14.2 hours,  $\text{NH}_4^+$  concentrations for both mesocosms were stable at  $0.03 \text{ mg-N L}^{-1}$  (Figure 4.3B). The addition of Phyto-Feast caused an immediate jump in  $\text{NH}_4^+$  concentrations to  $0.1 \text{ mg-N L}^{-1}$  for both mesocosms. Following the addition,  $\text{NH}_4^+$  concentrations stayed relatively stable at  $0.1 \text{ mg-N L}^{-1}$  before showing a small increase in the mussel mesocosm. The increase in the mussel mesocosm spanned 5 hours before returning to a relatively stable conditions at hour 42. There were no noticeable changes in  $\text{NH}_4^+$  concentration for either mesocosm until hour 55. Over the next 9 hours,  $\text{NH}_4^+$  concentrations increased to  $0.11 \text{ mg-N L}^{-1}$  in the control mesocosm while concentrations in the mussel mesocosm reached  $0.14 \text{ mg-N L}^{-1}$ . The initial increase in  $\text{NH}_4^+$  concentrations at hour 42 was attributed to a small, but prolonged excretion event while the increase in  $\text{NH}_4^+$  concentrations at hour 55

were not be attributed to only mussel excretion. With increases in both mesocosm happening at hour 55, part of the increase of  $\text{NH}_4^+$  in the mussel mesocosm would be attributed to hydrolysis of organic nitrogen due to phytoplankton decay. With this experiment going for a longer period, compared to Experiment 1, the assertion that  $\text{NH}_4^+$  concentration would increase due to phytoplankton decay is applicable. With the first  $\text{NH}_4^+$  increase in the mussel mesocosm hypothesized as an excretion event, it was important to understand what was happening with the gape and heart rate.

Different from Experiment 1, the gape position was not constant throughout the low food availability period. Initially, the mussel gape was in the open position before going through two opening and closing events at hours 2 and hour 7 (Figure 4.3C). During the initial gaping event, the gape closed for approximately 4.2 hours, while during the second gaping event it closed for approximately 5.4 hours. Instead of showing a gape response after the addition of Phyto-Feast, the mussel gape remained open for the next 25.7 hours with minimal movements. At hour 38, the mussel gape position closed for 7.6 hours before re-opening. While gaping events two and three were similar to each other, the heart rate showed different responses for the two position changes.

Throughout the first two experiments, the mussel heart rate started to show a trend of being influenced by changes in gape position. During the first two gaping events, the heart rate remained stable at 6.3 bpm before slowly increasing to 7.5 bpm at the end of the second gaping event. During the 25.7 hour span where the mussel gape remained open, the heart rate showed small fluctuations between 7.5 and 7.2 bpm. Similar to the heart rate increasing to 7.5 bpm before the gape re-opened at end of the second gaping event, the heart rate decreased before the mussel gape began to close at hour 38. At hour 43, over halfway through the gape closure, the heart rate had decreased to approximately 4.7 bpm. The heart rate then increased to 6.7 bpm as the gape reopened. For the remainder of the experiment, the heart rate fluctuated between 6.7 and 6 bpm.

Unfortunately, over the final 18 hours, the gape sensor experienced technical issues and

there was no data to compare it to. Over the entire experiment, the mussel had an average heart rate of  $6.6 \pm 0.7$  bpm.

#### 4.2.2 Experiment 2B

Figure 4.4 shows a visual representation of how phytoplankton concentrations,  $\text{NH}_4^+$  concentration, heart rate, and gape response changed over the course of 40 hours in Experiment 2B. All of the figures are represented by time in hours on the x-axis with tick marks every four hours. Figure 4.4A shows changes in phytoplankton concentrations (RFU) of the overlying water in both the mussel and control mesocosm. Figure 4.4B shows the changes in overlying water  $\text{NH}_4^+$  concentrations ( $\text{mg-N L}^{-1}$ ) for both the control and mussel mesocosm. Both of these graphs represent the changes in the mussel mesocosm with a brown filled region while the control mesocosm is represented by a red line. Figure 4.4C shows both the changes in gape position and the heart rate. Gape position is represented by the brown filled region with which position indicated on the left y-axis (open or closed). The heart rate is denoted by the red line with right y-axis showing the beats per min (bpm). Figure 4.4 indicates that phytoplankton and  $\text{NH}_4^+$  concentrations do not change until after the Phyto-Feast spike but both heart rate and gape position were changing prior to the food spike.

During the low food availability period, the overlying water had an average phytoplankton concentration of 135 RFU for the control mesocosm while the mussel mesocosm had an average of 112 RFU. The addition of Phyto-Feast at hour 6.2 caused the phytoplankton concentrations to jump to 5,173 and 5,530 RFUs in the control and mussel mesocosm respectively (Figure 4.4A). The phytoplankton concentrations in both tanks decreased exponentially over the span of 32 hours until it reached 610 RFUs in the control mesocosm and 665 RFUs in the mussel mesocosm which translate to a phytoplankton first-order settling rate of  $0.07 \text{ hr}^{-1}$  for both mesocosms. The  $\text{NH}_4^+$

concentrations, like the phytoplankton concentrations, remained stable during the low food availability period.

During the low food availability conditions,  $\text{NH}_4^+$  concentrations were negligible since there was a minimal amount of phytoplankton for the mussel to consume and to decay. Prior to the addition of Phyto-Feast,  $\text{NH}_4^+$  concentrations in both mesocosms were stable at  $0.03 \text{ mg-N L}^{-1}$ . With the addition of Phyto-Feast,  $\text{NH}_4^+$  concentrations jumped to  $0.1 \text{ mg-N L}^{-1}$  at hour 6.2 in both mesocosms (Figure 4.4B). Following the Phyto-Feast addition, the  $\text{NH}_4^+$  concentrations in the control mesocosm stayed relatively stable throughout the entire experiment with no considerable increases or decreases.

Conversely,  $\text{NH}_4^+$  concentration in the mussel mesocosm quickly decreased to  $0.09 \text{ mg-N L}^{-1}$  at hour 9 and remained stable for five hours before linearly increasing to  $0.11 \text{ mg-N/L}$  over the next 31 hours. After the Phyto-Feast spike, the  $\text{NH}_4^+$  concentrations in the mussel tank experienced abrupt decreases followed rapid increases back to a normal trend. These three events are not believed to be attributed to mussel but more sensor error. However, the increase in  $\text{NH}_4^+$  concentrations from  $0.09$  to  $0.11 \text{ mg-N L}^{-1}$  is attributed to an extended excretion event. While  $\text{NH}_4^+$  concentrations in the mussel mesocosm experience subtle changes, gape responses were sudden and irregular.

Unlike phytoplankton and  $\text{NH}_4^+$  concentrations, it was impossible to ensure the gape position remained stable prior to the addition of Phyto-Feast. At hour two, 4.2 hours before the phytoplankton addition, the mussel gape closed for 12.9 hours (Figure 4.4C). However, immediately after the addition of Phyto-Feast, the mussel gape slightly reopened and slowly continued to re-open until abruptly returning to an open position at hour 14.9. The gape position went through small position changes over the next 17.7 hours but nothing substantial. At hour 32.6, the mussel gape closed for 2 hours before slightly reopening for the remainder of the experiment, similar to the gaping event prior to the Phyto-Feast addition. Like gape position, the heart rate was not stable prior to the addition of phytoplankton.

During Experiment 2B, the mussel heart rate was continually changing and was not affected by the addition of Phyto-Feast. Initially the heart rate was at 5 bpm, then increased to approximately 6.4 bpm during the first gape closure of the mussel. However, the heart rate quickly dropped to 4.8 bpm by hour 7.2. The heart remained below 5 bpm for five hours before increasing to 5.5 as the gape reopened. Over the next 17.8 hours, the heart rate average 5.4 bpm, but went through small up and down periods before increasing to 5.8 bpm at hour 32. This was followed by a quick decrease 4.6 bpm by hour 39, which coincides with the gape closing. Both times the mussel closed its gape, the heart rate decreased and remained lower than when the gape was open. Lower than the previous two experiments, the mussel had an average heart rate of  $5.3 \pm 0.4$  bpm.

#### 4.2.3 Ammonium Mass Flux Comparison between Experiment 2A and 2B

Experiment 2A and 2B experienced the same environmental conditions, enabling a direct comparison of the  $\text{NH}_4^+$  mass flux between the trials. The bar graph in figure 4.5 shows a comparison of the mass flux for the mussel and control mesocosm for each trial. The  $\text{NH}_4^+$  mass flux was determined by comparing the  $\text{NH}_4^+$  concentrations immediately following the Phyto-Feast addition with the  $\text{NH}_4^+$  concentration approximately 33 hours after the spike. In Experiment 2A, the control mesocosm had a negligible  $\text{NH}_4^+$  mass flux while the mussel mesocosm had a mass flux of  $0.02 \text{ mg-N hr}^{-1}$ . This resulted in a difference of approximately  $0.02 \text{ mg-N hr}^{-1}$  between the two tanks. Experiment 2B showed similar results. The control mesocosm had an  $\text{NH}_4^+$  mass flux of  $0.01 \text{ mg-N hr}^{-1}$  while the mussel mesocosm had a mass flux of  $0.03 \text{ mg-N hr}^{-1}$ . This resulted in a difference of approximately  $0.02 \text{ mg-N d}^{-1}$ . Comparing the two trials, both mussel tanks had a higher  $\text{NH}_4^+$  mass flux of approximately  $0.02 \text{ mg-N hr}^{-1}$  attributed to excretion events following the addition of Phyto-Feast.



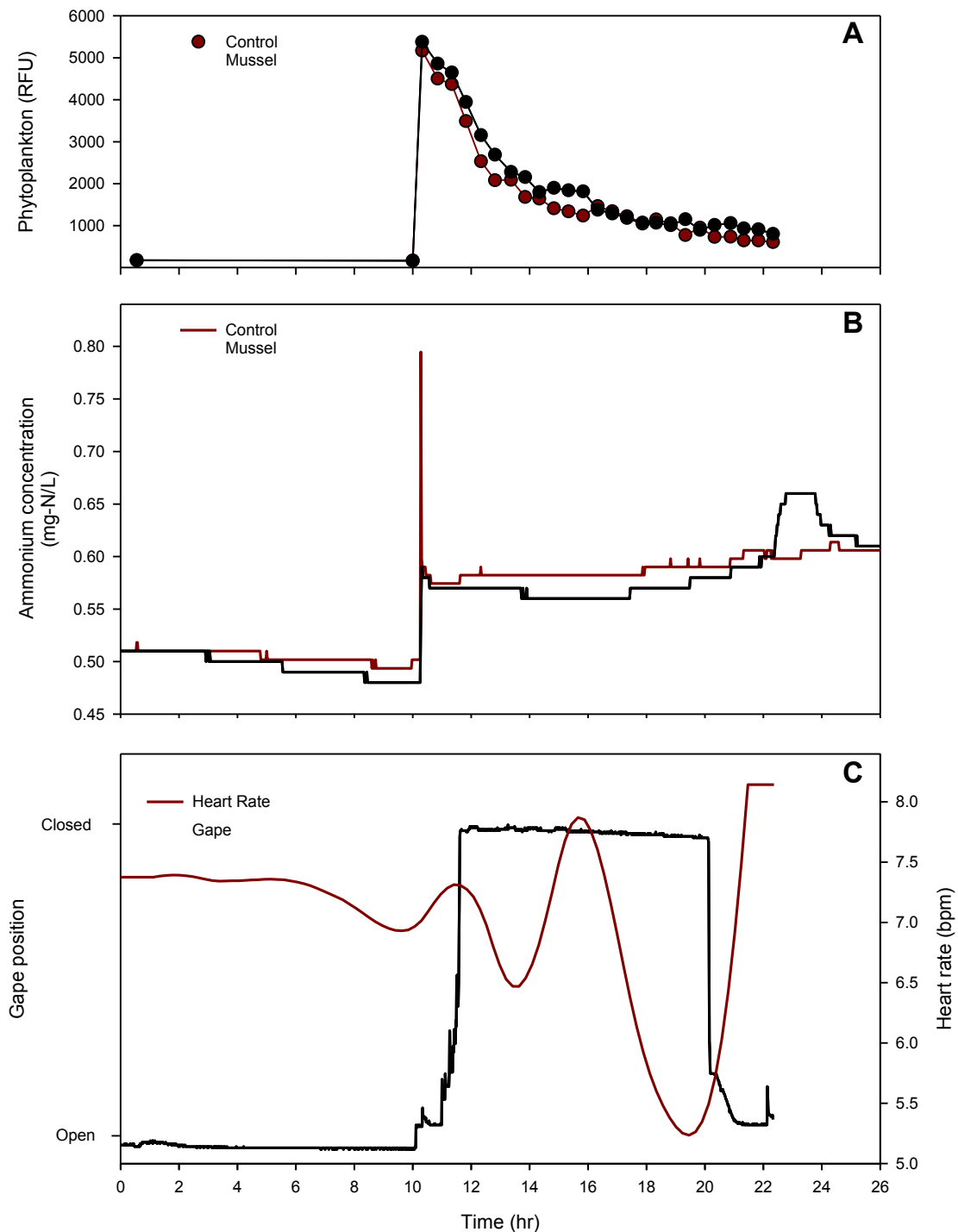


Figure 4.1 Experiment 1 results: (a) phytoplankton concentrations in overlying water, (b) changes in  $\text{NH}_4^+$  concentrations for mussel and control mesocosms ( $\text{mg-N L}^{-1}$ ), and (c) changes in the mussels heart rate (bpm) and gape response (open or closed). The blue dashed lines mark changes in gape position.

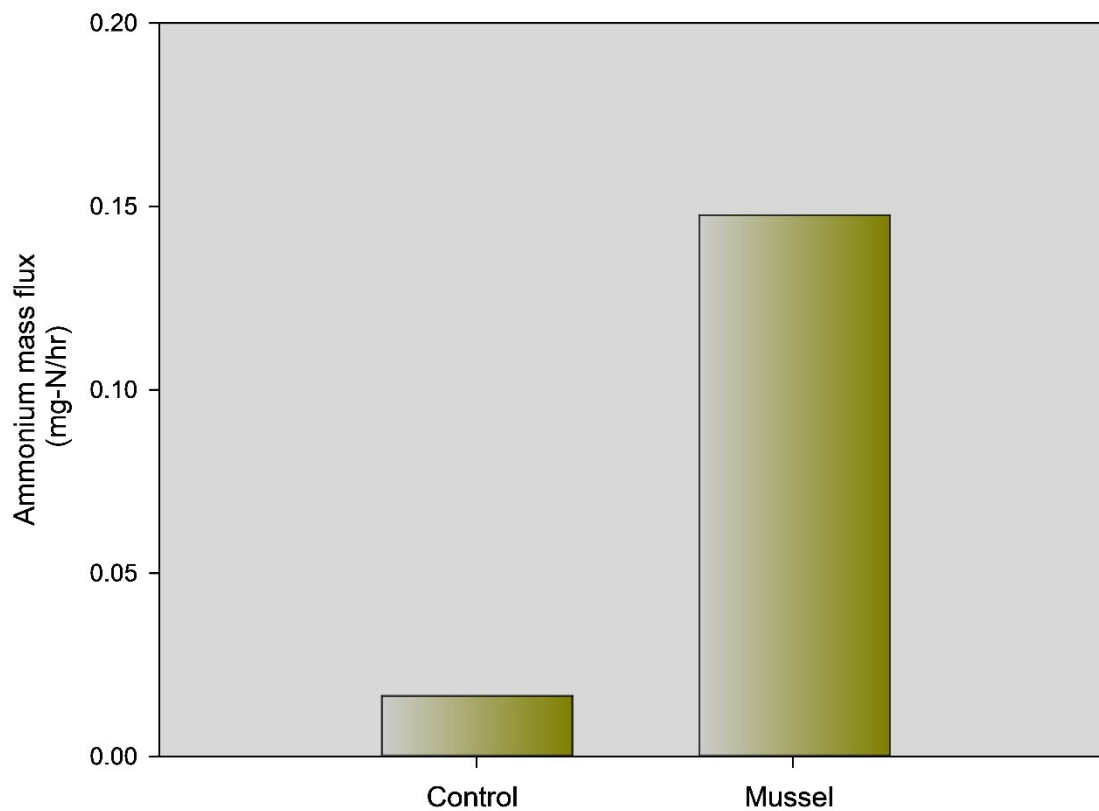


Figure 4.2  $\text{NH}_4^+$  mass flux immediately after Phyto-Feast addition for both control and mussel microcosms in Experiment 1.

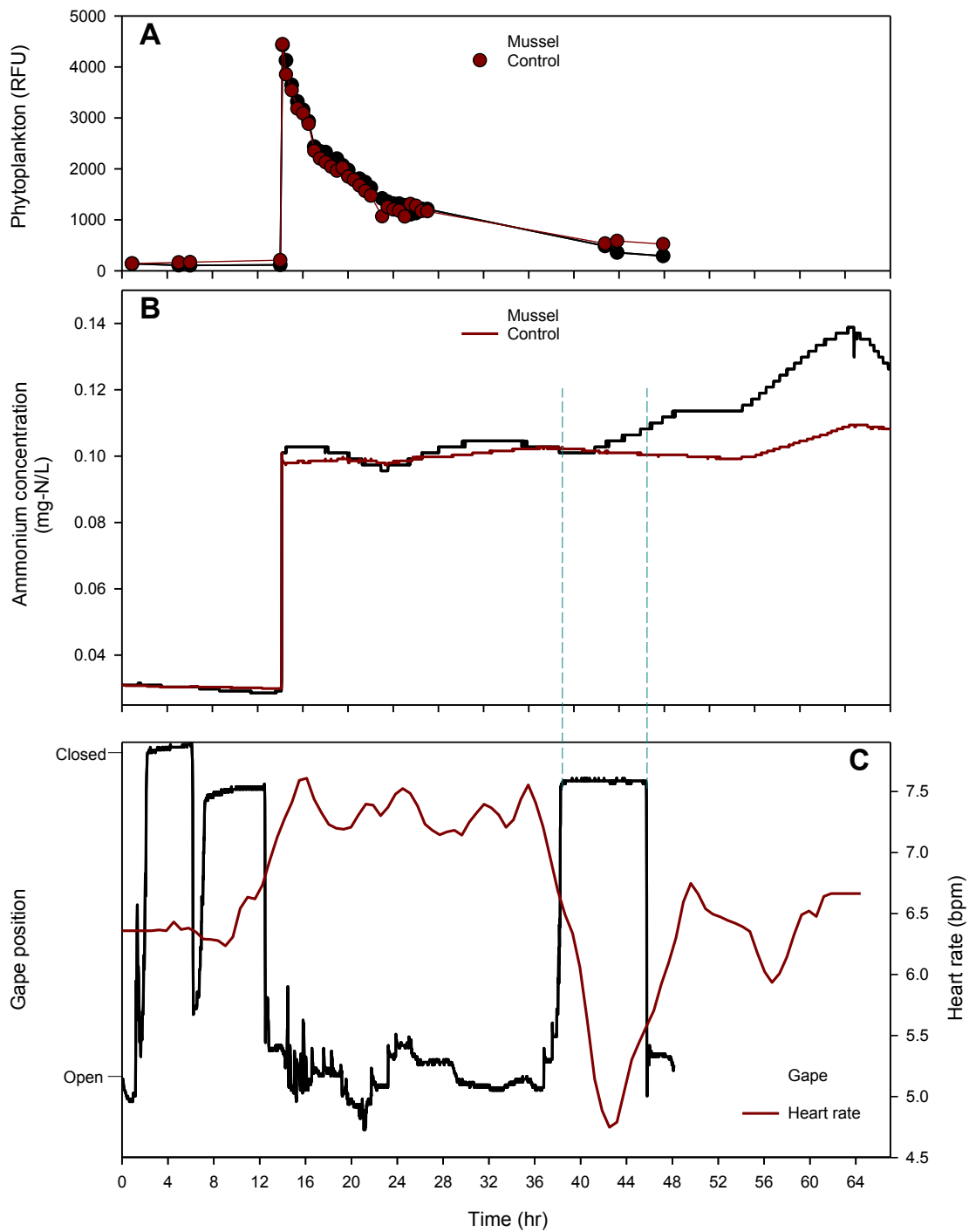


Figure 4.3 Experiment 2A results: (a) phytoplankton concentrations in overlying water, (b) changes in  $\text{NH}_4^+$  concentrations for mussel and control mesocosms ( $\text{mg-N L}^{-1}$ ), and (c) changes in the mussels heart rate (bpm) and gape response (open or closed). The blue dashed lines mark changes in gape position.

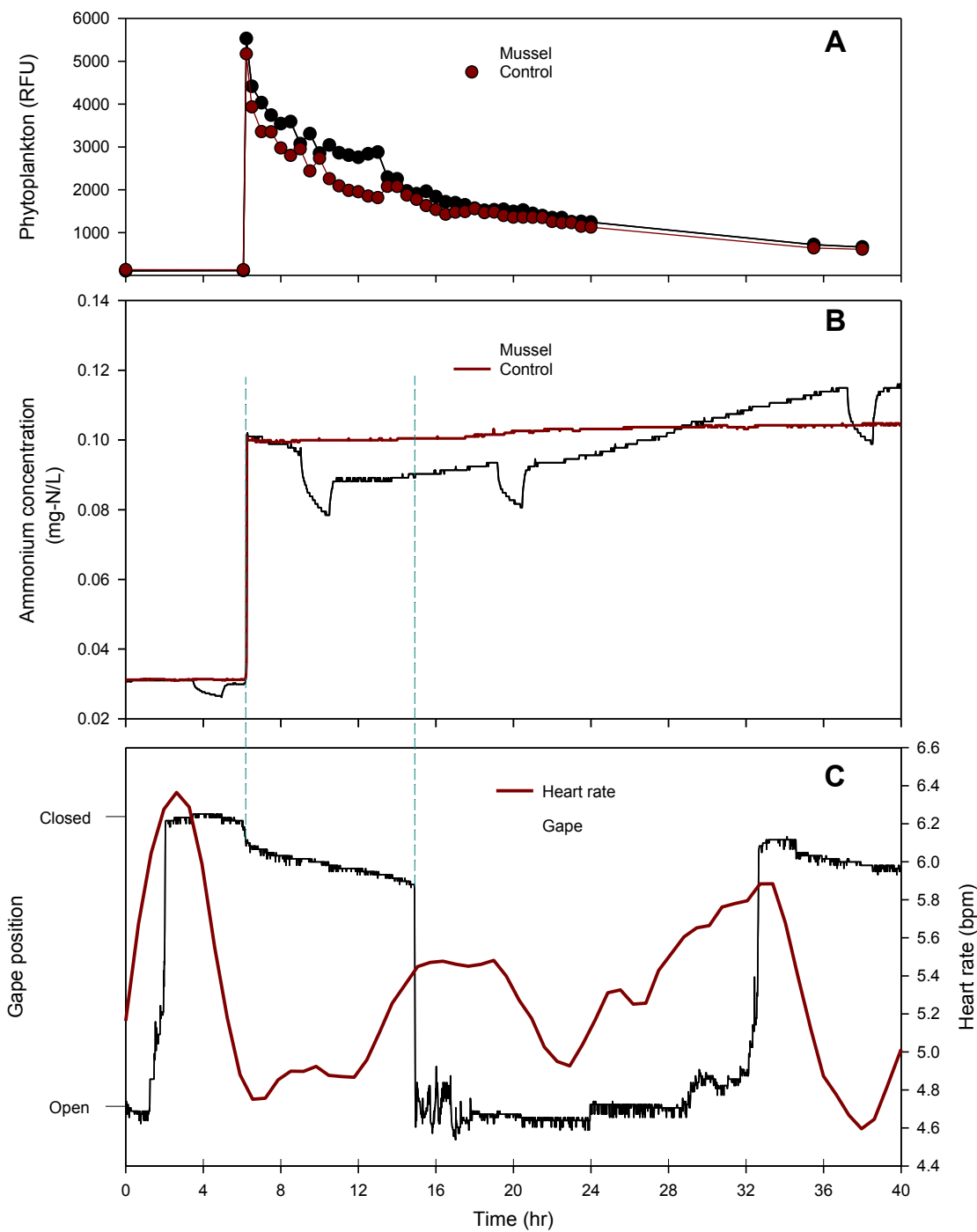


Figure 4.4 Experiment 2B results: (a) phytoplankton concentrations in overlying water, (b) changes in  $\text{NH}_4^+$  concentrations for mussel and control mesocosms ( $\text{mg-N L}^{-1}$ ), and (c) changes in the mussels heart rate (bpm) and gape response (open or closed). The blue dashed lines mark changes in gape position.

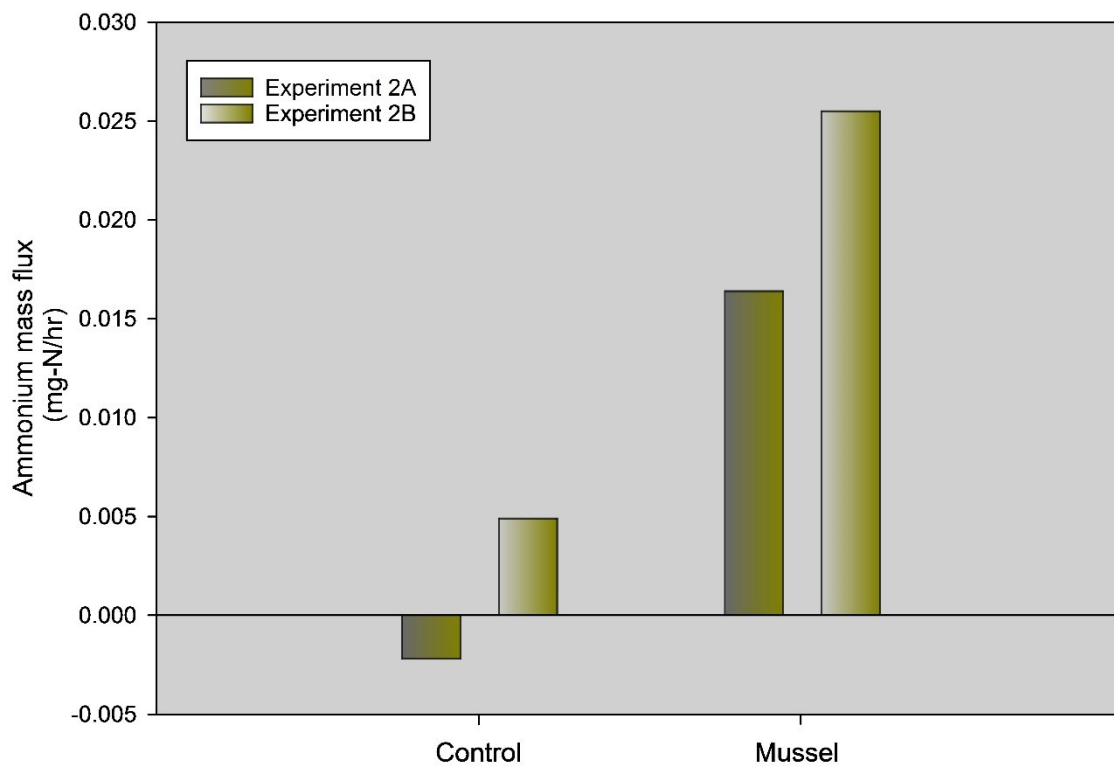


Figure 4.5  $\text{NH}_4^+$  mass flux immediately after Phyto-Feast addition for both control and mussel microcosms in experiments 2A and 2B.

CHAPTER 5  
AMMONIUM EXCRETION, HEART RATE, AND GAPE RESPONSE  
BY ONE MUSSEL IN A 10 L MICROCOSM

This chapter summarizes how  $\text{NH}_4^+$  concentration, heart rate, and gape respond to increases in phytoplankton concentrations for Experiments 3A and 3B. This is followed by a comparison of  $\text{NH}_4^+$  mass fluxes for the mussel and control microcosm. Lastly, this chapter will discuss the results from all of the experiments and how they compare to results found in the literature. After analyzing the results from Experiment 2, it was concluded that reducing the volume of the experimental system would ensure the mussel was near the sensor and increase the ability to track changes in ammonium concentrations. Therefore, Experiment 3 consisted of two trials that were conducted in a smaller environment, a microcosm.

### 5.1 Results of Experiment 3

#### 5.1.1 Experiment 3A

Figure 5.1 shows how phytoplankton concentration,  $\text{NH}_4^+$  concentration, heart rate and gape response changed over the course of 42 hours in Experiment 3A. All of the graphs show time in hours on the x-axis with tick marks every four hours. Figure 5.1A shows changes in phytoplankton concentrations (RFU) for both the mussel and control mesocosm. Figure 5.1B shows the changes in  $\text{NH}_4^+$  concentrations ( $\text{mg-N L}^{-1}$ ) in the overlying water for both the control and mussel microcosm. These figures use the brown filled region to represent the mussel microcosm while the control microcosm is represented by a red line. Figure 5.1C shows changes in, the gape position and the heart rate. Gape position is represented by the brown filled region with position being indicated on the left y-axis (open or closed). Heart rate is denoted by the red line with right y-axis showing the beats per min (bpm).

With experiment 3A starting at the end of a five-day, low food availability period, it was expected that the phytoplankton concentrations would be negligible. Prior to the Phyto-Feast addition, the phytoplankton concentrations in control microcosm had an average of 139 RFU, while the mussel microcosm had an average of 162 RFU. Immediately after the addition of Phyto-Feast at hour six, the phytoplankton concentrations jumped to 6,114 and 6,451 RFU for the control and mussel microcosm respectively (Figure 5.1A). The relative phytoplankton concentrations then decreased exponentially to 712 RFU for the control microcosm and 445 RFU for the mussel microcosm over the next 22.1 hours, which translates to a phytoplankton first-order settling rate of  $0.06 \text{ hr}^{-1}$  for both microcosms. While phytoplankton concentrations decreased exponentially, it was hypothesized that  $\text{NH}_4^+$  concentrations would increase over time.

Prior to the phytoplankton addition, both the control and mussel microcosm had negligible  $\text{NH}_4^+$  concentrations. The addition of Phyto-Feast at six hours caused an immediate increase in  $\text{NH}_4^+$  concentrations to  $0.17 \text{ mg-N L}^{-1}$  for both the mussel and control microcosm-(Figure 5.1B). For 16 hours, the  $\text{NH}_4^+$  concentration in the control microcosm remained relatively stable at  $0.17 \text{ mg-N L}^{-1}$  before gradually increasing to  $0.25 \text{ mg-N L}^{-1}$  over a 20 hour span. In the mussel microcosm,  $\text{NH}_4^+$  concentrations remained constant at  $0.17 \text{ mg-N L}^{-1}$  before dropping to  $0.08 \text{ mg-N L}^{-1}$  at hour 16.3. While it was expected that the  $\text{NH}_4^+$  concentrations would increase and not decrease in the mussel microcosm, this is attributed to mussel removing the  $\text{NH}_4^+$  from the overlying water during filtration. However, following the large decrease, the  $\text{NH}_4^+$  concentration in the mussel microcosm increased while the concentration in control microcosm remained constant. At hour 16.3, the difference between the control and mussel microcosm was  $0.09 \text{ mg-N L}^{-1}$  but by hour 32, the difference had become negligible. Therefore, over a 15.3 hour time span, the mussel increased the  $\text{NH}_4^+$  concentration in their microcosm by approximately  $0.1 \text{ mg-N L}^{-1}$ . For the first time, the increase in  $\text{NH}_4^+$  concentration in the

mussel microcosm came after a change in gape position, which is shown by the blue dashed lines. This increase in  $\text{NH}_4^+$  concentration is attributed to an extended excretion event. However, with some of the increase happening during an increase in the control microcosm, the decay of phytoplankton accounts for part of the increase in  $\text{NH}_4^+$  concentrations.

Figure 5.1C shows that the mussel gape opened twice while only closed once in Experiment 3A. During the end of the low food availability period, the mussel gape stayed in an open position, with slight changes (Figure 5.1C). Instead of showing an immediate response to the phytoplankton addition, the mussel gape did not close until approximately one hour after the increase in phytoplankton concentration. At hour 7, the mussel gape closed and remained closed for 11.4 hours before reopening at hour 18.4. The blue dashed lines show that following the gape re-opening, the  $\text{NH}_4^+$  concentrations in the mussel microcosm started to increase. Over the next 20 hours, the gape position was open with no substantial movement while  $\text{NH}_4^+$  concentrations continued to increase. At hour 38.5, the mussel gape closed and remained closed for the duration of the experiment. Different from the first gaping event, the second gape closure was tighter than the closure that happened following the addition of phytoplankton. Similar to gape position, the heart rate showed minimal changes prior to the phytoplankton addition as compared to after it.

Prior to the addition of Phyto-Feast, the heart rate remained relatively stable between 6.6 bpm and 6.2 bpm (Figure 5.1C). Immediately after the addition of Phyto-Feast, the heart rate decreased from 6.5 to 5.2 bpm over 4.5 hours, which coincided with the gape closing. The heart rate then noticeably increased to 5.9 bpm followed by a small drop before increasing to 6.6 bpm while the gape was re-opening at hour 20.5. The heart rate remained at approximately 6.6 bpm for two hours before decreasing down to 5.8 bpm at hour 26. Over the next 10 hours, the heart rate remained between 5.8 and 6.1 bpm



before increasing to 6.8 bpm during a three hour time span. Over the 42 hours, the mussel had an average heart rate of  $6.1 \pm 0.4$  bpm.

### 5.1.2 Experiment 3B

Figure 5.2 shows how phytoplankton concentrations,  $\text{NH}_4^+$  concentration, and gape position changed over the course of 40 hours in Experiment 3B. Figure 5.2A shows changes in phytoplankton concentrations (RFUs) for the mussel and control microcosm. Figure 5.2B shows the changes in  $\text{NH}_4^+$  concentrations ( $\text{mg-N L}^{-1}$ ) in the overlying water for the control and mussel microcosm. These figures represent changes in the mussel microcosm with a brown filled region while the control microcosm is represented by a red line. Figure 5.2C shows the changes in mussel gape position on the y-axis as either opened or closed. Unfortunately, the heart rate sensor experienced technical issues and the results were not able to be used. All of the figures are represented by time in hours on the x-axis with tick marks every four hours. Figure 5.2 shows that phytoplankton and  $\text{NH}_4^+$  concentrations changed immediately after the Phyto-Feast spike while gape position was not immediately effected.

As the first six hours of the experiment were during the end of the five-day, low food availability period, it was expected that the phytoplankton concentrations would be minimal until the addition of Phyto-Feast. At the end of the low food availability period, the phytoplankton concentration had an average 99 RFU for the control microcosm and 87 RFU mussel microcosm. The addition of Phyto-Feast at hour six caused the phytoplankton concentrations to increase to 2,890 RFU and 3,133 RFUs for the control and mussel microcosms respectively (Figure 5.2A). Over the next 28 hours, the phytoplankton concentrations then decreased exponentially until reaching 323 RFU for the control microcosm and 178 RFU for the mussel microcosm, which translates to a phytoplankton first-order settling rate of  $0.06 \text{ hr}^{-1}$  for both microcosms. Similar to

phytoplankton concentrations,  $\text{NH}_4^+$  concentrations were negligible prior to the addition of phytoplankton.

With a limited food source, it was expected that  $\text{NH}_4^+$  concentrations would remain stable prior to the addition of Phyto-Feast. Before the addition of Phyto-Feast  $\text{NH}_4^+$  concentrations in both microcosms remained constant at  $0.05 \text{ mg-N L}^{-1}$ . Following the addition of Phyto-Feast,  $\text{NH}_4^+$  concentrations in both microcosms jumped to  $0.17 \text{ mg-N L}^{-1}$  and remained stable in both microcosm for 3.3 hours (Figure 5.2B). Nine hours after the increase in phytoplankton, the  $\text{NH}_4^+$  concentrations in the mussel microcosm decreased to  $0.13 \text{ mg-N L}^{-1}$  while  $\text{NH}_4^+$  concentration in the control microcosm were stable at  $0.18 \text{ mg-N L}^{-1}$ . At this point, the control microcosm had a higher  $\text{NH}_4^+$  concentration of  $0.05 \text{ mg-N L}^{-1}$ . At hour 24,  $\text{NH}_4^+$  concentrations in the mussel microcosm started to noticeably increase, when compared to the concentration in the control microcosm. By hour 34, the mussel microcosm had higher  $\text{NH}_4^+$  concentrations than the control microcosm. By the end of the experiment,  $\text{NH}_4^+$  concentrations were  $0.02 \text{ mg-N L}^{-1}$  higher in the mussel microcosm than the control microcosm. After the decrease in  $\text{NH}_4^+$  concentrations, the mussel microcosm showed a  $0.07 \text{ mg-N L}^{-1}$  increase compared to the control microcosm. With the  $\text{NH}_4^+$  increase spanning 16 hours, this increase is attributed to an extended excretion event with a minimal addition due to the decay of phytoplankton. Following the same trend as Experiment 3A,  $\text{NH}_4^+$  concentrations in the mussel microcosm did not show a noticeable increase until after the mussel gape re-opened.

Prior to the increase in phytoplankton concentrations, the mussels gape remained stable in the open position. Instead of immediately responding to the addition of Phyto-Feast, the mussel gape did not close until 3.5 hours after the phytoplankton addition- figure 5.2C. During the gape closure, the  $\text{NH}_4^+$  concentration decreased in the mussel tank and remained relatively stable during the 14.5 hour closure period. The re-opening at hour 24 coincides with the beginning of the  $\text{NH}_4^+$  increase in the mussel microcosm,

which can be seen with the blue dashed lines-figure 5.2. For the remainder of the experiment, the mussel gape remained in the open position with minimal gape changes.

### 5.1.3 Ammonium Mass Flux Comparison between Experiments 3A and 3B

Microcosms in Experiments 3A and 3B experienced the same environmental alterations, resulting in the ability to directly compare of the ammonium mass flux between the two experiments Figure 5.3. The bar graphs show the ammonium mass flux for the mussel and control microcosm. The  $\text{NH}_4^+$  mass flux represents the difference in  $\text{NH}_4^+$  concentrations immediately following the Phyto-Feast addition and approximately 33 hours after. In Experiment 3A, the control microcosm had an  $\text{NH}_4^+$  mass flux of  $0.03 \text{ mg-N hr}^{-1}$  while the mussel microcosm had a mass flux of  $0.024 \text{ mg-N hr}^{-1}$ . This results in a larger mass flux for the control microcosm. Despite the fact the control microcosm showed a larger mass flux in Experiment 3A, the opposite happened in Experiment 3B. In Experiment 3B, the mussel microcosm had an  $\text{NH}_4^+$  mass flux of  $0.02 \text{ mg-N hr}^{-1}$  compared to  $0.015 \text{ mg-N hr}^{-1}$  in the control microcosm. Therefore, the mussel microcosm saw a  $0.005 \text{ mg-N hr}^{-1}$  increase in  $\text{NH}_4^+$  after the phytoplankton addition. However, the analysis for both experiments did not take into account the decrease in  $\text{NH}_4^+$  concentration in the mussel microcosm.

Considering the decrease in  $\text{NH}_4^+$  concentration in the mussel microcosm, the  $\text{NH}_4^+$  mass flux in the overlying water was greater in the mussel microcosm after the re-opening of the mussel gape Figure 5.4. Rather than looking at the mass flux over 33 hours, this mass flux looked at the difference in ammonium concentrations immediately after the gape re-opens and 16.5 hours later. This resulted in an  $\text{NH}_4^+$  mass flux of approximately  $0.04 \text{ mg-N hr}^{-1}$  for the control microcosm compared to approximately  $0.1 \text{ mg-N hr}^{-1}$  for the mussel microcosm in Experiment 3A. This results in larger  $\text{NH}_4^+$  mass flux of  $0.06 \text{ mg-N hr}^{-1}$  for the mussel microcosm. Similarly, the mussel microcosm in

Experiment 3B a larger  $\text{NH}_4^+$  mass flux by  $0.03 \text{ mg-N hr}^{-1}$ ,  $0.03 \text{ mg-N hr}^{-1}$  for the control microcosm and  $0.06 \text{ mg-N hr}^{-1}$  for the mussel microcosm. Following the mussel gape re-opening,  $\text{NH}_4^+$  mass fluxes are larger for both trials in the mussel microcosms.

## 5.2 Experimental Discussion

This discussion compares results obtained during this study with results from other published research. The discussion will focus only on  $\text{NH}_4^+$  mass fluxes from Experiment 3, because the smaller volume of overlying water resulted in the increased ability to detect changes of  $\text{NH}_4^+$  concentrations in the overlying water. As the results from the gape and heart rate sensors were not directly influenced by the overlying water volume, the results from all experiments will be compared with published research.

In aquatic ecosystems, areas with mussels are expected to have higher  $\text{NH}_4^+$  concentrations as a result of filtering suspended particles and excreting  $\text{NH}_4^+$  back into the substrate and overlying water.<sup>67</sup> Even though Experiment 3A showed lower  $\text{NH}_4^+$  concentrations in the mussel microcosm compared to control microcosm, both trials showed  $\text{NH}_4^+$  concentrations decreased before increasing in the mussel microcosm, while  $\text{NH}_4^+$  concentrations in control microcosm remained relatively stable. As the mussel filtered the overlying water, removing nutrients and phytoplankton,  $\text{NH}_4^+$  concentrations decreased before increasing through excretion of the unused nutrients into the substrate and overlying water.<sup>68</sup> As filtered water passes through the digestive system, suspended particles are sorted based on their chemical composition and absorbed for growth while excess nutrients are released through biodeposits or excretion.<sup>42,69</sup> Following the filtration of phytoplankton, mussels go through a digestion period of approximately  $13 \pm 6$  hours before peaks in  $\text{NH}_4^+$  concentrations are expected.<sup>70</sup> While the digestion time for Experiment 3A and 3B were approximately 23 and 26 hours, the longer values could be attributed to environmental conditions or variations in phytoplankton composition.

At times of increased nutrient concentrations, mussels are expected to have higher excretion concentrations when compared to times when there are limited amounts of phytoplankton.<sup>40, 71</sup> Comparing the  $\text{NH}_4^+$  mass fluxes from Experiment 3 with literature values, there are mixed results. Depending on species, size, and time of the year,  $\text{NH}_4^+$  excretion can be as high as  $33.7 \mu\text{g NH}_3\text{-N hr}^{-1} \text{ g}^{-1}$ ,  $40 \mu\text{g-N hr}^{-1}$ , or  $2.5 \mu\text{mol NH}_4^+ \text{ hr}^{-1} \text{ mussel}^{-1}$ .<sup>71-73</sup> Using the allometric function  $M = aL^b$  where  $M$  is the dry mussel mass,  $L$  is the measured shell length, and  $a$  and  $b$  are previously determined parameters, the mussel in Experiment 3 was approximately 100 grams of dry biomass.<sup>74</sup> Therefore, converting the mass fluxes after the re-opening of the mussels (Figure 5.4), excretion rates in Experiment 3A were  $0.6 \mu\text{g-N hr}^{-1} \text{ g}^{-1}$ ,  $60 \mu\text{g-N hr}^{-1}$ , and  $3.3 \mu\text{mol NH}_4^+ \text{ hr}^{-1}$ , while excretion rates in Experiment 3B were  $0.3 \mu\text{g-N hr}^{-1} \text{ g}^{-1}$ ,  $30 \mu\text{g-N hr}^{-1}$ , and  $1.7 \mu\text{mol NH}_4^+ \text{ hr}^{-1}$ . Comparing experimental excretion rates with values found in literature<sup>71</sup>, the excretion rates were an order of magnitude of two lower when the excretion rate was a function of mussel biomass. However, when comparing strictly the excretion rate on a per mussel basis, the experimental values were comparable with the latter two literature values<sup>72, 73</sup>. Unfortunately, with size and species influencing excretion rate, excretion rate on a per mass basis is a better indicator for individual mussels. Even though a phytoplankton was added to microcosms, variations in experimental excretion rates can be explained by environmental conditions.

With the experimental  $\text{NH}_4^+$  excretion values showing some inconsistencies, explanations point to stressful environmental conditions. Excretion rates can be lower at elevated temperatures due to thermal stress. At higher temperatures, mussels remove less suspended particles from the overlying water but show a higher excretion rate due to stress.<sup>18</sup> Even though temperatures were constant and not at abnormally high temperatures,  $70^\circ$  Fahrenheit could still lower the excretion rates. Another stress related factor, at times of low food availability, more of the filtered particles will be used for growth or stored as a reserve for future periods of low-food availability. This results in

smaller amounts of nutrients being excreted or biodeposited.<sup>24</sup> With the amount of nutrients available influencing mussel excretion, phytoplankton composition is a big factor. When the phytoplankton is high in valuable nutrients, more can be used for growth, subsequently decreasing the amount of  $\text{NH}_4^+$  excretion. Although, when there are limited amounts of valuable nutrients, mussels will also have lower excretion rates.<sup>24, 38</sup> Even though a store-bought phytoplankton was added to provide essential nutrients to the mussels, over time excretion rates will decrease during lab experiments.<sup>75</sup> As much as microcosms can simulate normal conditions, experimental habitats are not the same as normal conditions and can influence mussel excretion rate.

Following the addition of Phyto-Feast in every experiment except 2A, the mussel gape position indicated a response to increased phytoplankton concentrations. In Experiments 1, 3A, and 3B, the gape of the mussel went from an opened position to a closed position before re-opening. Following increases in phytoplankton concentrations, mussels respond with gape positions opening or closing. During a constant period of higher concentrations, the gape position will close.<sup>53</sup> Sometimes when the composition of the phytoplankton are not ideal, gape position closes as a way to conserve energy by not have to sort through the suspended particles.<sup>42</sup> Automated imaging has indicated that following low-food availability, gape position will open. When the gape position is already open, there is not a noticeable change.<sup>48</sup> In 2B, the Hall-sensor indicated a small opening in mussel gape following the addition of Phyto-Feast. With automated imaging only being able to take pictures of the mussel above the substrate, it is limited in determining how the burrowed portion of the gape is responding.

Both trials in Experiment 2 showed that the gape position closed prior to the addition of Phyto-Feast. During periods of low-food availability, gape position closes as a way to conserve energy until phytoplankton and nutrient concentrations increase.<sup>38</sup> Even with closed gapes, mussels are able to immediately detect changes in phytoplankton concentrations, resulting in the gape opening. Otherwise, as phytoplankton concentrations

remain minimal, mussels will pedal feed as a way to find food.<sup>54</sup> When the mussel moves, there are small but quick gape changes over an extended period that can only be detected at higher frequencies.<sup>76</sup> In Experiments 2A and 2B, the gape closure prior to the addition of Phyto-Feast is attributed to conserving energy or quick position changes due to pedal feeding that were undetectable. In 2B, the small re-opening of the gape position can be attributed to the detection of phytoplankton before maximizing the gape opening. It is important to note that Experiment 2A, 2B, and 3A showed variations in the “tightness” of the gape closure. While there is nothing in the literature explaining the difference in amount of gape closure, it should be something to look at in the future to determine if there is a physiological difference.

Research has shown the mussel heart can range from 13 bpm to 7, with light and mussel movement being the largest influence. Periods of darkness cause the mussel to experience a lower heart rate, while burrowing events cause increases in heart rate.<sup>59, 77</sup> On average, all four of the experiments with heart rate data had similar heart rates. However, when the gape position is closed, the heart rate decreased. When the gape position closes, oxygen consumption as the mantle cavity requires less ventilation.<sup>78</sup> As the filtered water moves through the mantle cavity of the mussel, it removes oxygen from the water.<sup>79</sup> Following Experiment 2A, a different mussel was used for experiments, which resulted in a lower range of heart rates. In the first two experiments, the mussel had average heart rates of  $7 \pm 0.7$  bpm and  $6.6 \pm 0.7$ , while the heart rate dropped to an average of  $5.3 \pm 0.4$  and  $6.1 \pm 0.4$  for Experiment 2B and 3A. With heart rate influenced by the amount of oxygen pumped through the mantle cavity, each mussel has a different respiration rate dependent on size and age. Larger mussels have higher respiration rates and as mussels get older, respiration rates decrease.<sup>55</sup> However, both mussels showed a similar trend that gape closure decreased the heart rate supporting that the decrease in heart rate is attributed to a lower oxygen consumption.<sup>78</sup> At the end of the experiment, it

is evident that each mussel has a different heart rate and that it was influenced by changes in gape position.



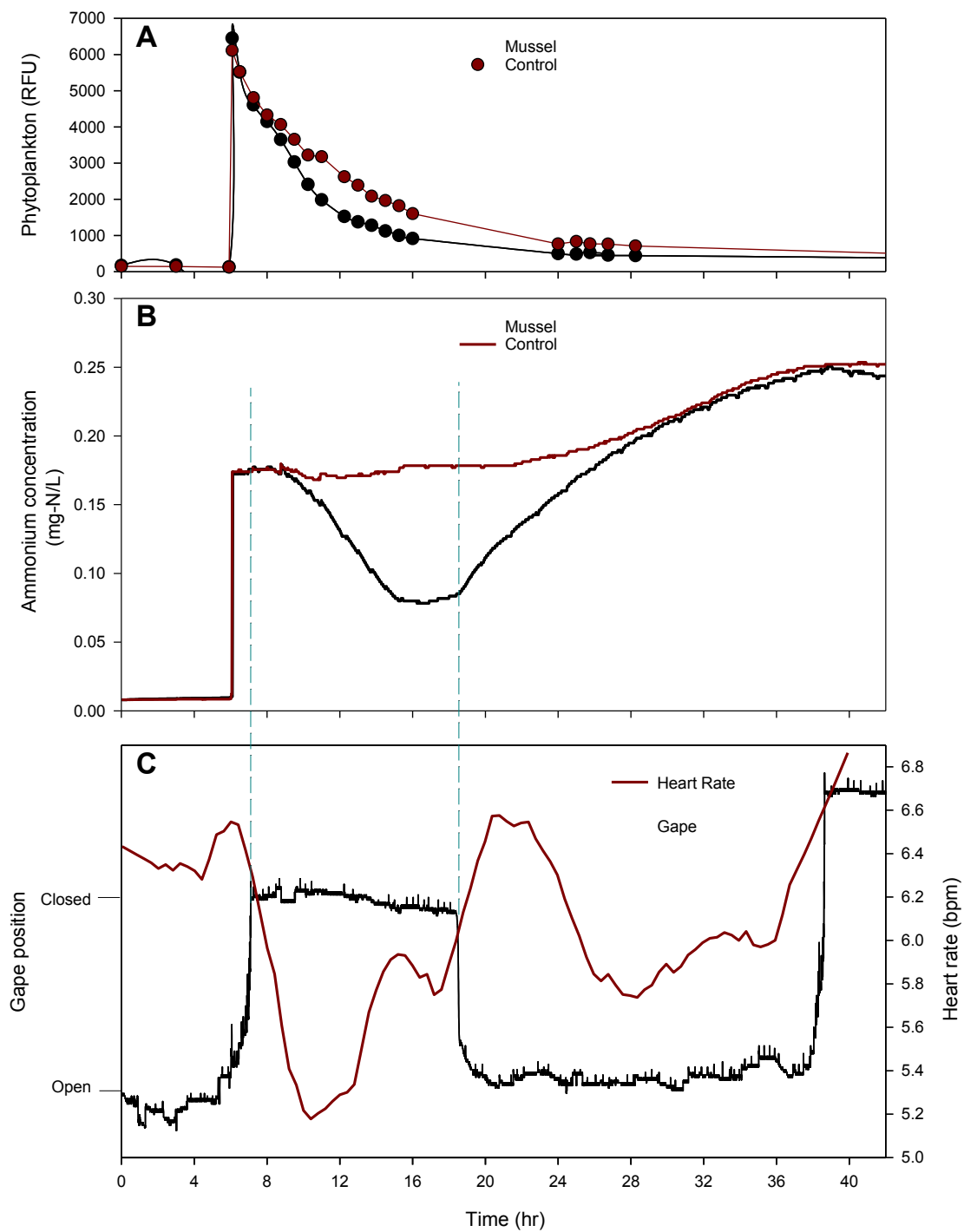


Figure 5.1 Experiment 3A results: (a) phytoplankton concentrations in overlying water, (b) changes in  $\text{NH}_4^+$  concentrations for mussel and control microcosms ( $\text{mg-N L}^{-1}$ ), and (c) changes in the mussels heart rate (bpm) and gape response (open or closed). The blue dashed lines mark changes in gape position.

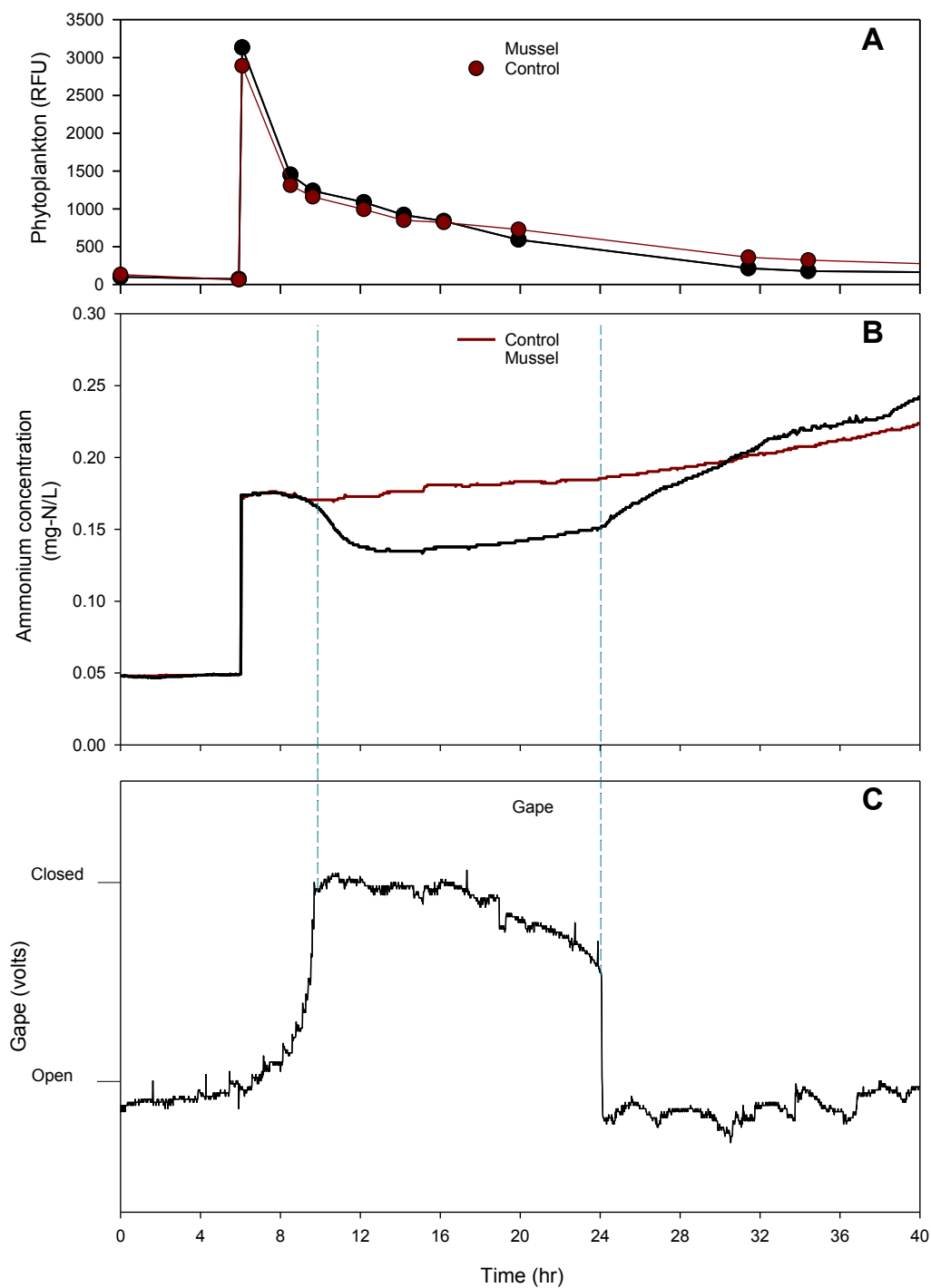


Figure 5.2 Experiment 3B results: (a) phytoplankton concentrations in overlying water, (b) changes in  $\text{NH}_4^+$  concentrations for mussel and control microcosms ( $\text{mg-N L}^{-1}$ ), and (c) mussels gape response (open or closed). The blue dashed lines mark changes in gape position.

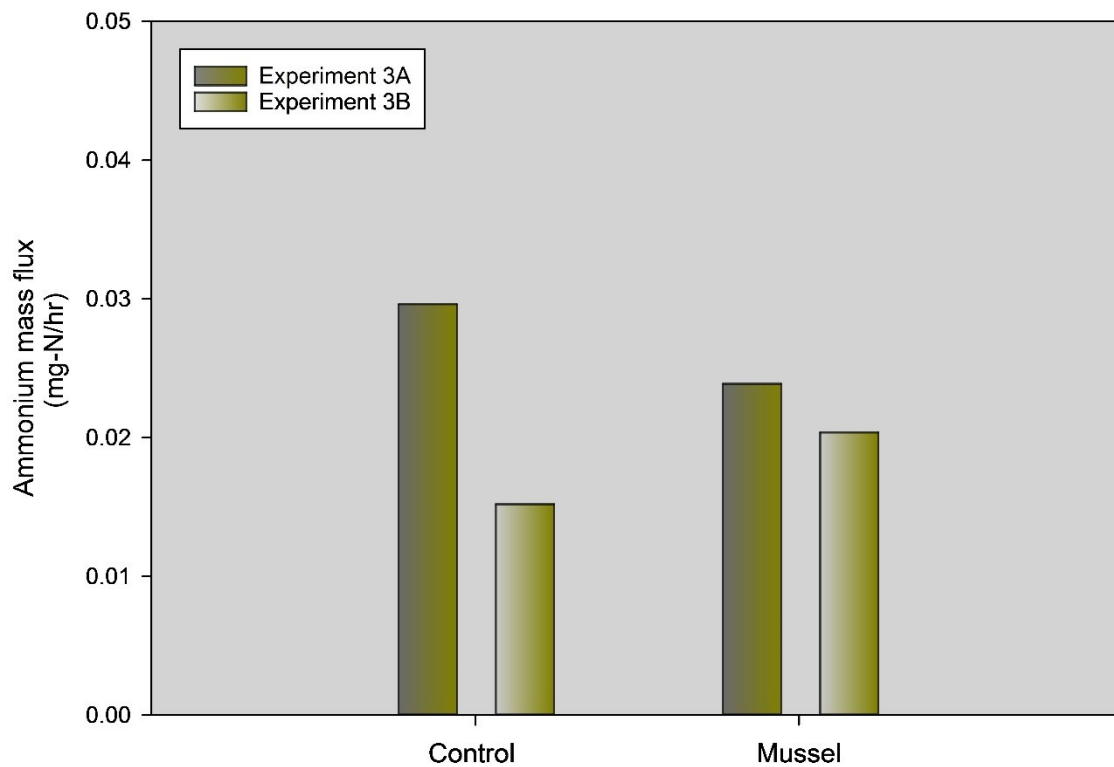


Figure 5.3  $\text{NH}_4^+$  mass flux immediately after Phyto-Feast addition for both control and mussel microcosms in experiments 3A and 3B.

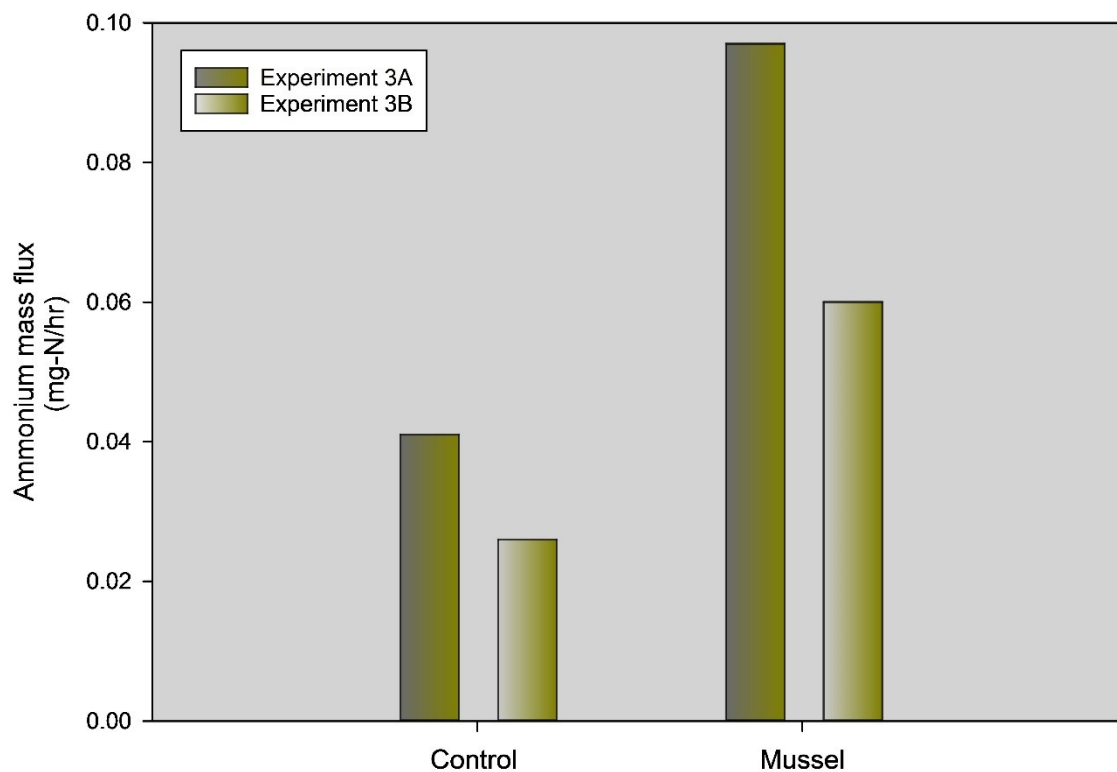


Figure 5.4  $\text{NH}_4^+$  mass flux after mussel gape re-opened following the addition of Phyto-Feast for both the control and mussel microcosm for experiment 3A and 3B.

## CHAPTER 6

### MODELING THE IMPACT FRESHWATER MUSSELS HAVE ON AQUATIC AMMONIUM CONCENTRATIONS VIA GAPE RESPONSE

This chapter describes the parameters and equations used for a dynamic model that simulated the changes in overlying water conditions for mussel beds. This is followed by comparing  $\text{NH}_4^+$  concentrations for six simulations with different mussel biomasses, phytoplankton concentrations, and variations in excretion rates as a function of gape response.

#### 6.1 Model Parameters

This STELLA model used mass balance equations to simulate the changes in five nitrogenous compounds in aquatic ecosystems (Figures 6.1-6.4). The dynamic model used stocks and flows to show changes in phytoplankton, organic nitrogen, nitrite, nitrate, and ammonium concentrations over a 2,160 hour (90 days) timeframe that was broken into six hour time steps. Figure 6.1 shows the stocks and flows for phytoplankton, Figure 6.2 shows ammonium in both the overlying and pore water, Figure 6.3 shows nitrate and organic nitrogen, and Figure 6.4 shows the stocks and flows for nitrite. While this research focused on how excretion rate of mussels impact  $\text{NH}_4^+$  concentrations in the overlying water, this chapter will only present the results from the simulation for  $\text{NH}_4^+$  concentrations. Ammonium in the overlying water had inputs of phytoplankton respiration/excretion, ammonium inflow, and ammonium diffusion from pore water with losses due to plant uptake of ammonium, nitrification, ammonium outflow, and ammonium diffusion to pore water (Equation 6.1). Mussel excretion does not go directly in the overlying water but instead diffuses from the pore water. The amount of ammonium excreted by mussels was a function of gape position, phytoplankton

concentration in the overlying water (mussel clearance converter, and mussel biomass.

All of the variable and rates used in the STELLA model are shown in tables 6.1 and 6.2.

$$\text{Equation 6.1 } n_{a,o,t} = n_{a,o,t-1} + \frac{n_{n,r,t}}{\tau} + ra + D_{n_{a,o,t}} - \frac{n_{a,o,t}}{\tau} - P_a - n - D_{n_{a,p,t}}$$

where,

$$n_{a,p,t} = \text{Pore Water Ammonium Concentration at time } t \text{ (mg - N L}^{-1}\text{)}$$

$$n_{a,p,t-1}$$

$$= \text{Pore Water Ammonium Concentration at time } t - 1 \text{ (mg - N L}^{-1}\text{)}$$

$$n_{a,o,t} = \text{Overlying Water Ammonium Concentration at time } t \text{ (mg - N L}^{-1}\text{)}$$

$$n_{a,o,t-1} = \text{Overlying Water Ammonium Concentration at time } t - 1 \text{ (mg - N L}^{-1}\text{)}$$

$$n_{n,r,t} = \text{River Water Ammonium Concentration at time } t \text{ (mg - N L}^{-1}\text{)}$$

$$hn = \text{Hydrolysis of Organic Nitrogen (mg - N L}^{-1} \text{ h}^{-1}\text{)}$$

$$n_{o,p,t} = \text{Pore Water Organic Nitrogen Concentration at time } t \text{ (mg - N L}^{-1}\text{)}$$

$$k_{hn}(T_p)$$

$$= \text{Temperature}$$

$$- \text{Dependent Organic Nitrogen Hydrolysis Rate (h}^{-1}\text{)}$$

$$T_p = \text{Pore Water Temperature (}^\circ\text{C)}$$

$$D_{n_{a,p,t}} = \text{Pore Water Ammonium Diffusion (mg - N L}^{-1} \text{ h}^{-1}\text{)}$$

$$k_{D_{n_{a,p,t}}} = \text{Pore Water Ammonium Diffusion Rate (h}^{-1}\text{)}$$

$$ex = \text{Mussel Excretion (h}^{-1}\text{)}$$

$$M_b = \text{Mussel Biomass (dry weight)(g)}$$

$$M_{ex} = \text{Mussel Excretion Rate of Ammonium (h}^{-1} \text{ g}^{-1} \text{ dry wgt.)}$$

$k_{eM}$  = Mussel Excretion Converter

$T_o$  = Overlying Water Temperature (°C)

$D_{n_{a,o,t}}$  = Diffusion of Ammonium in the Overlying Water ( $mg - N L^{-1} h^{-1}$ )

$k_{D_{n_{a,o,t}}}$  = Overlying Water Ammonium Diffusion Rate ( $h^{-1}$ )

$fi_a$  = Flow in of Ammonium ( $mg - N L^{-1} h^{-1}$ )

$\tau$  = Hydraulic Retention Time (h)

$ra$  = Phytoplankton Respiration/Excretion ( $mg - N L^{-1} h^{-1}$ )

$a_{o,t}$  = Overlying Water Phytoplankton Concentration at time t ( $mg - N L^{-1}$ )

$k_{ra}(T_o)$  = Temperature

– Dependent Phytoplankton Respiration/Excretion Rate ( $h^{-1}$ )

$fo_a$  = Flow out of Ammonium ( $mg - N L^{-1} h^{-1}$ )

$P_a$  = Plant Uptake of Ammonium ( $mg - N L^{-1} h^{-1}$ )

$g$  = Phytoplankton Growth ( $mg - N L^{-1} h^{-1}$ )

$U_{in}$  = Fraction of Inorganic Nitrogen Uptake

$n_{n,o,t}$  = Overlying Water Nitrate Concentration at time t ( $mg - N L^{-1}$ )

$k_a$  = Half Saturation Constant for Ammonium Preference

$a_{o,t}$  = Overlying Water Phytoplankton Concentration at time t ( $mg - N L^{-1}$ )

$k_g(T, N, I)$  = First – Order Growth Rate

– as a function of temperature, nutrients, and light ( $h^{-1}$ )

$k_{g,T}$  = Maximum Phytoplankton Growth Rate ( $h^{-1}$ )

$\varphi$  = Light Attenuation Factor

$N$  = Nitrification ( $mg - N L^{-1} h^{-1}$ )

$k_n(T_o)$  = Overlying Water Temperature –

Dependent Nitrification Rate ( $h^{-1}$ )

## 6.2 Stella Model

Figure 6.5-6.10 show  $\text{NH}_4^+$  concentrations from the STELLA model for six different simulations, two mussel biomasses, 100 and 2000 grams, each at three phytoplankton concentrations,  $1 \text{ mg-N L}^{-1}$ ,  $5 \text{ mg-N L}^{-1}$ , and  $10 \text{ mg-N L}^{-1}$ . In all six figures, the x-axis shows the time in hours while the y-axis displays  $\text{NH}_4^+$  concentrations in the overlying water as  $\text{mg-N L}^{-1}$ . In each figure,  $\text{NH}_4^+$  concentrations are shown for six different gape responses. In the figures 6.5-6.10, the black line represents  $\text{NH}_4^+$  concentrations the overlying water when mussel excretion is not influenced by gape. The pink line represents  $\text{NH}_4^+$  concentrations during random opening and closing events. The other four lines represent the  $\text{NH}_4^+$  concentrations for a twelve hour opening and closing cycle with different lengths of closure periods. The yellow line represents a daily twelve hour cycle without any extended closure periods. The blue line represents a two day opening and closing cycle followed by a two day closing event. Similarly, the red and green lines represent a five day and a ten day daily opening and closing cycle followed by the same length closing period. Throughout the entire simulation, these three scenarios rotate between an opening and closing cycle with an extended closure period. In all of the simulations, the excretion rates used were from experiment 3A. When the gape position was open, the excretion rate was constant at  $1.1 \times 10^{-4} \text{ mg-N hr}^{-1} \text{ L}^{-1} \text{ g dry biomass}^{-1}$  while when it was closed it was  $3.2 \times 10^{-6} \text{ mg-N hr}^{-1} \text{ L}^{-1} \text{ g dry biomass}^{-1}$ . In the simulations where the mussel excretion rate was not a function of gape, the excretion rate of  $1.1 \times 10^{-4} \text{ mg-N hr}^{-1} \text{ L}^{-1} \text{ g dry biomass}^{-1}$ . Figures 6.5-6.10 indicate that using gape changes to predict the impact mussels have on  $\text{NH}_4^+$  concentrations will be different than when there is a constant excretion rate.

Initially, the simulation was done for an aquatic ecosystem with a mussel biomass of 100 grams, which is approximately the weight of one pocketbook mussel (Figure 6.5-6.7). Figure 6.5 shows the results when there was a phytoplankton concentration of  $1 \text{ mg-N L}^{-1}$ , Figure 6.6 shows the results for  $5 \text{ mg-N L}^{-1}$ , and Figure 6.7 shows the results



for 10 mg-N L<sup>-1</sup>. Comparing the figures for a mussel biomass of 100 grams, NH<sub>4</sub><sup>+</sup> concentrations in the overlying water increased with increasing in phytoplankton concentrations. With NH<sub>4</sub><sup>+</sup> concentrations being influenced by more than just mussel excretion, it was expected to see variations in NH<sub>4</sub><sup>+</sup> concentrations as phytoplankton concentrations increased. At low mussel biomass, NH<sub>4</sub><sup>+</sup> concentrations will increase as more phytoplankton respire/excrete ammonium and through the hydrolysis of organic nitrogen left by dead phytoplankton. When excretion rate was not a function of gape, phytoplankton concentration of 1 mg-N L<sup>-1</sup> had the lowest NH<sub>4</sub><sup>+</sup> concentration of 0.09 mg-N L<sup>-1</sup> while phytoplankton concentration of 5 and 10 mg-N L<sup>-1</sup> resulted in NH<sub>4</sub><sup>+</sup> concentrations of 0.11 mg-N L<sup>-1</sup> and 0.12 mg-N L<sup>-1</sup>. Comparing these results to when the excretion rate was a function of gape, only one simulation showed lower NH<sub>4</sub><sup>+</sup> concentrations for all gaping events.

As the model was run with excretion being a function of gape, the five simulations showed similar results for the various phytoplankton concentrations. Comparing strictly the NH<sub>4</sub><sup>+</sup> concentrations when the excretion rate was a function of gape, random and 12 hour gaping events resulted in the highest concentrations for all three phytoplankton concentrations. Both simulations showed a negligible difference in overlying NH<sub>4</sub><sup>+</sup> concentrations. As for the simulations when the gape position went through extended closure periods, the NH<sub>4</sub><sup>+</sup> concentrations would increase while the gape went through a 12 hour cycle before slightly decreasing during the extended gape closure period. All three extended gape closure simulations initially followed the 12 hour cycle until the first gape closure, where NH<sub>4</sub><sup>+</sup> concentrations dropped and were unable to reach the same concentrations as the 12 hour cycle. Similar to the simulations with random and a 12 hour opening and closing, the three extended gape closure simulations oscillated in the same range of NH<sub>4</sub><sup>+</sup> concentrations. At the end of the simulation for phytoplankton concentrations of 1 mg-N L<sup>-1</sup>, the 12 hour cycle had final NH<sub>4</sub><sup>+</sup> concentration of 0.07 mg-N L<sup>-1</sup> while the 10 day concentration was 0.06 mg-N L<sup>-1</sup>. Likewise, at the end of the

simulations with phytoplankton concentrations of both 5 and 10 mg-N L<sup>-1</sup>, the 12 hour cycle had 0.12 mg-N L<sup>-1</sup> and 0.18 mg-N L<sup>-1</sup> compared to 0.1 mg-N L<sup>-1</sup> and 0.16 mg-N L<sup>-1</sup> for the ten day extend gape closure. As typical mussel beds consist of more than one mussel, simulations were ran with a mussel biomass of 2000 grams, which is approximately 20 pocketbook mussels.

Figures 6.8-6.10 show NH<sub>4</sub><sup>+</sup> concentrations from simulations that were ran with a mussel biomass of 2000 grams with the same variations in phytoplankton. Differing from the simulations with 100 grams, when mussel excretion rate was not a function of gape but constant, NH<sub>4</sub><sup>+</sup> concentrations stabilized at approximately 0.7 mg-N L<sup>-1</sup> for all three phytoplankton concentrations. However, when excretion rate was a function of gape, NH<sub>4</sub><sup>+</sup> concentrations showed the same grouping as simulations when the mussel biomass was 100 grams. Random and 12 hour gapping events were together while two, five, and ten day extended closures oscillated at lower NH<sub>4</sub><sup>+</sup> concentrations. Unlike the first simulations, NH<sub>4</sub><sup>+</sup> concentrations flattened out for all of the gape events. When phytoplankton biomass was 1 mg-N L<sup>-1</sup>, the NH<sub>4</sub><sup>+</sup> concentrations were 0.39 mg-N L<sup>-1</sup> for the twelve hour cycle and 0.26 mg-N L<sup>-1</sup> for the ten day extended gape closure. Showing the same trend, simulations with phytoplankton concentrations of both 5 and 10 mg-N L<sup>-1</sup> finished with NH<sub>4</sub><sup>+</sup> concentrations of 0.37 mg-N L<sup>-1</sup> and 0.37 mg-N L<sup>-1</sup> for the 12 hour cycle compared to 0.25 mg-N L<sup>-1</sup> and 0.25 mg-N L<sup>-1</sup> for the ten day extend gape closure. Based on these results, specific NH<sub>4</sub><sup>+</sup> concentrations do not change with increasing phytoplankton concentrations, but instead are governed by changes in gape position.

Two trends that were evident at the end of the simulations were, 1) the influence phytoplankton has on NH<sub>4</sub><sup>+</sup> concentrations in the overlying water when there is not an abundance of mussels and, 2) the influence gape changes have on NH<sub>4</sub><sup>+</sup> concentrations when there is a large mussel biomass. In Figures 6.5-6.7, the mussel biomass remains constant, but increases in phytoplankton concentrations showed a continual increase in NH<sub>4</sub><sup>+</sup> concentrations even though the mussel excretion rate was not influenced by

phytoplankton concentrations. When phytoplankton concentrations are greater than 10 mg-N L<sup>-1</sup>, NH<sub>4</sub><sup>+</sup> concentrations will be higher when excretion rate is a function of gape. However, at 5 mg-N L<sup>-1</sup>, only random and 12 hour gapping events resulted in higher NH<sub>4</sub><sup>+</sup> concentrations while at 1 mg-N L<sup>-1</sup> all gapping events resulted in lower NH<sub>4</sub><sup>+</sup> concentrations. Comparing those results with the results from the simulations with a biomass of 2000, the NH<sub>4</sub><sup>+</sup> concentration stabilized at approximately 0.7 for all three phytoplankton concentrations. The other two inputs in the model were phytoplankton respiration/excretion and the hydrolysis of organic nitrogen, which happens after phytoplankton die. The model shows that phytoplankton has a greater impact on NH<sub>4</sub><sup>+</sup> concentrations when there is not an abundance of mussels as there is nothing there to remove it. However, when there is an abundance of mussels, NH<sub>4</sub><sup>+</sup> concentrations are influenced more by gape position than phytoplankton concentrations.

Figures 6.8-6.10 indicate that when excretion rate is a function of gape, the simulation predicts lower NH<sub>4</sub><sup>+</sup> concentrations than when there is a constant excretion rate. As mussels go through extended gape closures, the NH<sub>4</sub><sup>+</sup> concentrations in the overlying water decrease. While daily 12 hour open and closing events result in approximately half the NH<sub>4</sub><sup>+</sup> concentrations when excretion rate is constant, extended gape closures longer than two days decrease NH<sub>4</sub><sup>+</sup> concentrations further. The two, five, and ten day extended closure cycles show that NH<sub>4</sub><sup>+</sup> concentrations will increase during the 12 hour opening and closing cycle but there is a major drop when the gape closed for an extended period. Even when it reopened, NH<sub>4</sub><sup>+</sup> concentrations started to increase before dropping again at the next extended gape closure. If extended gape closures are not a part of a normal cycle, but instead caused by risk of predation or environmental disturbance, the NH<sub>4</sub><sup>+</sup> concentrations will increase to a certain threshold before decreasing during another extended gape closure.<sup>58, 76</sup>

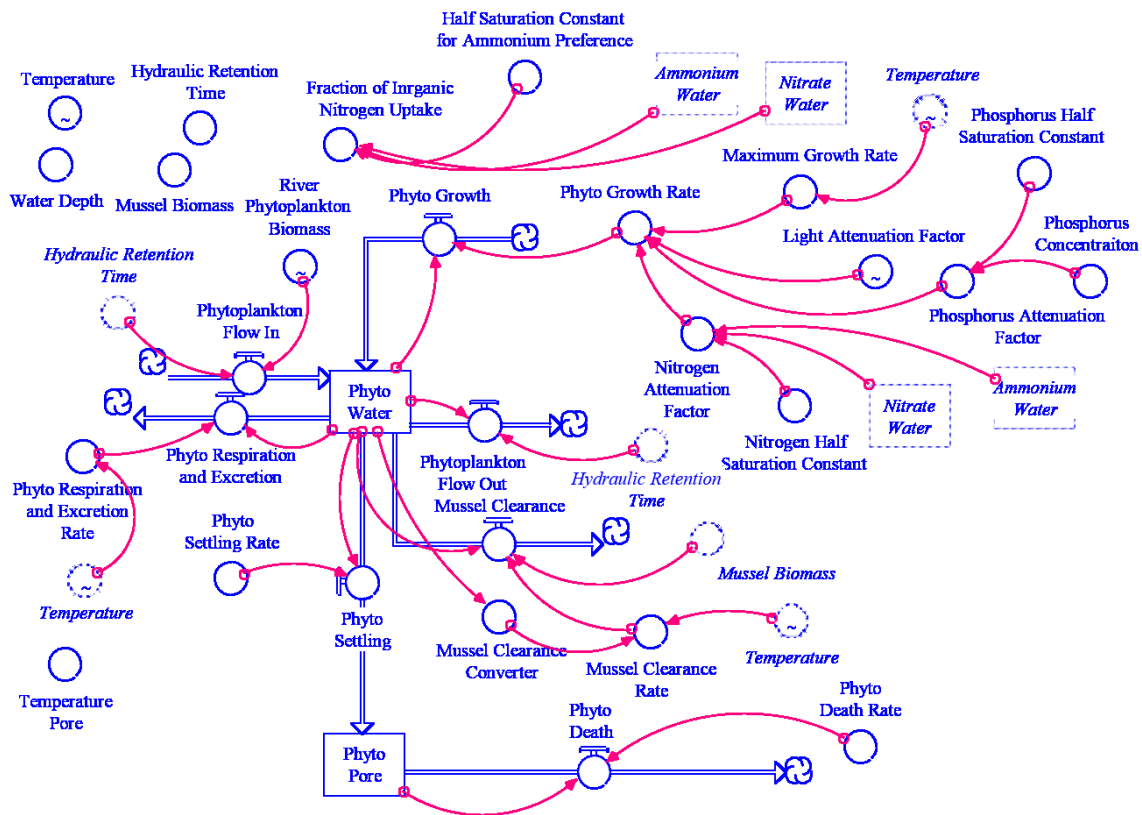


Figure 6.1 Stocks, flows, and converters for phytoplankton in the STELLA model adapted from Brill Dissertation.<sup>80</sup>

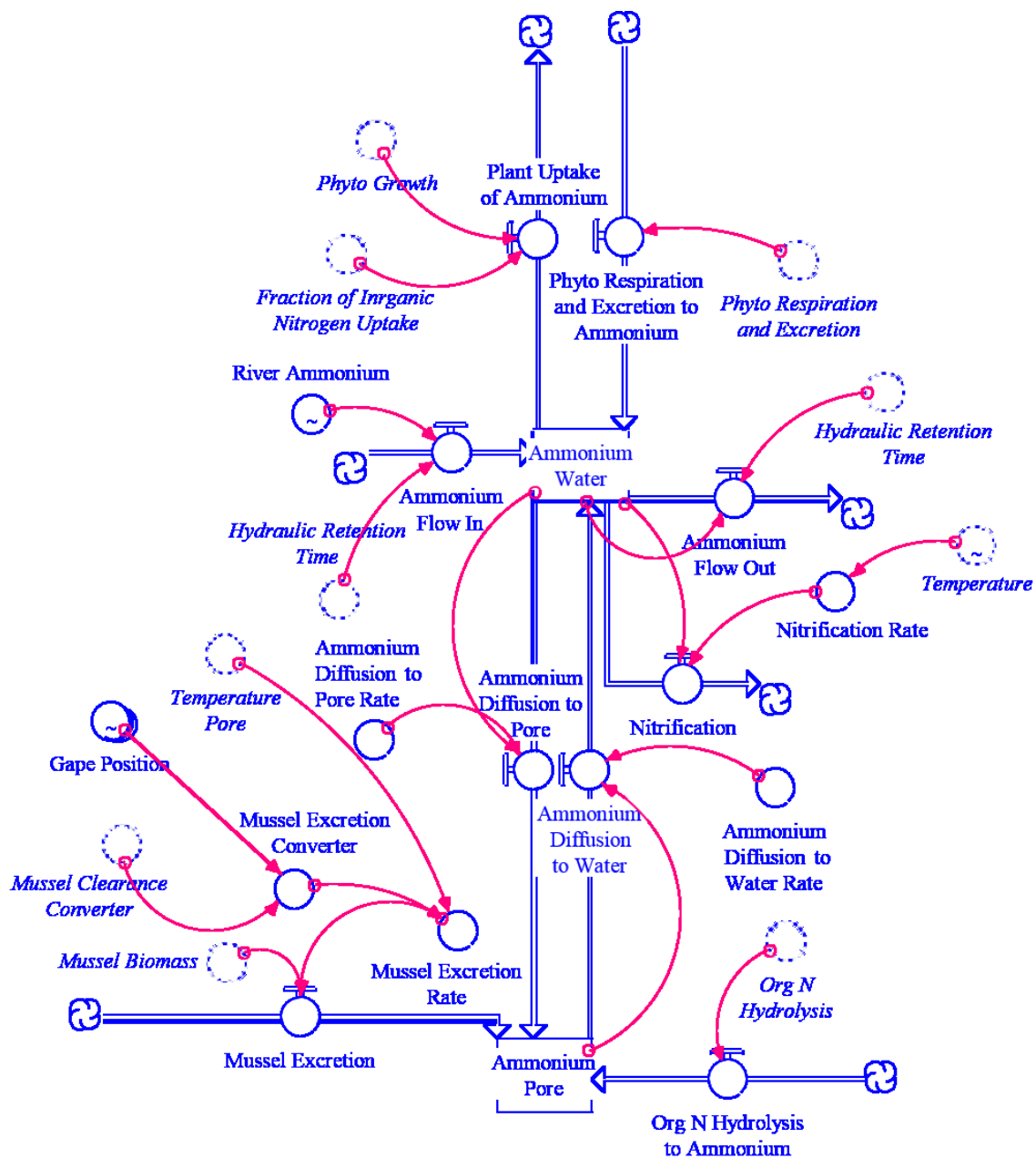


Figure 6.2 Stocks, flows, and converters for ammonium in the STELLA model adapted from Brill Dissertation.<sup>80</sup>

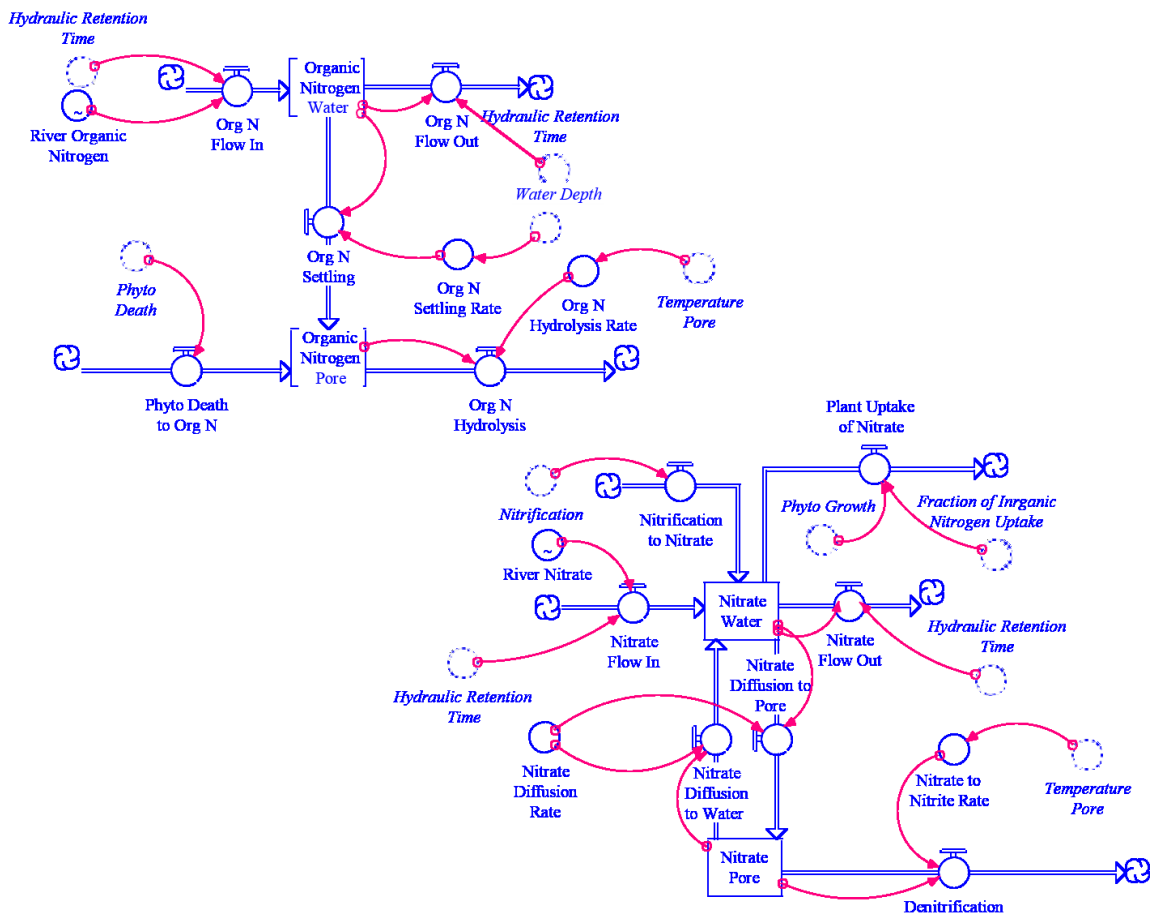


Figure 6.3 Stocks, flows, and converters for both organic nitrogen and nitrate in the STELLA model adapted from Brill Dissertation.<sup>80</sup>

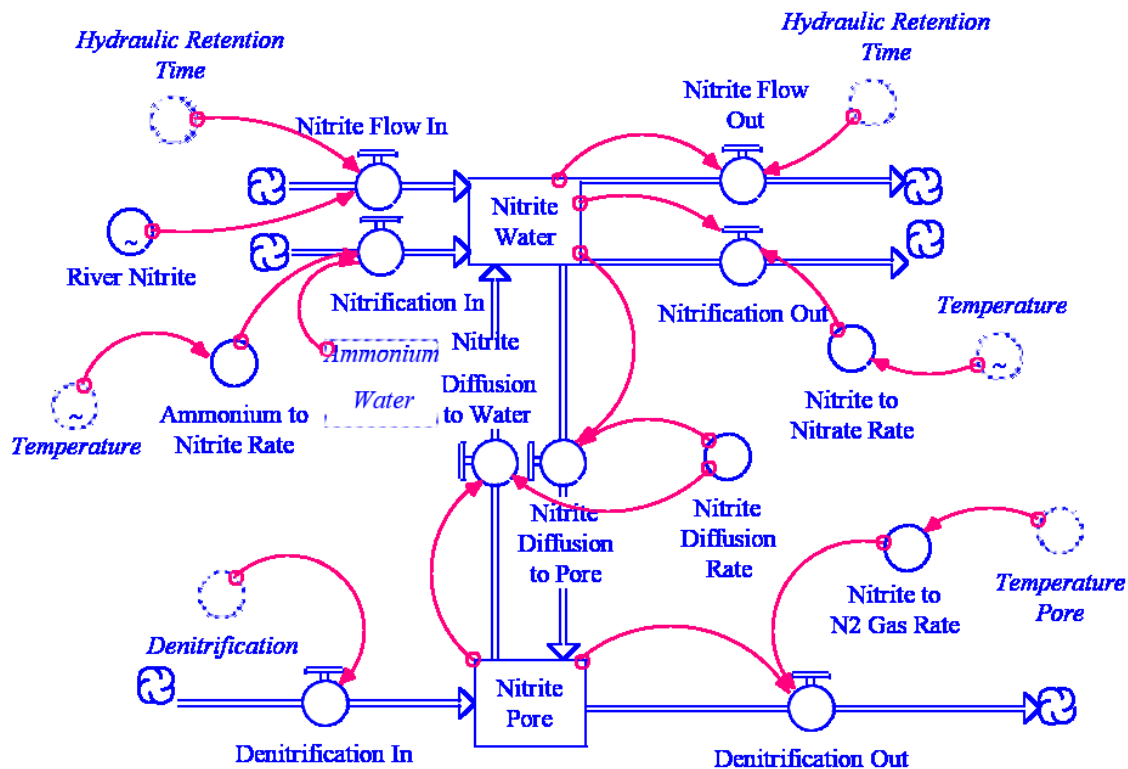


Figure 6.4 Stocks, flows, and converters for nitrite in the STELLA model adapted from Brill Dissertation.<sup>80</sup>

Table 6.1 Variables used in the development of the STELLA model.

Variable	Definition	Units
ai	Nitrification of Ammonium to Nitrite	mg-N L <sup>-1</sup> h <sup>-1</sup>
a <sub>o,t</sub>	Overlying Water Phytoplankton Concentration at time t	mg-N L <sup>-1</sup>
a <sub>o,t-1</sub>	Overlying Water Phytoplankton Concentration at time t-1	mg-N L <sup>-1</sup>
a <sub>p,t</sub>	Pore Water Phytoplankton Concentration at time t	mg-N L <sup>-1</sup>
a <sub>p,t-1</sub>	Pore Water Phytoplankton Concentration at time t-1	mg-N L <sup>-1</sup>
cl	Mussel Clearance	mg-N L <sup>-1</sup> h <sup>-1</sup>
d	Phytoplankton Death to Organic Nitrogen	mg-N L <sup>-1</sup> h <sup>-1</sup>
D <sub>na,o,t</sub>	Overlying Water Ammonium Diffusion	mg-N L <sup>-1</sup> h <sup>-1</sup>
D <sub>na,p,t</sub>	Pore Water Ammonium Diffusion	mg-N L <sup>-1</sup> h <sup>-1</sup>
D <sub>ni,o,t</sub>	Overlying Water Nitrite Diffusion	mg-N L <sup>-1</sup> h <sup>-1</sup>
D <sub>ni,p,t</sub>	Pore Water Nitrite Diffusion	mg-N L <sup>-1</sup> h <sup>-1</sup>
D <sub>nn,o,t</sub>	Overlying Water Nitrate Diffusion	mg-N L <sup>-1</sup> h <sup>-1</sup>
D <sub>nn,p,t</sub>	Pore Water Nitrate Diffusion	mg-N L <sup>-1</sup> h <sup>-1</sup>
ex	Mussel Excretion	h <sup>-1</sup>
g	Phytoplankton Growth	mg-N L <sup>-1</sup> h <sup>-1</sup>
H	Water Depth	m
hn	Hydrolysis of Organic Nitrogen	mg-N L <sup>-1</sup> h <sup>-1</sup>
ig	Denitrification of Nitrite to Nitrogen Gas	mg-N L <sup>-1</sup> h <sup>-1</sup>
in	Nitrification for Nitrite to Nitrate	mg-N L <sup>-1</sup> h <sup>-1</sup>
k <sub>ai</sub> (T <sub>o</sub> )	Overlying Temperature-dependent conversion rate of Ammonium to Nitrite	h <sup>-1</sup>
k <sub>am</sub>	Half Saturation Constant for Ammonium Preference	mg-N L <sup>-1</sup>
k <sub>cl</sub>	Mussel Clearance Converter	h <sup>-1</sup> g <sup>-1</sup> dry wt.
k <sub>d</sub> (T <sub>p</sub> )	Phytoplankton Death to Organic Nitrogen Rate	h <sup>-1</sup>



Table 6.1 continued

Variable	Definition	Units
$k_{Dna,o,t}$	Overlying Water Ammonium Diffusion Rate	$h^{-1}$
$k_{Dna,p,t}$	Pore Water Ammonium Diffusion Rate	$h^{-1}$
$k_{Dni,t}$	Nitrite Diffusion Rate	$h^{-1}$
$k_{Dnn,t}$	Nitrate Diffusion Rate	$h^{-1}$
$k_{eM}$	Mussel Excretion Converter	$h^{-1} g^{-1}$ dry wt.
$k_g(T_o, N, I)$	First-Order Growth Rate as a function of overlying water temp., nutrients, and light	$h^{-1}$
$k_{g,T_o}$	Maximum Phytoplankton Growth rate	$h^{-1}$
$k_{hn}(T_p)$	Pore Temperature-Dependent Organic Nitrogen Hydrolysis Rate	$h^{-1}$
$k_{ig}(T_p)$	Pore Temperature-dependent conversion rate of Nitrite to Nitrogen Gas	$h^{-1}$
$k_{in}(T_o)$	Overlying Temperature-dependent conversion rate of Nitrite to Nitrate	$h^{-1}$
$k_n(T_o)$	Overlying Temperature-Dependent Nitrification Rate	$h^{-1}$
$k_{ni}(T_p)$	Pore Temperature-Dependent conversion rate of Nitrate to Nitrite	$h^{-1}$
$k_{ra}(T_o)$	Temperature-dependent phytoplankton respiration/excretion rate	$h^{-1}$
$M_b$	Mussel Biomass (dry weight)	g
$M_{cl}$	Mussel Clearance Rate	$h^{-1} g^{-1}$ dry wt.
$M_{ex}$	Mussel Excretion Rate of Ammonium	$h^{-1} g^{-1}$ dry wt.
$n$	Nitrification	$mg-N L^{-1} h^{-1}$
$ni$	Denitrification of Nitrate to Nitrite	$mg-N L^{-1} h^{-1}$
$n_{a,o,t}$	Overlying Water Ammonium Concentration at time t	$mg-N L^{-1}$
$n_{a,o,t-1}$	Overlying Water Ammonium Concentration at time t-1	$mg-N L^{-1}$
$n_{a,p,t}$	Pore Water Ammonium Concentration at time t	$mg-N L^{-1}$
$n_{a,p,t-1}$	Pore Water Ammonium Concentration at time t-1	$mg-N L^{-1}$
$n_{a,r,t}$	River Water Ammonium Concentration at time t	$mg-N L^{-1}$
$n_{i,o,t}$	Overlying Water Nitrite Concentration at time t	$mg-N L^{-1}$

Table 6.1 continued

Variable	Definition	Units
$n_{i,p,t}$	Pore Water Nitrite Concentration at time t	mg-N L <sup>-1</sup>
$n_{i,p,t-1}$	Pore Water Nitrite Concentration at time t-1	mg-N L <sup>-1</sup>
$n_{i,r,t}$	River Water Nitrite Concentration at time t	mg-N L <sup>-1</sup>
$n_{n,o,t}$	Overlying Water Nitrate Concentration at time t	mg-N L <sup>-1</sup>
$n_{n,o,t-1}$	Overlying Water Nitrate Concentration at time t-1	mg-N L <sup>-1</sup>
$n_{n,p,t}$	Pore Water Nitrate Concentration at time t	mg-N L <sup>-1</sup>
$n_{n,p,t-1}$	Pore Water Nitrate Concentration at time t-1	mg-N L <sup>-1</sup>
$n_{n,r,t}$	River Water Nitrate Concentration at time t	mg-N L <sup>-1</sup>
$n_{o,o,t}$	Overlying Water Organic Nitrogen Concentration at time t	mg-N L <sup>-1</sup>
$n_{o,o,t-1}$	Overlying Water Organic Nitrogen Concentration at time t-1	mg-N L <sup>-1</sup>
$n_{o,p,t}$	Pore Water Organic Nitrogen Concentration at time t	mg-N L <sup>-1</sup>
$n_{o,p,t-1}$	Pore Water Organic Nitrogen Concentration at time t-1	mg-N L <sup>-1</sup>
$n_{o,r,t}$	River Water Organic Nitrogen Concentration at time t	mg-N L <sup>-1</sup>
$P_a$	Plant Uptake of Ammonium	mg-N L <sup>-1</sup> h <sup>-1</sup>
$P_n$	Plant Uptake of Nitrate	mg-N L <sup>-1</sup> h <sup>-1</sup>
$ra$	Phytoplankton Respiration/Excretion	mg-N L <sup>-1</sup> h <sup>-1</sup>
$T_o$	Overlying Water Temperature	°C
$T_p$	Pore Water Temperature	°C
$\tau$	Hydraulic Retention Time	h
$U_{in}$	Fraction of Inorganic Nitrogen Uptake	
$V_{s,o}$	Organic Nitrogen Settling Rate	m h <sup>-1</sup>
$V_{s,a}$	Rate of Phytoplankton Settling	m h <sup>-1</sup>
$\phi$	Light Attenuation Factor	
$\phi_{n,p}$	Minimum of Nitrogen or Phosphorous Light Attenuation Factor	

Source: Variables used were adapted from Brill Dissertation<sup>80</sup>

Table 6.2 Range of variables and rates used for the dynamic STELLA model.

Model Variable	Units	Sensitivity Analysis Range
Nitrification Rate	$h^{-1}$	0.0001 to 0.21
Denitrification Rate	$h^{-1}$	0.0005 to 0.0996
Light	---	0 to 1
Temperature	$^{\circ}C$	5 to 35
Hydraulic Retention Time	h	0.5 to 48
Maximum Phytoplankton Growth Rate	$h^{-1}$	0.0417 to 0.0833
Phytoplankton Death Rate	$h^{-1}$	0.0021 to 0.0104
Phytoplankton Settling Rate	$mh^{-1}$	0 to 0.0833
Phytoplankton Respiration/Excretion	$h^{-1}$	0.0004 to 0.0208
Organic Nitrogen Hydrolysis Rate	$h^{-1}$	0.00004 to 0.0083
Organic Nitrogen Settling Rate	$mh^{-1}$	0 to 0.0833
Mussel Biomass	g	0 to 250
Mussel Phytoplankton Clearance Rate	$h^{-1} g^{-1}$	0 to 0.000714
Mussel Ammonium Excretion Rate	$h^{-1} g^{-1}$	0 to 4

Source: Variables and rates used were adapted from Brill disseration<sup>80</sup>

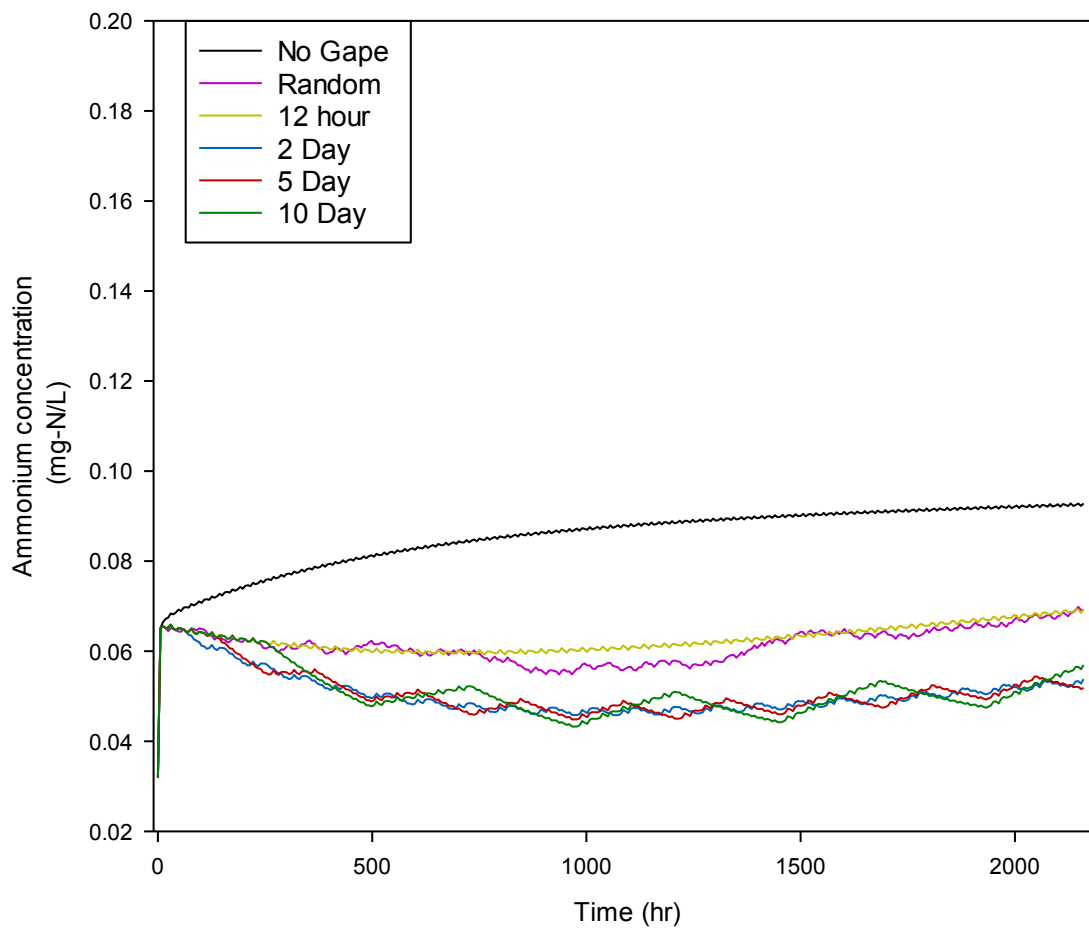


Figure 6.5 Simulated overlying water  $\text{NH}_4^+$  concentrations for one mussel and phytoplankton biomass one  $\text{mg L}^{-1}$  during various gape position changes.

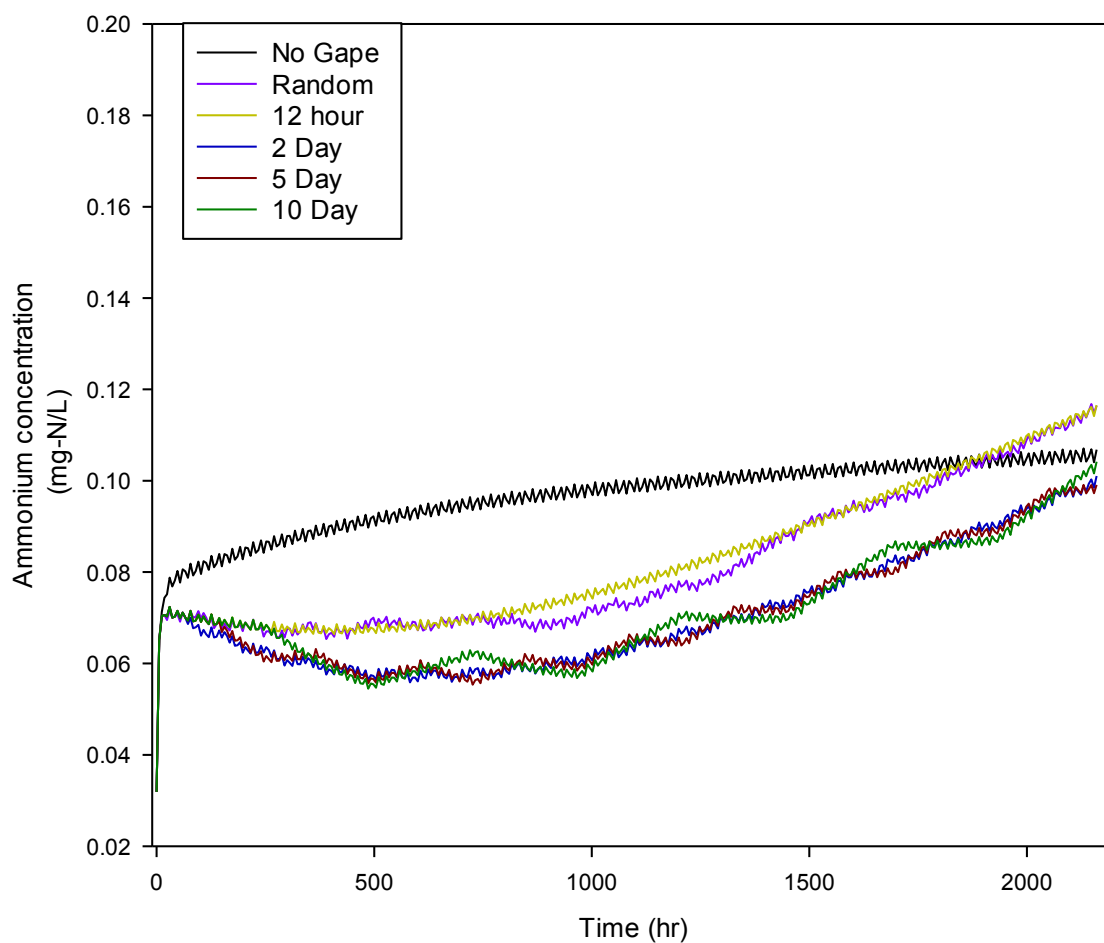


Figure 6.6 Simulated overlying water  $\text{NH}_4^+$  concentrations for one mussel and phytoplankton biomass five  $\text{mg L}^{-1}$  during various gape position changes.

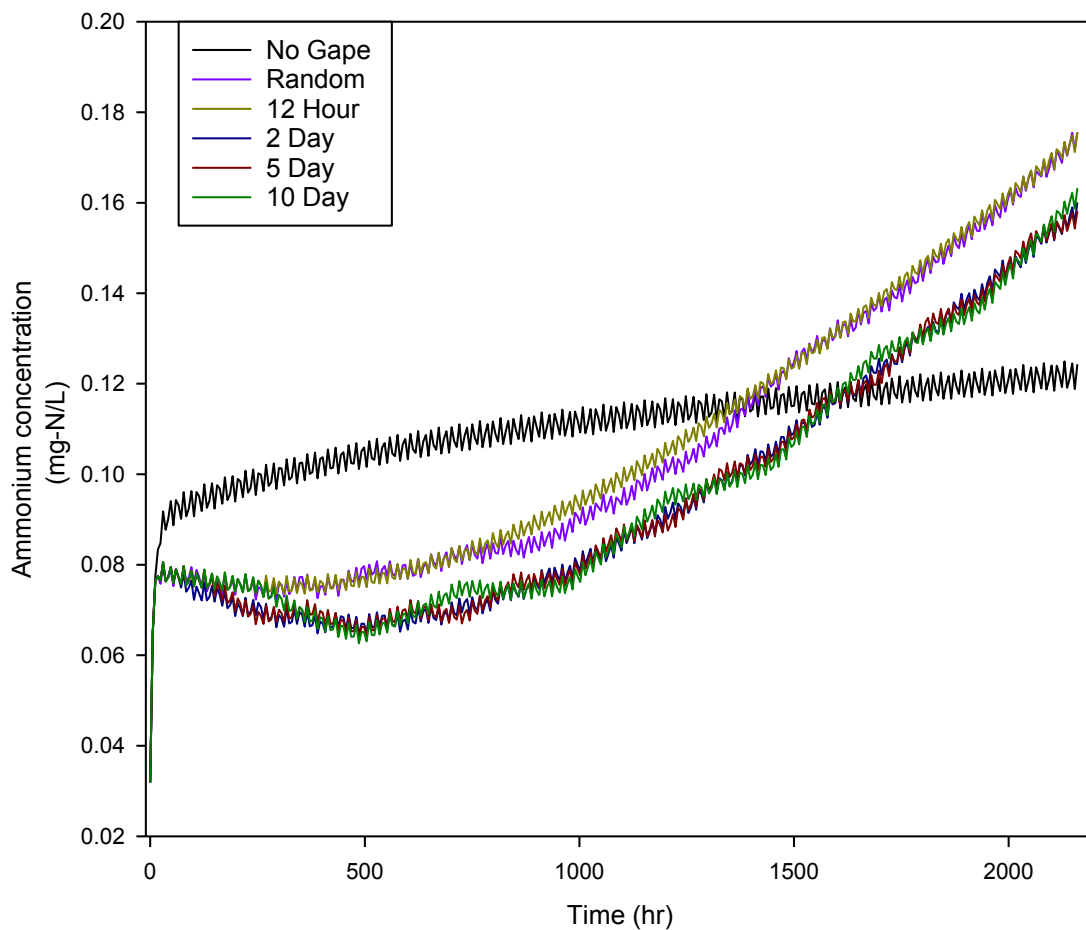


Figure 6.7 Simulated overlying water  $\text{NH}_4^+$  concentrations for one mussel and phytoplankton biomass of  $10 \text{ mg L}^{-1}$  during various gape position changes.

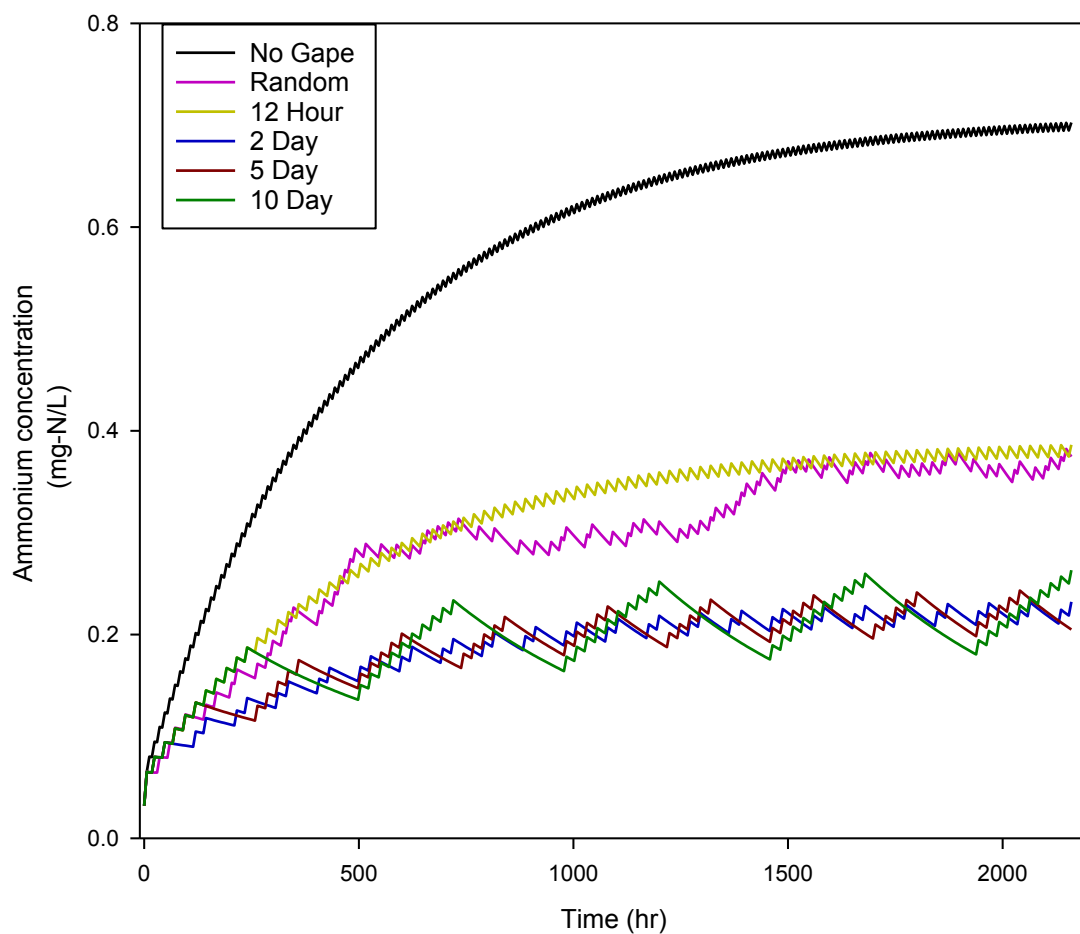


Figure 6.8 Simulated overlying  $\text{NH}_4^+$  concentrations for 200 mussels and phytoplankton biomass of one  $\text{mg L}^{-1}$  during various gape position changes.

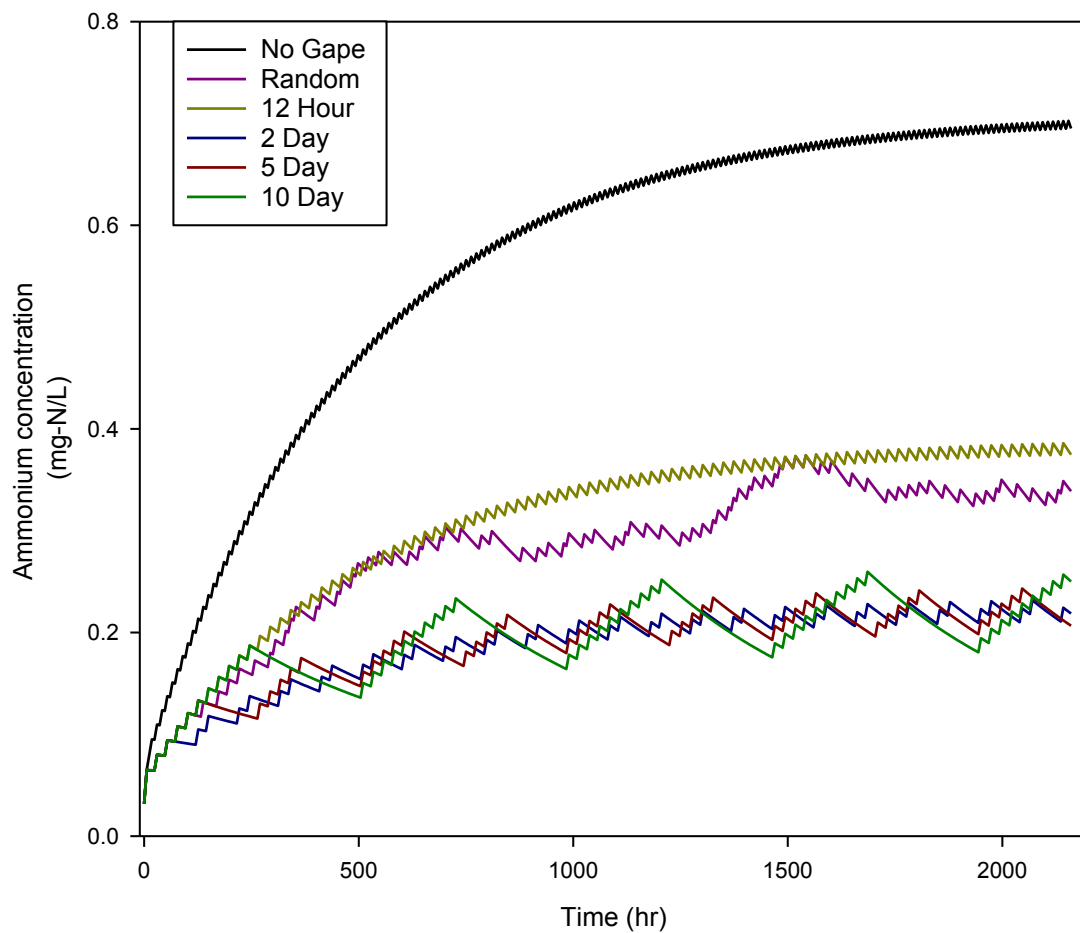


Figure 6.9 Simulated overlying  $\text{NH}_4^+$  concentrations for 200 mussel and phytoplankton biomass of five  $\text{mg L}^{-1}$  during various gape position changes.



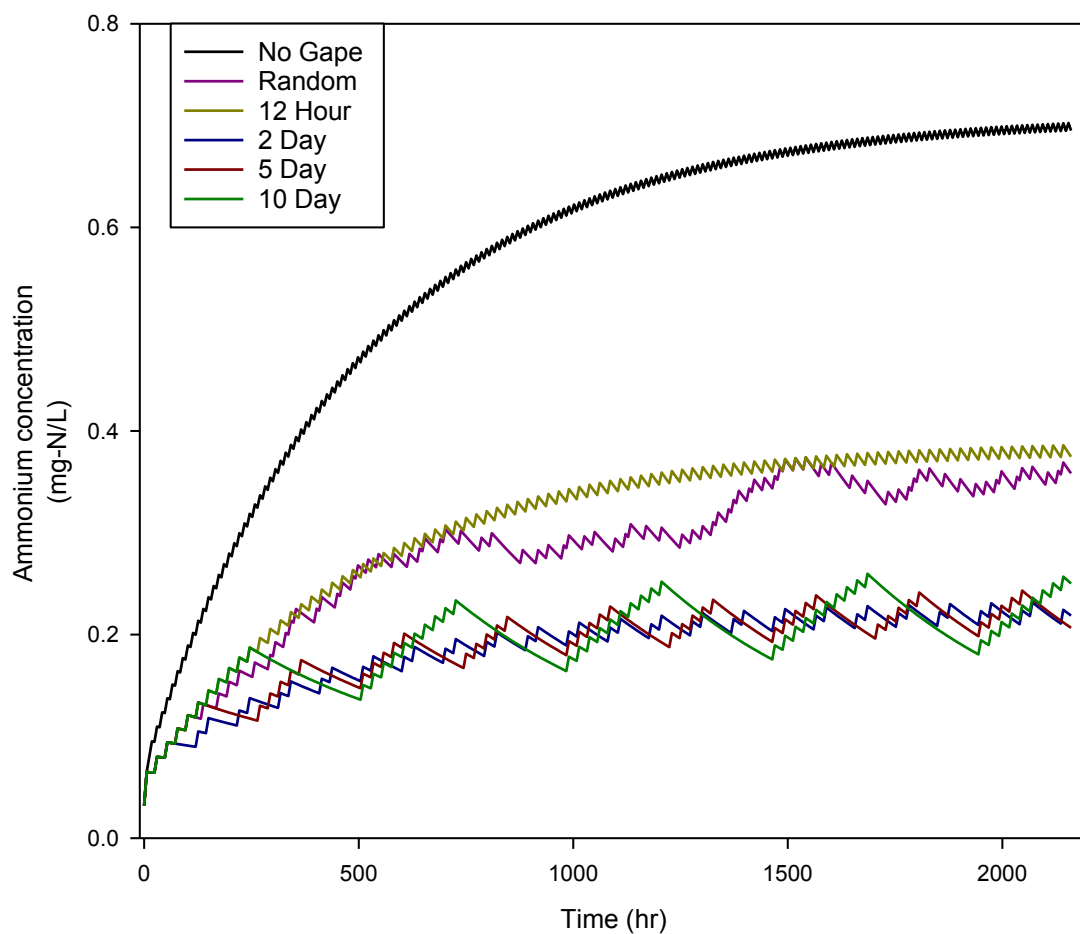


Figure 6.10 Simulated overlying  $\text{NH}_4^+$  concentrations for 200 mussel and phytoplankton biomass of  $10 \text{ mg L}^{-1}$  during various gape position changes.

## REFERENCES

1. Nations, U., UN Foundation Roundtable: The World at Six Billion. In 1999; p 8128.
2. Galloway, J. N.; Cowling, E. B., Reactive nitrogen and the world: 200 years of change. *Ambio* **2002**, *31*, (2), 64.
3. NAE Manage the nitrogen cycle.  
<http://www.engineeringchallenges.org/cms/8996/9132.aspx>
4. Howarth, R. W., Coastal nitrogen pollution: A review of sources and trends globally and regionally. *Harmful Algae* **2008**, *8*, (1), 14-20.
5. Meinch, T., Water Works plans to sue three counties. *The Des Moines Register* 2015.
6. EPA Northern Gulf of Mexico Hypoxic Zone.  
<http://water.epa.gov/type/watersheds/named/msbasin/zone.cfm> (1/16),
7. Li, L.; Zheng, B.; Liu, L., Biomonitoring and Bioindicators Used for River Ecosystems: Definitions, Approaches and Trends. *Procedia Environmental Sciences* **2010**, *2*, 1510-1524.
8. Green, R. H.; Singh, S. M.; Bailey, R. C., Bivalve molluscs as response systems for modelling spatial and temporal environmental patterns. *Science of the Total Environment* **1985**, *46*, (1), 147-169.
9. Green, R. H.; Bailey, R. C.; Hinch, S. G.; Metcalfe, J. L.; Young, V. H., Use of Freshwater Mussels ( Bivalvia: Unionidae) to Monitor the Nearshore Environment of Lakes. *Journal of Great Lakes Research* **1989**, *15*, (4), 635-644.
10. Wasmund, N.; Nausch, G.; Hansen, A., Phytoplankton succession in an isolated upwelled Benguela water body in relation to different initial nutrient conditions. *Journal of Marine Systems* **2014**.
11. Vaughn, C. C.; Gido, K. B.; Spooner, D. E., Ecosystem processes performed by unionid mussels in stream mesocosms: Species roles and effects of abundance. *Hydrobiologia* **2004**, *527*, (1), 35-47.
12. Vaughn, C. C.; Spooner, D. E., Unionid mussels influence macroinvertebrate assemblage structure in streams. *J. N. Am. Benthol. Soc.* **2006**, *25*, (3), 691-700.
13. Manis, E.; Royer, T. V.; Johnson, L. T.; Leff, L. G., Denitrification in agriculturally impacted streams: seasonal changes in structure and function of the bacterial community. *PloS one* **2014**, *9*, (8), e105149.
14. NOAA EPA-supported scientists find average but large Gulf dead zone.  
[http://www.noaanews.noaa.gov/stories2014/20140804\\_deadzone.html](http://www.noaanews.noaa.gov/stories2014/20140804_deadzone.html)
15. Alexander, R. B.; Smith, R. A.; Schwarz, G. E.; Boyer, E. W.; Nolan, J. V.; Brakebill, J. W., Differences in phosphorus and nitrogen delivery to the Gulf of Mexico from the Mississippi River Basin. *Environmental science & technology* **2008**, *42*, (3), 822.
16. Spooner, D. E.; Vaughn, C. C., Context-dependent effects of freshwater mussels on stream benthic communities. *Freshwater Biology* **2006**, *51*, (6), 1016-1024.
17. Riisgard, H. U.; Kittner, C.; Seerup, D. F., Regulation of opening state and filtration rate in filter- feeding bivalves (*Cardium edule*, *Mytilus edulis*, *Mya arenaria*) in response to low algal concentration. *J. Exp. Mar. Biol. Ecol.* **2003**, *284*, (1-2), 105-127.
18. Spooner, D.; Vaughn, C., A trait- based approach to species' roles in stream ecosystems: climate change, community structure, and material cycling. *Oecologia* **2008**, *158*, (2), 307-317.
19. Graf, D. L.; Cummings, K. S., Palaeoheterodont diversity ( Mollusca: Trigonioidea + Unionoidea): what we know and what we wish we knew about freshwater mussel evolution. *Zoological Journal of the Linnean Society* **2006**, *148*, (3), 343-394.
20. Services, U. S. F. a. W. America's Mussels: Silent Sentinels.  
<http://www.fws.gov/midwest/Endangered/clams/mussels.html>

21. Strayer, D., Understanding how nutrient cycles and freshwater mussels (Unionoida) affect one another. *The International Journal of Aquatic Sciences* **2014**, 735, (1), 277-292.
22. Haag, W. R.; Rypel, A. L., Growth and longevity in freshwater mussels: Evolutionary and conservation implications. *Biological Reviews* **2011**, 86, (1), 225-247.
23. USGS, Freshwater Mussels of the Upper Mississippi River System. In 2006.
24. Christian, A. D.; Crump, B. G.; Berg, D. J., Nutrient release and ecological stoichiometry of freshwater mussels (Mollusca:Unionidae) in 2 small, regionally distinct streams. *Journal of the North American Benthological Society* **2008**, 27, (2), 440-450.
25. Layzer, J. B.; Madison, L. M., Microhabitat use by freshwater mussels and recommendations for determining their instream flow needs. *Regulated Rivers: Research & Management* **1995**, 10, (2-4), 329-345.
26. Haag, W. R., *North American Freshwater Mussels: Natural History, Ecology, and Conservation*. Cambridge University Press: 2012.
27. Bogan, A. E., Freshwater bivalve extinctions (mollusca: Unionoida): A search for causes. *Integrative and Comparative Biology* **1993**, 33, (6), 599-609.
28. Strayer, D. L.; Caraco, N. F.; Cole, J. J.; Findlay, S.; Pace, M. L., Transformation of freshwater ecosystems by bivalves: a case study of zebra mussels in the Hudson River. *BioScience* **1999**, 48, (1), 19.
29. Kryger, J.; Riisgård, H., Filtration rate capacities in 6 species of European freshwater bivalves. *Oecologia* **1988**, 77, (1), 34-38.
30. Naimo, T., A review of the effects of heavy metals on freshwater mussels. *Ecotoxicology* **1995**, 4, (6), 341-362.
31. Norton, J. M., Nitrification in Agricultural Soils. In *Nitrogen in Agricultural Systems*, American Society of Agronomy: 2008; Vol. 49.
32. Mulvaney, R. L. In *Nitrification of Different Nitrogen Fertilizers*, Illinois Fertilizer Conference Proceedings, 1994; 1994.
33. Smith, K. A.; Jackson, D. R.; Pepper, T. J., Nutrient losses by surface run-off following the application of organic manures to arable land. 1. Nitrogen. *Environmental Pollution* **2001**, 112, (1), 41-51.
34. Smith, D. R.; Owens, P. R.; Leytem, A. B.; Warnemuende, E. A., Nutrient losses from manure and fertilizer applications as impacted by time to first runoff event. *Environmental Pollution* **2007**, 147, (1), 131-137.
35. Pathak, H.; Pathak, D., Eutrophication: Impact of Excess Nutrient Status in Lake Water Ecosystem. *Environmental & Analytical Toxicology* **2012**, 2, (5), 5.
36. Li, Y.; Waite, A. M.; Gal, G.; Hipsey, M. R., Do phytoplankton nutrient ratios reflect patterns of water column nutrient ratios? A numerical stoichiometric analysis of Lake Kinneret. *Procedia Environmental Sciences* **2012**, 13, 1630-1640.
37. Beman, M. J.; Arrigo, K. R.; Matson, P. A., Agricultural runoff fuels large phytoplankton blooms in vulnerable areas of the ocean. *Nature* **2005**, 434, (7030), 211.
38. Saurel, C.; Gascoigne, J. C.; Palmer, M. R.; Kaiser, M. J., In situ mussel feeding behavior in relation to multiple environmental factors: Regulation through food concentration and tidal conditions. *Limnology and Oceanography* **2007**, 52, (5), 1919-1929.
39. Pascoe, P.; Parry, H.; Hawkins, A., Observations on the measurement and interpretation of clearance rate variations in suspension-feeding bivalve shellfish. *Aquatic Biology* **2009**, 6, 181-190.
40. Jansen, H. M.; Strand, Ø.; Verdegem, M.; Smaal, A., Accumulation, release and turnover of nutrients (C-N-P-Si) by the blue mussel *Mytilus edulis* under oligotrophic conditions. *Journal of Experimental Marine Biology and Ecology* **2012**, 416-417, 185-195.
41. Jordan, T. E.; Valiela, I., A nitrogen budget of the ribbed mussel, *Geukensia demissa*, and its significance in nitrogen flow in a New England salt marsh [Massachusetts]. *A nitrogen budget of the ribbed mussel, Geukensia demissa, and its*

- significance in nitrogen flow in a New England salt marsh [Massachusetts]* **1982**, 27, (1), 75-90.
42. Prins, T.; Smaal, A.; Pouwer, A., Selective ingestion of phytoplankton by the bivalves *Mytilus edulis* L. and *Cerastoderma edule* (L.). *Hydrobiological Bulletin* **1991**, 25, (1), 93-100.
43. Strauss, E. A.; Mitchell, N. L.; Lamberti, G. A., Factors regulating nitrification in aquatic sediments: effects of organic carbon, nitrogen availability, and pH. *Canadian Journal of Fisheries and Aquatic Sciences* **2002**, 59, (3), 554-563.
44. Rysgaard, S.; Risgaard-Petersen, N.; Sloth, N., Nitrification, denitrification, and nitrate ammonification in sediments of two coastal lagoons in Southern France. *The International Journal of Aquatic Sciences* **1996**, 329, (1), 133-141.
45. Rittmann, B. E.; McCarty, P. L., *Environmental Biotechnology : Principles and Applications*. Boston : McGraw-Hill: Boston, 2001.
46. Gough, H. M.; Gascho Landis, A. M.; Stoeckel, J. A., Behaviour and physiology are linked in the responses of freshwater mussels to drought. *Freshwater Biology* **2012**, 57, (11), 2356-2366.
47. Robson, A. A.; De Leaniz, C. G.; Wilson, R. P.; Halsey, L. G., Behavioural adaptations of mussels to varying levels of food availability and predation risk. *J. Molluscan Stud.* **2010**, 76, 348-353.
48. Maire, O.; Amouroux, J. M.; Duchene, J. C.; Gremare, A., Relationship between filtration activity and food availability in the Mediterranean mussel *Mytilus galloprovincialis*. *Mar. Biol.* **2007**, 152, (6), 1293-1307.
49. Helm, M. M.; Trueman, E. R., The effect of exposure on the heart rate of the mussel, *Mytilus edulis* L. *Comparative Biochemistry And Physiology* **1967**, 21, (1), 171-177.
50. da Silva Cândido, L. T.; Brazil Romero, S. M., Heart rate and burrowing behavior in the mussel *Anodontites trapesialis* (Bivalvia: Mycetopodidae) from lotic and lentic sites. *Comparative biochemistry and physiology. Part A, Molecular & integrative physiology* **2006**, 145, (1), 131.
51. Braby, C. E., Following the heart: temperature and salinity effects on heart rate in native and invasive species of blue mussels (genus *Mytilus*). *Journal of Experimental Biology* **2006**, 209, (13), 2554-2566.
52. Clausen, I.; Riisgård, H., Growth, filtration and respiration in the mussel *Mytilus edulis*: no evidence for physiological regulation of the filter- pump to nutritional needs. *Marine Ecology Progress Series* **1996**, 141, 37-45.
53. Clausen, I.; Riisgard, H. U., Growth, filtration and respiration in the mussel *Mytilus edulis*: No evidence for physiological regulation of the filter-pump to nutritional needs. *Mar. Ecol.-Prog. Ser.* **1996**, 141, (1-3), 37-45.
54. Vaughn, C. C.; Hakenkamp, C. C., The functional role of burrowing bivalves in freshwater ecosystems. In *Freshw. Biol.*, 2001; Vol. 46, pp 1431-1446.
55. Sukhotin, A. A.; Pörtner, H. O., Age- dependence of metabolism in mussels *Mytilus edulis* (L.) from the White Sea. *Journal of Experimental Marine Biology and Ecology* **2001**, 257, (1), 53-72.
56. Burnett, N. P.; Seabra, R.; De Pirro, M.; Wethey, D. S.; Woodin, S. A.; Helmuth, B.; Zippay, M. L.; Sarà, G.; Monaco, C.; Lima, F. P., An improved noninvasive method for measuring heartbeat of intertidal animals. *Limnology and Oceanography: Methods* **2013**, 11, 91-100.
57. Taylor, H. D.; Kruger, A.; J., N. J., Embedded electronics for a mussel-based biological sensor. In *Sensors Applications Symposium*, IEEE: Galveston, TX, 2013; pp 148-151.
58. Wilson, R.; Reuter, P.; Wahl, M., Muscling in on mussels: new insights into bivalve behaviour using vertebrate remote- sensing technology. *International Journal on Life in Oceans and Coastal Waters* **2005**, 147, (5), 1165-1172.

59. Bakhmet, I. N.; Khalaman, V. V., Heart rate variation patterns in some representatives of Bivalvia. *Biology Bulletin* **2006**, *33*, (3), 276-280.
60. Depledge, M. H.; Andersen, B. B., A computer- aided physiological monitoring system for continuous, long- term recording of cardiac activity in selected invertebrates. *Comparative Biochemistry and Physiology -- Part A: Physiology* **1990**, *96*, (4), 473-477.
61. Anderson, T. R., Modelling the influence of food C:N ratio, and respiration on growth and nitrogen excretion in marine zooplankton and bacteria. *Journal of Plankton Research* **1992**, *14*, (12).
62. Rizzo, D. M.; Mouser, P. J.; Whitney, D. H.; Mark, C. D.; Magarey, R. D.; Voinov, A. A., The comparison of four dynamic systems- based software packages: Translation and sensitivity analysis. *Environmental Modelling and Software* **2006**, *21*, (10), 1491-1502.
63. Costanza, R.; Voinov, A., Modeling ecological and economic systems with STELLA: Part III. In 2001; Vol. 143, pp 1-7.
64. Costanza, R.; Gottlieb, S., Modelling ecological and economic systems with STELLA: Part II. *Ecological Modelling* **1998**, *112*, (2), 81-84.
65. Minnesota, U. o., Mussel Anatomy-side. In James Ford Bell Museum: Minneapolis, 2003.
66. IDNR, Freshwater Mussels of Iowa. In Iowa Department of Natural Resources: 2002.
67. Higgins, T.; Grennan, J.; McCarthy, T. K., Effects of recent zebra mussel invasion on water chemistry and phytoplankton production in a small Irish lake. *Aquatic Invasions* **2008**, *3*, (1), 14-20.
68. Howard, J. K.; Cuffey, K. M., The functional role of native freshwater mussels in the fluvial benthic environment. *Freshw. Biol.* **2006**, *51*, (3), 460-474.
69. Shumway, S. E.; Cucci, T. L.; Newell, R. C.; Yentsch, C. M., Particle selection, ingestion, and absorption in filter- feeding bivalves. *Journal of Experimental Marine Biology and Ecology* **1985**, *91*, (1), 77-92.
70. Bril, J. S.; Durst, J. J.; Hurley, B. M.; Just, C. L.; Newton, T. J., Sensor data as a measure of native freshwater mussel impact on nitrate formation and food digestion in continuous-flow mesocosms. *Journal of Medical Entomology* **2014**, *33*, (2), 417-424.
71. Huang, S. C.; Newell, R. I. E., Seasonal variations in the rates of aquatic and aerial respiration and ammonium excretion of the ribbed mussel, *Geukensia demissa* (Dillwyn). *Journal of Experimental Marine Biology and Ecology* **2002**, *270*, (2), 241-255.
72. Bayne, B. L.; Scullard, C., Rates of nitrogen excretion by species of *Mytilus* (Bivalvia: Mollusca). *J. Mar. Biol. Ass.* **1977**, *57*, (2), 355-369.
73. Smaal, A.; Vonck, A., Seasonal variation in C, N and P budgets and tissue composition of the mussel *Mytilus edulis*. *Marine Ecology Progress Series* **1997**, *153*, 167-179.
74. Newton, T.; Zigler, S.; Rogala, J.; Gray, B.; Davis, M., Population Assessment and Potential Functional Roles of Native Mussels in the Upper Mississippi River. *Aquatic Conservation-Marine and Freshwater Ecosystems* **2011**, *21*.
75. Bracken, M. E. S., Invertebrate-mediated nutrient loading increases growth of intertidal macroalga. *Journal of Phycology* **2004**, *40*, (6), 1032-1041.
76. Robson, A.; Thomas, G.; Garcia De Leaniz, C.; Wilson, R., Valve gape and exhalant pumping in bivalves: optimization of measurement. *Aquatic Biology* **2009**, *6*, 191-200.
77. da Silva Cândido, L. T.; Brazil Romero, S. M., Heart rate and burrowing behavior in the mussel *Anodontites trapesialis* (Bivalvia: Mycetopodidae) from lotic and lentic sites. *Comparative biochemistry and physiology. Part A, Molecular & integrative physiology* **2006**, *145*, (1), 131.
78. Famme, P., Effect of shell valve closure by the mussel *Mytilus edulis* L. on the rate of oxygen consumption in declining oxygen tension. *Comparative Biochemistry and Physiology -- Part A: Physiology* **1980**, *67*, (1), 167-170.

79. Jorgensen, C. B.; Mohlenberg, F.; Sten-Knudsen, O., Nature of relation between ventilation and oxygen consumption in filter feeders. *Marine Ecology* **1986**, *29*, 16.
80. Bril, J. Assessing the Effects of Native Freshwater Mussels on Aquatic Nitrogen Dynamics. The University of Iowa, 2012.